

PRINCETON AERONAUTICAL
PAPERBACKS

1. LIQUID PROPELLANT ROCKETS

David Altman, James M. Carter, S. S. Penner, Martin Summerfield.
High Temperature Equilibrium, Expansion Processes, Combustion
of Liquid Propellants, The Liquid
Propellant Rocket Engine.
196 pages. \$2.95

2. SOLID PROPELLANT ROCKETS

Clayton Huggett, C. E. Bartley and Mark M. Mills.
Combustion of Solid Propellants, Solid Propellant Rockets.
176 pages. \$2.45

3. GASDYNAMIC DISCONTINUITIES

Wallace D. Hayes. 76 pages. \$1.45

4. SMALL PERTURBATION THEORY

W. R. Sears. 72 pages. \$1.45

5. HIGHER APPROXIMATIONS IN
AERODYNAMIC THEORY. M. J. Lighthill.

156 pages. \$1.95

6. HIGH SPEED WING THEORY

Robert T. Jones and Doris Cohen.
248 pages. \$2.95

7. FUNDAMENTAL PHYSICS OF GASES

Karl F. Herzfeld, Virginia Griffing, Joseph O. Hirschfelder,
C. F. Curtiss, R. B. Bird and Ellen L. Spotz.
149 pages. \$1.95

8. FLOW OF RAREFIED GASES

Samuel A. Schaaf and Paul L. Chambré.
63 pages. \$1.45

9. TURBULENT FLOW

Galen B. Schubauer and C. M. Tchen.
131 pages. \$1.45

10. STATISTICAL THEORIES OF TURBULENCE

C. C. Lin.
68 pages. \$1.45

PRINCETON UNIVERSITY PRESS • PRINCETON, N.J.

NUMBER 9
PRINCETON AERONAUTICAL
PAPERBACKS
COLEMAN duP. DONALDSON, GENERAL EDITOR

TURBULENT
FLOW

BY GALEN B. SCHUBAUER
AND C. M. TCHEN

PRINCETON, NEW JERSEY
PRINCETON UNIVERSITY PRESS
1961

© COPYRIGHT, 1959, BY PRINCETON UNIVERSITY PRESS

L. C. CARD NO. 61-12665

Reproduction, translation, publication, use, and disposal by and for the United States Government and its officers, agents, and employees acting within the scope of their official duties, for Government use only, is permitted. At the expiration of ten years from the date of publication, all rights in material contained herein first produced under contract Nonr-03201 shall be in the public domain.

PRINTED IN THE UNITED STATES OF AMERICA

HIGH SPEED AERODYNAMICS
AND JET PROPULSION

BOARD OF EDITORS

THEODORE VON KÁRMÁN, *Chairman*
HUGH L. DRYDEN
HUGH S. TAYLOR

COLEMAN DUP. DONALDSON, General Editor, 1956–
Associate Editor, 1955–1956

JOSEPH V. CHARYK, General Editor, 1952–
Associate Editor, 1949–1952

MARTIN SUMMERFIELD, General Editor, 1949–1952

RICHARD S. SNEDEKER, Associate Editor, 1955–

- I. Thermodynamics and Physics of Matter. Editor: F. D. Rossini
- II. Combustion Processes. Editors: B. Lewis, R. N. Pease, H. S. Taylor
- III. Fundamentals of Gas Dynamics. Editor: H. W. Emmons
- IV. Theory of Laminar Flows. Editor: F. K. Moore
- V. Turbulent Flows and Heat Transfer. Editor: C. C. Lin
- VI. General Theory of High Speed Aerodynamics. Editor: W. R. Sears
- VII. Aerodynamic Components of Aircraft at High Speeds. Editors:
A. F. Donovan, H. R. Lawrence
- VIII. High Speed Problems of Aircraft and Experimental Methods.
Editors: A. F. Donovan, H. R. Lawrence, F. Goddard, R. R.
Girruth
- IX. Physical Measurements in Gas Dynamics and Combustion.
Editors: R. W. Ladenburg, B. Lewis, R. N. Pease, H. S. Taylor
- X. Aerodynamics of Turbines and Compressors. Editor: W. R.
Hawthorne
- XI. Design and Performance of Gas Turbine Power Plants. Editors:
W. R. Hawthorne, W. T. Olson
- XII. Jet Propulsion Engines. Editor: O. E. Lancaster

PRINCETON, NEW JERSEY
PRINCETON UNIVERSITY PRESS

→ AST
92515
626
(RECAP)

PREFACE

The favorable response of many engineers and scientists throughout the world to those volumes of the Princeton Series on High Speed Aerodynamics and Jet Propulsion that have already been published has been most gratifying to those of us who have labored to accomplish its completion. As must happen in gathering together a large number of separate contributions from many authors, the general editor's task is brightened occasionally by the receipt of a particularly outstanding manuscript. The receipt of such a manuscript for inclusion in the Princeton Series was always an event which, while extremely gratifying to the editors in one respect, was nevertheless, in certain particular cases, a cause of some concern. In the case of some outstanding manuscripts, namely those which seemed to form a complete and self-sufficient entity within themselves, it seemed a shame to restrict their distribution by their inclusion in one of the large and hence expensive volumes of the Princeton Series.

In the last year or so, both Princeton University Press, as publishers of the Princeton Series, and I, as General Editor, have received many enquiries from persons engaged in research and from professors at some of our leading universities concerning the possibility of making available at paperback prices certain portions of the original series. Among those who actively campaigned for a wider distribution of certain portions of the Princeton Series, special mention should be made of Professor Irving Glassman of Princeton University, who made a number of helpful suggestions concerning those portions of the Series which might be of use to students were the material available at a lower price.

In answer to this demand for a wider distribution of certain portions of the Princeton Series, and because it was felt desirable to introduce the Series to a wider audience, the present Princeton Aeronautical Paperbacks series has been launched. This series will make available in small paper-backed volumes those portions of the larger Princeton Series which it is felt will be most useful to both students and research engineers. It should be pointed out that these paperbacks constitute but a very small part of the original series, the first seven published volumes of which have averaged more than 750 pages per volume.

For the sake of economy, these small books have been prepared by direct reproduction of the text from the original Princeton Series, and no attempt has been made to provide introductory material or to eliminate cross references to other portions of the original volumes. It is hoped that these editorial omissions will be more than offset by the utility and quality of the individual contributions themselves.

Coleman duP. Donaldson, General Editor

PUBLISHER'S NOTE: Other articles from later volumes of the clothbound series, *High Speed Aerodynamics and Jet Propulsion*, may be issued in similar paperback form upon completion of the original series.

Berücksichtigt und Technische Universität Berlin eGeschwinn

Angemeldet

Heruntergeladen am | 10.02.18 09:57

CONTENTS

B. Turbulent Flow	3
Galen B. Schubauer, Fluid Mechanics Section, National Bureau of Standards, Washington, D. C.	
C. M. Tchen, Aerodynamics Section, National Bureau of Standards, Washington, D. C.	
<i>Chapter 1. Introduction</i>	
1. Subject Treatment	3
2. Nature of Turbulent Flow	4
3. Diffusiveness of Turbulence	7
<i>Chapter 2. General Hydrodynamical Equations for the Turbulent Motion of a Compressible Fluid</i>	
4. Equations of Continuity and Momentum	8
5. Equation of Kinetic Energy	11
6. Equation of Energy and Enthalpy	13
<i>Chapter 3. Turbulent Boundary Layer of a Compressible Fluid</i>	
7. Introduction	15
8. Fundamental Equations of Motion of a Compressible Boundary Layer	17
9. Relationships between Velocity, Pressure, and Temperature Distributions	18
10. Phenomena of Transport of Properties in a Turbulent Fluid	25
11. Reynolds Analogy between Heat Transfer and Skin Friction	32
12. Basis of Skin Friction Theories	35
13. Empirical Laws of Skin Friction	41
14. Comparison between Experiments and Theories	44
<i>Chapter 4. General Treatment of Incompressible Mean Flow along Walls</i>	
15. Power Laws	47
16. Wall Law and Velocity-Defect Law	50
17. Logarithmic Formulas	52
18. Smooth Wall Incompressible Skin Friction Laws	55
19. Effect of Pressure Gradient	57
20. Equilibrium Boundary Layers According to Clauser	63
21. Law of the Wake According to Coles	67
22. Mixing Length and Eddy Viscosity in Boundary Layer Flows	71
23. Effect of Roughness	75
24. Integral Methods for Calculating Boundary Layer Development	81
25. Three-Dimensional Effects	84

CONTENTS

Chapter 5. Free Turbulent Flows

26. Types and General Features	86
27. Laws of Mean Spreading and Decay	87
28. General Form and Structure	91
29. Transport Processes in Free Turbulent Flow	96
30. Velocity Distribution Formulas for Jets and Wakes	101
31. Effect of Density Differences and Compressibility on Jets with Surrounding Air Stationary	104
32. Effect of Axial Motion of Surrounding Air on Jets	107

Chapter 6. Turbulent Structure of Shear Flows

33. The Nature of the Subject	112
34. References on Structure of Shear Turbulence	113
35. Cited References	118

SECTION B

TURBULENT FLOW

G. B. SCHUBAUER

C. M. TCHEN

CHAPTER 1. INTRODUCTION

B.1. Subject Treatment. Since turbulent flows and their effects are encountered in nearly every case where fluid motion is involved, it becomes important to know their behavior. It is also important to understand the reason for their behavior, not only to formulate laws for practical use, but to satisfy our desire to know and to be able to explain the phenomena with which we deal.

These dual requirements have been kept in mind in writing this account, and some degree of balance has been attempted. However, greater emphasis is placed on the characteristics of mean flow resulting from the action of turbulence than on the turbulent motions themselves. Since the effects of compressibility and aerodynamic heating are assuming increasing importance in modern technology, these have been included wherever possible. The general equations of motion and energy are accordingly expressed in terms of a compressible fluid, and combined thermodynamic and aerodynamic formulations are presented in relation to boundary layer and skin friction effects at high speeds.

Due to the fact that most of the basic concepts by which we attempt to understand the behavior of turbulent flows are as yet conceived only in terms of incompressible flow, much of the subject must still be treated in these terms. Therefore the more penetrating treatment of wall-bounded flows on the one hand and free turbulent flows on the other are dealt with in terms of incompressible, isothermal flow. The specific subjects covered under these general headings are boundary layers, pipe and channel flows, jets, wakes, and mixing regions. In the case of jets the effects of compressibility and of temperature and density differences are treated.

It would be misleading to imply that complete coverage can be given to all of the varied aspects of turbulent flow in the space allotted to it here. Certain omissions are therefore inevitable. These include much of the structure of turbulent flow embracing the wealth of information derived from hot wire measurements and its theoretical interpretation. A

bibliography of literature references is however supplied. This omission may be partially excused on the grounds that the reader may turn for such material to Townsend's book [1] on this general subject. Statistical theories of turbulence are likewise excluded, and justifiably so since they are the subject of Sec. C. Another fruitful source of information is the book by Batchelor [2].

B,2. Nature of Turbulent Flow. When entering into the subject of turbulent flow it is essential to understand that the kind of flows with which we shall be dealing belong to a particular class known as shear flows. These comprise flow fields in which relative velocities have been induced by shear stresses, and they are distinguished by having arisen in this way rather than by the action of pressures. They are therefore rotational flows as opposed to potential flows, and they are usually more restricted since their extent is governed by the range of action of the stresses. They may be bounded by solid walls or they may be free. Common examples are boundary layers, pipe and channel flows, jets, and wakes.

It is equally important that we know why we restrict ourselves to shear flow. The reason is that only in such flows can turbulent motions arise and sustain themselves. When turbulence is found in a stream that has no measurable mean shear, the turbulent motions themselves represent the decaying remnant of shear flows that existed somewhere upstream. Such a condition is not uncommon where upstream objects have created wakes. Grids or coarse screens placed across a stream are commonly used to create a homogeneous field of turbulence for experimental study. We shall not be concerned with this case.

Our main task will be to describe turbulent shear flows and to examine their laws of behavior. For the most part we shall be concerned with mean flows, but we shall have some opportunity as we go along to look into the flow itself, to find out what it contains, and to see reasons for certain behavior patterns. Some generalizations which apply to the mechanics of turbulent flows as a class can be made, and these we now take up. The more quantitative and precise aspects must be left to later articles on specific subjects. Since there is much about turbulent flow that has not been put on a firm theoretical basis, some amount of rationalization is involved, and this necessarily reflects individual viewpoints. It is hoped that the following discussion will stimulate thought and show that turbulent flow is a phenomenon that should arouse our curiosity.

We begin first with the somewhat controversial questions: What is turbulent flow, and why does it exist? When tangential stresses are applied to a fluid having internal friction, shearing motions are set up in line with the stresses and in conformity to the shape of the boundaries. Within this flow field, various kinds of secondary motions become possible. Regu-

lar ones, when they occur, are readily accounted for in terms of pressure gradients resulting from the curvature of the main flow, usually imposed by the shape of the boundaries. Irregular ones, called turbulence, are by far the more common, and their direct cause is less obvious. Their occurrence does not depend on the shape of the boundaries, but like all secondary flows, they must depend on a generating mechanism which produces motions in directions other than that of the applied shear. We must look for this mechanism within the flow itself. Our inquiry can be divided into two parts, the first having to do with how the motions begin, and the second being concerned with how the motions maintain themselves.

To consider the first part, it is necessary to recall the transition problem treated in Sec. A. In many important cases a shear flow is laminar over the initial part of its course and then becomes turbulent and remains so for the remainder of its course. According to present evidence the initial onset of turbulence occurs suddenly by a breakdown of the laminar flow in localized regions. The cause of the breakdown is attributed to instability of the laminar flow under the action of disturbances. While conditions may be altered by the roughness of a surface or pressure gradient, a characteristic feature is the completeness of the turbulent state in the patches which grow following the breakdown. It is now well known that turbulence is convected downstream in the manner of any other fluid property, and, except in special cases where the flow is impeded to such a degree that turbulence can hold its position, it is washed away from the point where it originates and is followed by laminar flow. Repeated breakdowns are therefore generally required to maintain a continuous supply of turbulence, and instability of laminar flow is an essential part of this process.

For the second part of the inquiry we turn our attention to some section downstream where all isolated patches have grown together and the flow is continuously turbulent. We now observe that turbulence which is convected on downstream is followed by other turbulence from upstream. A steady state is maintained if the turbulence leaving is as vigorous as that arriving. The question now is whether instability plays a similar role in this sustaining process as it played in initiating the turbulence originally. Evidently it does not if turbulent motions already present can reinforce themselves to counteract the damping action of viscosity. Since turbulent motions produce frictional stresses against which the mean flow does work, a mechanism does exist by which turbulent motions capture kinetic energy from the mean flow. This is expressed by the well-known production term in the energy equations, consisting of the turbulent shear stress times the mean local velocity gradient. In short, turbulence carries with it the mechanism for sustaining itself, and this is sufficient to balance losses or gains by diffusion and convection and losses by viscous damping and still maintain a steady state at each point.

Nothing has yet been said about the character of the motions themselves. Naturally we should like to know whether the sustaining mechanism dictates some particular form of motion. It is a known fact that even though the energizing of turbulence is expressible in terms of shear stresses, turbulent pressure gradients are required, and they must arise from interactions within the flow itself. These interactions can be imagined to take the form of collisions between fluid elements; but since all streams are connected, the interaction paths are curved and continuous. The resulting motions may best be described as a superposition of eddies with various orientations. The shearing action stretches the eddies with axes lying along directions in which the fluid is being strained and intensifies their vorticity. Some concentrated vortex motions can therefore be expected to exist in the complex jumble of motions.

Before we can proceed further we must consider the various scales of motion encountered in turbulent flow and examine their role. It is generally assumed that the largest scale is that characteristic of the size of the mean flow field, such as the thickness of a boundary layer. Next come the turbulent motions where the superimposed jumble of eddies have various sizes ranging from near that of the mean flow down to the so-called micro-scales. All turbulent motions are agents responsible for shearing stress in the presence of a mean shear, and therefore all extract energy from the mean flow to sustain themselves. However, this action decreases with decreasing scale, and from an over-all point of view it is generally assumed that the energy enters the turbulence by way of the larger eddies. Correspondingly, the damping action of viscosity is assumed to be negligible in the mean flow and among the larger eddies but to increase progressively with decreasing size until it finally becomes dominant among the smallest eddies. The effect of viscosity is the more removed from the larger eddies as the Reynolds number becomes higher.

It is obvious that if energy enters the turbulence more by way of the large eddies than by the small ones and leaves more by way of the small eddies than by the large ones, there must be a transfer of energy from larger scales to smaller scales. The succession of transfer is generally regarded as taking place from size to size down the scale, with the number of stages increasing with the Reynolds number.

Except for the laminar sublayer next to a wall and its immediate vicinity, it is an observed fact that if the Reynolds number is sufficiently high for transition to have occurred, the succession of transfer is already long. In the usual terms, the turbulent energy spectrum is broad. This signifies that turbulent flows as a class show comparatively minor effects of Reynolds number in their over-all character. The mean velocity distribution, for example, changes little with Reynolds number, and the mean flow field shows a tendency to remain similar in form as it grows to

B,3 · DIFFUSIVENESS OF TURBULENCE

larger sizes. The turbulent velocities which contain the bulk of the turbulent energy likewise tend to maintain a constant ratio to the mean local velocity. This general condition is termed "Reynolds number similarity." This and the related property of preservation of form from section to section, commonly called "self preservation," are very important features of turbulent flow. They give to the flow a permanence of form and a continuity of behavior that simplify description and make possible certain general laws.

B,3. Diffusiveness of Turbulence. It is a well-known fact that frictional effects, mean velocity distributions, rate of spreading, and other features of turbulent flow bear little resemblance to those found in laminar flow. These differences can be attributed to a diffusiveness of turbulence that far exceeds molecular diffusion and has a more intimate connection with the mean flow. The mechanism of turbulent diffusion is commonly compared to that of molecular diffusion wherein a molecule moves and collides with another and so by a process of random walk migrates farther and farther from some initial point. Turbulent movements may also be likened to a random walk, and now bulk currents wander randomly in generally curved paths producing a cumulative increase in the distance from an initial point.

Except for the region near a wall where turbulent movements are inhibited, the bulk-lot transfers by turbulent motions so surpass transfer by molecular motions that the latter has little effect other than to smooth out the spotty condition of properties in their new neighborhood. Thus, molecular diffusion may often be neglected as far as the rate of transport is concerned. Where it cannot be neglected, molecular and turbulent diffusion are assumed to be additive.

When we concern ourselves with mean flow, we intentionally ignore the turbulent motions themselves and deal in effect with a fictitious "laminar flow" of a fluid behaving as though it had special properties. The analogy to laminar flow involves endowing the fluid with properties called "eddy viscosity" and "eddy heat conductivity," or more generally, "eddy diffusion coefficient." If we attempt to account for behavior in terms of an eddy viscosity, our fluid appears to be a very peculiar one. It might be described as non-Newtonian because of the dependence of the viscosity on rate of shear. We find further that the viscosity varies from point to point in one part of the flow and remains practically constant in other parts. Moreover, the numerical value is often hundreds of times larger than that of ordinary viscosity and bears no definite relation to it. What is even more unconventional is the fact that eddy viscosity increases with the size of the flow field and increases with over-all velocity. The fluid flow in a large pipe, for example, behaves as though

it had a larger viscosity than the same fluid flowing in a small pipe. Furthermore, at high rates of flow the viscosity appears to be larger than at low rates of flow.

Our fictitious fluid properties are governed by an intimate connection to the flow itself, and the apparent anomalies arise because of this fact. As we know, the transporting agents are the turbulent motions, and taken as a whole their velocities are proportional to some velocity characterizing that of the mean flow. This connection between transporting motions and the flow field stands in marked contrast to the independence of molecular motions which do the transporting in laminar flow.

In every case we must refer back to the turbulence mechanisms in order ultimately to understand any kind of property with which we have endowed the fluid. Phenomenological theories have been employed for this purpose, of which one of the better known examples is the mixing length theory proposed by Prandtl. Ideally, of course, we should like to use the fundamental equations of motion for this purpose, but so far this has not been possible. These questions are discussed in more detail in Art. 10.

CHAPTER 2. GENERAL HYDRODYNAMICAL EQUATIONS FOR THE TURBULENT MOTION OF A COMPRESSIBLE FLUID

B.4. Equations of Continuity and Momentum. The procedure introduced by Reynolds [3] and Lorentz [4], whereby equations of motion and energy balance for an incompressible turbulent flow are obtained, is well known. Briefly the turbulent motion is regarded as consisting of the sum of a mean part and a fluctuating part, and the sum is introduced into the Navier-Stokes equations. The resulting equations give considerable insight into the character of turbulent motions and serve as a basis for attacking mean flow problems and also for analyzing the turbulence into harmonic components.

We now follow the same procedure for compressible turbulent flow. The purpose in doing this is primarily to investigate the coupling between the mean motion and its fluctuations, and to establish the general fundamental equations from which some general properties become apparent. Later on, these equations may be simplified by approximations retaining the significant terms applicable in a particular problem, such as the customary boundary layer approximations.

The additional difficulties encountered in compressible turbulent flow are two-fold: First, the hydrodynamical equations are nonlinear, with the nonlinear terms not only containing the velocity components and their

it had a larger viscosity than the same fluid flowing in a small pipe. Furthermore, at high rates of flow the viscosity appears to be larger than at low rates of flow.

Our fictitious fluid properties are governed by an intimate connection to the flow itself, and the apparent anomalies arise because of this fact. As we know, the transporting agents are the turbulent motions, and taken as a whole their velocities are proportional to some velocity characterizing that of the mean flow. This connection between transporting motions and the flow field stands in marked contrast to the independence of molecular motions which do the transporting in laminar flow.

In every case we must refer back to the turbulence mechanisms in order ultimately to understand any kind of property with which we have endowed the fluid. Phenomenological theories have been employed for this purpose, of which one of the better known examples is the mixing length theory proposed by Prandtl. Ideally, of course, we should like to use the fundamental equations of motion for this purpose, but so far this has not been possible. These questions are discussed in more detail in Art. 10.

CHAPTER 2. GENERAL HYDRODYNAMICAL EQUATIONS FOR THE TURBULENT MOTION OF A COMPRESSIBLE FLUID

B.4. Equations of Continuity and Momentum. The procedure introduced by Reynolds [3] and Lorentz [4], whereby equations of motion and energy balance for an incompressible turbulent flow are obtained, is well known. Briefly the turbulent motion is regarded as consisting of the sum of a mean part and a fluctuating part, and the sum is introduced into the Navier-Stokes equations. The resulting equations give considerable insight into the character of turbulent motions and serve as a basis for attacking mean flow problems and also for analyzing the turbulence into harmonic components.

We now follow the same procedure for compressible turbulent flow. The purpose in doing this is primarily to investigate the coupling between the mean motion and its fluctuations, and to establish the general fundamental equations from which some general properties become apparent. Later on, these equations may be simplified by approximations retaining the significant terms applicable in a particular problem, such as the customary boundary layer approximations.

The additional difficulties encountered in compressible turbulent flow are two-fold: First, the hydrodynamical equations are nonlinear, with the nonlinear terms not only containing the velocity components and their

derivatives, such as was the case for incompressible flow, but also containing the product of velocity by density. The latter must moreover satisfy the conditions imposed by the equation of continuity and the equation of heat conduction. Second, in an incompressible flow the Reynolds equations have a form similar to the original Navier-Stokes equations, provided additional fictitious forces, called Reynolds stresses, are introduced. These stresses also characterize the turbulent friction and give the rate of production of turbulence when multiplied by mean velocity gradients. However, in a compressible flow, such fictitious stresses are more complicated and involve other roles in addition to the production of turbulence.

It is well to mention briefly why averages are used and what they mean. Turbulent motions of fluid elements are so complex that they cannot be treated individually. By averaging we can obtain mean motions which include turbulent properties statistically. The average can be taken at a given point over a certain interval of time, or over a certain region at a particular instant of time, or finally over a great number of realizations represented by identical fields at corresponding points and instants. These are the three kinds of Eulerian mean values, termed respectively, temporal, spatial, and statistical mean values. Finally we can follow the motion of an individual particle as a function of time and find the temporal and statistical mean value of any physical property associated with the particle. This would be the Lagrangian mean value. It is beyond our scope to discuss the different mean values. We shall adhere to the Eulerian description in which any one of the three averages may be used as far as the formalism is concerned. Commonly used methods of measurement and observation require the use of the temporal mean value, and this mean value will subsequently be inferred. The time interval does not need to be considered for present purposes, especially when we are concerned with steady motion.

The motion of the fluid is decomposed into a mean motion with velocity components U_i , parallel to the x_i axis, with the running indices $i = 1, 2, 3$, and the superimposed turbulent motions or fluctuations, with velocity components u_i .¹ The velocity components of the total motion will be $U_i + u_i$. Likewise the scalar quantities, pressure, density, and temperature are also decomposed into their mean parts and fluctuating parts, and are respectively

$$\bar{p} + p', \quad \rho = \bar{\rho} + \rho', \quad T = \bar{T} + T'$$

where \bar{p} denotes the mean pressure and p' its fluctuations, and ρ and T

¹ In this section as well as in Sec. C a departure from the usual notation of the Series wherein \bar{u} is used to denote the mean velocity in the x direction and u' the fluctuation about its mean value has been necessary in order to eliminate the confusion that would result in referring to the fluctuations that might exist simultaneously at two points.

B · TURBULENT FLOW

are respectively the instantaneous local density and the instantaneous local temperature. The bars denote mean parts, and the primes denote turbulent parts. Other physical quantities like viscosity, coefficient of heat condition, and specific heat are considered to have negligible fluctuating parts compared to their mean parts.

The Navier-Stokes equation for the total motion is written as follows:

$$(\bar{\rho} + \rho') \left[\frac{\partial}{\partial t} + (U_i + u_i) \frac{\partial}{\partial x_i} \right] (U_i + u_i) = \frac{\partial}{\partial x_i} (\sigma_{ji} + \sigma'_{ji}) \quad (4-1)$$

Here σ_{ji} is a stress tensor [5, p. 574] defined by

$$\sigma_{ji} = - \left(\bar{p} + \frac{2}{3} \mu \tilde{\zeta} \right) \delta_{ij} + \mu \left(\frac{\partial U_j}{\partial x_i} + \frac{\partial U_i}{\partial x_j} \right) \quad (4-2)$$

where $\zeta = \partial(U_k + u_k)/\partial x_k$; $\tilde{\zeta} = \partial U_k / \partial x_k$; μ is the viscosity supposed to be variable, but with a negligible fluctuating part; and δ_{ij} is the Kronecker delta having the value 1 for $i = j$ and 0 for $i \neq j$. In those equations a summation is understood for repeated indices.² A similar expression for σ'_{ji} can be written but this is omitted here.

The variables U , and u , must moreover satisfy the equation of continuity

$$\frac{\partial}{\partial t} (\bar{\rho} + \rho') + \frac{\partial}{\partial x_i} [(\bar{\rho} + \rho')(U_i + u_i)] = 0 \quad (4-3)$$

With the aid of Eq. 4-3, the equation of motion (Eq. 4-1) may also be written in the following form:

$$\frac{\partial}{\partial t} [(\bar{\rho} + \rho')(U_i + u_i)] = \frac{\partial}{\partial x_i} [(\sigma_{ji} + \sigma'_{ji}) - (\bar{\rho} + \rho')(U_i + u_i)(U_j + u_j)] \quad (4-4)$$

One way of obtaining the momentum equations for the mean and fluctuating motions is to start from Eq. 4-4 instead of Eq. 4-1. By averaging we obtain the following momentum equation for the mean motion:

$$\frac{\partial}{\partial t} (\bar{\rho} U_i + \bar{\rho}' u_i) + \frac{\partial}{\partial x_i} (\bar{\rho} U_i U_i) = \frac{\partial \sigma_{ji}}{\partial x_j} - \frac{\partial}{\partial x_i} [\bar{\rho} u_i u_j + U_i \bar{\rho}' u_j + U_j \bar{\rho}' u_i] \quad (4-5)$$

Similarly by averaging Eq. 4-3, the continuity equation for the mean motion is

$$\frac{\partial \bar{\rho}}{\partial t} + \frac{\partial}{\partial x_i} (\bar{\rho} U_i + \bar{\rho}' u_i) = 0 \quad (4-6)$$

Corresponding equations could be written for the fluctuating motion, but this will not be done.

² The indicial notations are advantageous in the general discussion of the equations of motion. However, in the following articles when dealing with properties in two dimensions the indicial notations will usually be abandoned in favor of x , y , U , and V .

B,5 · EQUATION OF KINETIC ENERGY

B,5. Equation of Kinetic Energy. The equation of kinetic energy for the mean motion is obtained by multiplying Eq. 4-5 by U_i . We obtain, after some transformation,

$$\begin{aligned} \frac{\partial}{\partial t} \left(\frac{1}{2} \bar{\rho} U_i^2 \right) + \frac{\partial}{\partial x_j} \left(\frac{1}{2} \bar{\rho} U_i^2 U_j \right) + U_i \left[\frac{\partial}{\partial t} (\overline{\rho' u_i}) + \frac{\partial}{\partial x_j} (\overline{\rho' u_i} U_j) \right] \\ = - \frac{\partial}{\partial x_j} [U_i (\bar{p} \delta_{ij} + \overline{\rho u_i u_j}) + \frac{1}{2} \overline{\rho' u_i} U_i^2] \\ + \frac{\partial U_i}{\partial x_j} (\bar{p} \delta_{ij} + \overline{\rho u_i u_j}) - \varphi_0 \quad (5-1) \end{aligned}$$

where

$$\begin{aligned} \varphi_0 &= - U_i \frac{\partial}{\partial x_j} \left[- \frac{2}{3} \mu \xi \delta_{ij} + \mu \left(\frac{\partial U_j}{\partial x_i} + \frac{\partial U_i}{\partial x_j} \right) \right] \\ &= \Phi_0 - \frac{\partial}{\partial x_j} \left\{ U_i \left[- \frac{2}{3} \mu \xi \delta_{ij} + \mu \left(\frac{\partial U_j}{\partial x_i} + \frac{\partial U_i}{\partial x_j} \right) \right] \right\} \quad (5-2a) \end{aligned}$$

and Φ_0 is defined by

$$\Phi_0 = - \frac{2}{3} \mu \xi^2 + \frac{1}{2} \mu \left(\frac{\partial U_j}{\partial x_i} + \frac{\partial U_i}{\partial x_j} \right)^2 \quad (5-2b)$$

It is remarked that Φ_0 is the Rayleigh dissipation function [5, p. 580]. In deriving Eq. 5-1, use has been made of Eq. 4-6. On the left-hand side of Eq. 5-1, we have the rate of change of kinetic energy,

$$\frac{\partial}{\partial t} \left(\frac{1}{2} \bar{\rho} U_i^2 \right) + \frac{\partial}{\partial x_j} \left(\frac{1}{2} \bar{\rho} U_i^2 U_j \right)$$

and the convection by density fluctuations,

$$U_i \left[\frac{\partial}{\partial t} (\overline{\rho' u_i}) + \frac{\partial}{\partial x_j} (\overline{\rho' u_i} U_j) \right]$$

On the right-hand side of Eq. 5-1, the term

$$\frac{\partial}{\partial x_j} [U_i (\bar{p} \delta_{ij} + \overline{\rho u_i u_j}) + \frac{1}{2} \overline{\rho' u_i} U_i^2]$$

accounts for the diffusion of energy by turbulence and pressure; the term $\overline{\rho' \xi}$ represents the rate of change of energy due to expansion; the term $\overline{\rho u_i u_j} \partial U_i / \partial x_j$ is the rate of production of turbulent energy from the energy of the mean flow, as a result of Reynolds stresses $\overline{\rho u_i u_j}$; and finally the term φ_0 , as given by Eq. 5-2a, is the action of viscosity, which takes the form of a dissipation Φ_0 , and a spatial transfer

$$- \frac{\partial}{\partial x_j} \left\{ U_i \left[- \frac{2}{3} \mu \xi \delta_{ij} + \mu \left(\frac{\partial U_j}{\partial x_i} + \frac{\partial U_i}{\partial x_j} \right) \right] \right\} \equiv \varphi_0 - \Phi_0 \quad (5-3a)$$

B · TURBULENT FLOW

It is remarked that the Reynolds stresses $\overline{\rho u_i u_j}$, which characterize the important nonlinear mechanism in the turbulent transfer, occur in two places, namely in the diffusion and in the production.

It is much easier to derive the equation of total kinetic energy, $K = \frac{1}{2}(U_i^2 + u_i^2)$. It suffices simply to multiply Eq. 4-4 by $(U_i + u_i)$ and obtain, after some transformation,

$$\begin{aligned} \frac{\partial}{\partial t} (\bar{\rho} \bar{K}) + \frac{\partial}{\partial x_j} (\bar{\rho} \bar{K} U_j) &= - \frac{\partial}{\partial t} \overline{\rho' K'} - \frac{\partial}{\partial x_j} (\overline{\rho' u_i K'} + \overline{\rho u_i K'} + \overline{U_i \rho' K'}) \\ &\quad + \overline{K \rho' u_i} - \overline{U_i \frac{\partial \bar{\rho}}{\partial x_j}} - \overline{u_j \frac{\partial \bar{\rho}'}{\partial x_i}} - \overline{\varphi} \end{aligned} \quad (5-4)$$

where

$$\varphi = \Phi - \frac{\partial}{\partial x_j} \left\{ (U_i + u_i) \left[-\frac{2}{3} \mu \xi \delta_{ij} + \mu \left(\frac{\partial U_j}{\partial x_i} + \frac{\partial U_i}{\partial x_j} + \frac{\partial u_j}{\partial x_i} + \frac{\partial u_i}{\partial x_j} \right) \right] \right\} \quad (5-2c)$$

$$\Phi = -\frac{2}{3} \mu \xi^2 + \frac{1}{2} \mu \left(\frac{\partial U_j}{\partial x_i} + \frac{\partial U_i}{\partial x_j} + \frac{\partial u_j}{\partial x_i} + \frac{\partial u_i}{\partial x_j} \right)^2 \quad (5-2d)$$

The quantities φ and Φ can be easily obtained by taking the mean values of Eq. 5-2c and 5-2d. Reynolds stress terms are included in Eq. 5-4 but only as diffusion terms. There is no energy production term associated with these stresses such as we find in Eq. 5-1 for the kinetic energy of mean motion. This is not surprising since the Reynolds stresses, which transfer energy from the mean motion into turbulent motion, must have a vanishing balance in the production of the total kinetic energy by reason of conservation. The molecular motion contributes a pure dissipation Φ and a spatial transfer $\varphi - \Phi$ which plays the role of viscous diffusion of energy. Its structure can be clarified by transforming either Eq. 5-2c or 5-3a. For the sake of abbreviation, let us take Eq. 5-3a and rewrite it as follows:

$$\begin{aligned} \Phi_0 - \varphi_0 &= -\frac{2}{3} \mu \xi^2 + \frac{1}{3} U_i \frac{\partial \mu \xi}{\partial x_j} + \frac{\mu}{2} \left(\frac{\partial U_j}{\partial x_i} + \frac{\partial U_i}{\partial x_j} \right)^2 \\ &\quad + U_i \frac{\partial}{\partial x_j} \left(\mu \frac{\partial U_i}{\partial x_j} \right) + U_i \frac{\partial \mu}{\partial x_j} \left(\frac{\partial U_j}{\partial x_i} - \xi \delta_{ij} \right) \\ &= \frac{1}{3} \mu \xi^2 + \frac{1}{3} U_i \frac{\partial \mu \xi}{\partial x_j} + \mu \left(\frac{\partial U_i}{\partial x_j} \frac{\partial U_j}{\partial x_i} - \frac{\partial U_i}{\partial x_i} \frac{\partial U_j}{\partial x_j} \right) \\ &\quad + \frac{\partial \mu}{\partial x_j} U_i \left(\frac{\partial U_j}{\partial x_i} + \frac{\partial U_i}{\partial x_j} - \xi \delta_{ij} \right) + \mu \frac{\partial^2}{\partial x_j^2} \left(\frac{U_i^2}{2} \right) \end{aligned}$$

Let us introduce

$$\chi_0 = \Phi_0 - \varphi_0 - \mu \frac{\partial^2}{\partial x_j^2} \left(\frac{U_i^2}{2} \right) \quad (5-3b)$$

B,6 · EQUATION OF ENERGY AND ENTHALPY

Then we obtain

$$x_0 = \frac{1}{3} \mu \tilde{\xi}^2 + \frac{1}{3} U_i \frac{\partial \mu \tilde{\xi}}{\partial x_i} + \mu \left(\frac{\partial U_i}{\partial x_j} \frac{\partial U_j}{\partial x_i} - \frac{\partial U_i}{\partial x_i} \frac{\partial U_j}{\partial x_j} \right) + \frac{\partial \mu}{\partial x_i} U_i \left(\frac{\partial U_j}{\partial x_i} + \frac{\partial U_i}{\partial x_j} - \tilde{\xi} \delta_{ij} \right) \quad (5-3c)$$

The last term vanishes if μ is taken as constant. The third term is not important, as can be shown by special examples, for instance, a boundary layer flow. The other terms are also not important if the effect of the compressibility is small. Hence $\Phi_0 - \varphi_0$ has predominantly the function of a spatial transfer. Similar formulas for $\Phi - \varphi$, $\Phi - \varphi$, or $\Phi' - \varphi'$ can readily be obtained, and so also can formulas for x , \tilde{x} , and x' , for example,

$$\tilde{x} = \frac{1}{3} \overline{\tilde{\xi}'^2} + \frac{1}{3} \overline{u_i \frac{\partial \mu \tilde{\xi}'}{\partial x_i}} + \mu \left(\overline{\frac{\partial u_i}{\partial x_j} \frac{\partial u_j}{\partial x_i}} - \overline{\frac{\partial u_i}{\partial x_i} \frac{\partial u_j}{\partial x_j}} \right) + x_0 \quad (5-3d)$$

B,6. Equation of Energy and Enthalpy. The production and transfer of heat in a turbulent flow is now considered. The derivation of the energy equation for the total motion is well known (see [6, p. 603] and also [7, p. 57]) and need not be repeated here. It is written as follows for constant specific heat and for variable thermal conductivity and viscosity:

$$(\bar{\rho} + \rho') \left[\frac{\partial}{\partial t} + (U_i + u_i) \frac{\partial}{\partial x_i} \right] \left[c_p (\bar{T} + T') \right] - \left[\frac{\partial}{\partial t} + (U_i + u_i) \frac{\partial}{\partial x_i} \right] (\bar{p} + p') = \Phi + \frac{\partial}{\partial x_i} \left[k \frac{\partial}{\partial x_i} (\bar{T} + T') \right] \quad (6-1)$$

where c_p is the specific heat at constant pressure; k is the thermal conductivity; $\bar{\rho}$, p' are the mean and fluctuating pressures; \bar{T} , T' are the mean and fluctuating temperatures; Φ is the dissipation function defined by Eq. 5-2d; and $c_p \bar{T}$ is the mean enthalpy. The energy equation (Eq. 6-1) can be separated into an equation for the mean motion and an equation for the fluctuating motion. Since the need for the latter equation is presently not apparent, only the energy equation for mean motion is developed and written as follows:

$$\begin{aligned} \frac{\partial}{\partial t} (\bar{\rho} c_p \bar{T}) + \frac{\partial}{\partial x_i} (\bar{\rho} c_p \bar{T} U_i) - \left[\frac{\partial \bar{p}}{\partial t} + \frac{\partial}{\partial x_i} (U_i \bar{p}) \right] + \frac{\partial}{\partial t} (c_p \bar{\rho} \bar{T}') \\ + \frac{\partial}{\partial x_i} (c_p \bar{\rho} \bar{T}' U_i) = - \frac{\partial}{\partial x_i} \left(c_p \bar{\rho} \bar{T}' u_i + \bar{\rho}' u_i \bar{T} - \bar{u}_i \bar{p}' - k \frac{\partial \bar{T}}{\partial x_i} \right) \\ - \left(\bar{p} \frac{\partial U_k}{\partial x_k} + \bar{p}' \frac{\partial u_k}{\partial x_k} \right) + \Phi \quad (6-2) \end{aligned}$$

B · TURBULENT FLOW

Finally, by introducing the mean and fluctuating value of the total energy content per unit mass E^0 , E , \bar{E} , and E' , such that

$$\begin{aligned} E^0 &= c_p \bar{T} + \frac{1}{2} U_*^2 \\ E &= c_p (\bar{T} + T') + \frac{1}{2} (U_* + u_i)^2 \\ \bar{E} &= c_p \bar{T} + \frac{1}{2} (U_*^2 + \bar{u}_i^2) \\ E' &= E - \bar{E} \end{aligned}$$

and adding Eq. 5-1 to Eq. 6-2, we obtain

$$\begin{aligned} \frac{D}{Dt} (\bar{\rho} E^0) + U_* \frac{D}{Dt} (\bar{\rho}' u_i) + \frac{D}{Dt} (c_p \bar{\rho}' \bar{T}') - \left(\frac{\partial \bar{p}}{\partial t} + \bar{u}_i \frac{\partial \bar{p}}{\partial x_j} \right) \\ = - \frac{\partial}{\partial x_j} \left(\bar{\rho}' u_i E^0 + U_* \bar{\rho} u_i \bar{u}_j + c_p \bar{\rho}' \bar{T}' \bar{u}_j - k \frac{\partial \bar{T}}{\partial x_j} \right) + \bar{\rho} u_i \bar{u}_j \frac{\partial U_*}{\partial x_j} + \Phi_0 - \varphi_0 \end{aligned} \quad (6-3a)$$

where the operator D/Dt on any function f denotes

$$\frac{Df}{Dt} = \frac{\partial f}{\partial t} + \frac{\partial}{\partial x_j} (f U_j)$$

The left-hand side of Eq. 6-3a expresses the rate of change of quantities $\bar{\rho} E^0$, $\bar{\rho}' u_i$, $\bar{\rho}' \bar{T}'$, and \bar{p} . These rates are the result of diffusion and turbulent energy production expressed by the terms on the right-hand side. Here we find the production term $-\bar{\rho} u_i \bar{u}_j \partial U_* / \partial x_j$, which decreases the energy of mean motion, and diffusion terms within the brackets which include Reynolds stress terms of transport of mass and temperature along with the better-known term $\bar{\rho} u_i \bar{u}_j$. Here also is the molecular contribution expressed by $\Phi_0 - \varphi_0$, which we have already noted in Eq. 5-3 as a spatial transfer and not an energy dissipation. No molecular dissipation appears in Eq. 6-3a because the kinetic energy dissipated appears in the form of heat.

The corresponding equation for \bar{E} may be obtained by adding Eq. 5-4 and 6-2. Thus

$$\begin{aligned} \frac{\partial}{\partial t} (\bar{\rho} \bar{E}) + \frac{\partial}{\partial x_j} (\bar{\rho} \bar{E} U_j) + \frac{\partial}{\partial t} (\bar{\rho}' E') \\ = - \frac{\partial}{\partial x_j} \left(\bar{\rho} u_i \bar{E}' + \bar{\rho}' u_i \bar{E} + \bar{\rho}' u_i \bar{E}' + U_* \bar{\rho}' \bar{E}' - k \frac{\partial \bar{T}}{\partial x_j} \right) + \Phi - \varphi \end{aligned} \quad (6-4a)$$

As would be expected, Eq. 6-4a, which accounts for both the mean and the turbulent energy, is of simpler form and does not contain the production term $\bar{\rho} u_i \bar{u}_j \partial U_* / \partial x_j$.

The diffusion terms in the energy equations (Eq. 6-3a and 6-4a) contain the thermal diffusion with flux $k \partial \bar{T} / \partial x_j$. This may be expressed as an

energy diffusion $\partial E^0/\partial x$, or $\partial \bar{E}/\partial x$, if we introduce χ_0 according to Eq. 5-3c and \bar{x} according to Eq. 5-3d. In this way, Eq. 6-3a and 6-4a become respectively

$$\begin{aligned} \frac{D}{Dt} (\bar{\rho} E^0) + U_i \frac{D}{Dt} (\overline{\rho' u_i}) + \frac{D}{Dt} (c_p \overline{\rho T'}) - \left(\frac{\partial \bar{p}}{\partial t} + \overline{u_j} \frac{\partial \bar{p}}{\partial x_j} \right) \\ = - \frac{\partial}{\partial x_i} \left(\overline{\rho' u_i} E^0 + U_i \overline{\rho u_i u_i} + c_p \overline{\rho T' u_i} - \frac{k}{c_p} \frac{\partial E^0}{\partial x_i} \right) \\ - \frac{\partial}{\partial x_i} \left[\mu \left(\frac{1}{Pr} - 1 \right) \frac{\partial}{\partial x_i} \left(\frac{U_i^2}{2} \right) \right] + \chi_0 \quad (6-3b) \end{aligned}$$

$$\begin{aligned} \frac{\partial}{\partial t} (\bar{\rho} \bar{E}) + \frac{\partial}{\partial x_i} (\bar{\rho} \bar{E} U_i) + \frac{\partial}{\partial t} (\overline{\rho' E'}) \\ = - \frac{\partial}{\partial x_i} \left(\overline{\rho u_i E'} + \overline{\rho' u_i \bar{E}} + \overline{\rho' u_i E'} + U_i \overline{\rho' E'} - \frac{k}{c_p} \frac{\partial \bar{E}}{\partial x_i} \right) \\ - \frac{\partial}{\partial x_i} \left[\frac{1}{2} \mu \left(\frac{1}{Pr} - 1 \right) \frac{\partial}{\partial x_i} (U_i^2 + \bar{u}_i^2) \right] + \bar{x} \quad (6-4b) \end{aligned}$$

where $Pr = \mu c_p / k$ is the Prandtl number. The specific heat c_p is taken as constant. Eq. 6-3b and 6-4b become much simpler if $Pr = 1$, and if χ_0 and \bar{x} are negligible.

Since in the incompressible case $\mu = \text{const}$, $Pr = 1$ and $\chi_0 = \bar{x} = 0$, we can reduce Eq. 6-3b and 6-4b respectively to

$$\frac{D}{Dt} (\rho E^0) - \left(\frac{\partial \bar{p}}{\partial t} + \overline{u_j} \frac{\partial \bar{p}}{\partial x_j} \right) = - \frac{\partial}{\partial x_i} \left(U_i \overline{\rho u_i u_i} + c_p \overline{\rho T' u_i} - \frac{k}{c_p} \frac{\partial E^0}{\partial x_i} \right) \quad (6-3c)$$

$$\frac{D}{Dt} (\rho \bar{E}) = - \frac{\partial}{\partial x_i} \left(\overline{\rho u_i E'} - \frac{k}{c_p} \frac{\partial \bar{E}}{\partial x_i} \right) \quad (6-4c)$$

Eq. 6-4c is the well-known equation of turbulent heat transfer in an incompressible flow. Here $\overline{\rho u_i E'}$ is the flux of energy transported by turbulent diffusion.

CHAPTER 3. TURBULENT BOUNDARY LAYER OF A COMPRESSIBLE FLUID

B,7. Introduction. When a fluid flows past the solid boundary of a body, a shear flow results. The condition of no-slip requires that the fluid immediately in contact with the wall be brought to rest. Next to it the fluid is retarded by the internal shear stresses. The retardation decreases with increasing distance from the wall and becomes vanishingly small in

energy diffusion $\partial E^0/\partial x$, or $\partial \bar{E}/\partial x$, if we introduce χ_0 according to Eq. 5-3c and \bar{x} according to Eq. 5-3d. In this way, Eq. 6-3a and 6-4a become respectively

$$\begin{aligned} \frac{D}{Dt} (\bar{\rho} E^0) + U_i \frac{D}{Dt} (\overline{\rho' u_i}) + \frac{D}{Dt} (c_p \overline{\rho T'}) - \left(\frac{\partial \bar{p}}{\partial t} + \overline{u_j} \frac{\partial \bar{p}'}{\partial x_j} \right) \\ = - \frac{\partial}{\partial x_i} \left(\overline{\rho' u_i} E^0 + U_i \overline{\rho u_i u_i} + c_p \overline{\rho T' u_i} - \frac{k}{c_p} \frac{\partial E^0}{\partial x_i} \right) \\ - \frac{\partial}{\partial x_i} \left[\mu \left(\frac{1}{Pr} - 1 \right) \frac{\partial}{\partial x_i} \left(\frac{U_i^2}{2} \right) \right] + \chi_0 \quad (6-3b) \end{aligned}$$

$$\begin{aligned} \frac{\partial}{\partial t} (\bar{\rho} \bar{E}) + \frac{\partial}{\partial x_i} (\bar{\rho} \bar{E} U_i) + \frac{\partial}{\partial t} (\overline{\rho' E'}) \\ = - \frac{\partial}{\partial x_i} \left(\overline{\rho u_i E'} + \overline{\rho' u_i \bar{E}} + \overline{\rho' u_i E'} + U_i \overline{\rho' E'} - \frac{k}{c_p} \frac{\partial \bar{E}}{\partial x_i} \right) \\ - \frac{\partial}{\partial x_i} \left[\frac{1}{2} \mu \left(\frac{1}{Pr} - 1 \right) \frac{\partial}{\partial x_i} (U_i^2 + \bar{u}_i^2) \right] + \bar{x} \quad (6-4b) \end{aligned}$$

where $Pr = \mu c_p / k$ is the Prandtl number. The specific heat c_p is taken as constant. Eq. 6-3b and 6-4b become much simpler if $Pr = 1$, and if χ_0 and \bar{x} are negligible.

Since in the incompressible case $\mu = \text{const}$, $Pr = 1$ and $\chi_0 = \bar{x} = 0$, we can reduce Eq. 6-3b and 6-4b respectively to

$$\frac{D}{Dt} (\rho E^0) - \left(\frac{\partial \bar{p}}{\partial t} + \overline{u_j} \frac{\partial \bar{p}'}{\partial x_j} \right) = - \frac{\partial}{\partial x_i} \left(U_i \overline{\rho u_i u_i} + c_p \overline{\rho T' u_i} - \frac{k}{c_p} \frac{\partial E^0}{\partial x_i} \right) \quad (6-3c)$$

$$\frac{D}{Dt} (\rho \bar{E}) = - \frac{\partial}{\partial x_i} \left(\overline{\rho u_i E'} - \frac{k}{c_p} \frac{\partial \bar{E}}{\partial x_i} \right) \quad (6-4c)$$

Eq. 6-4c is the well-known equation of turbulent heat transfer in an incompressible flow. Here $\overline{\rho u_i E'}$ is the flux of energy transported by turbulent diffusion.

CHAPTER 3. TURBULENT BOUNDARY LAYER OF A COMPRESSIBLE FLUID

B,7. Introduction. When a fluid flows past the solid boundary of a body, a shear flow results. The condition of no-slip requires that the fluid immediately in contact with the wall be brought to rest. Next to it the fluid is retarded by the internal shear stresses. The retardation decreases with increasing distance from the wall and becomes vanishingly small in

B · TURBULENT FLOW

a relatively short distance. The layer in which this occurs is called the boundary layer. A knowledge of the flow behavior within this layer is of prime importance, especially when effects associated with compressibility and aerodynamic heating come into play.

The turbulent boundary layer occurs more generally than the laminar boundary layer, but is less well understood theoretically. The exceedingly complex character of turbulent flow and the inadequacy of theories of turbulence make an exact mathematical treatment of the flow impossible at present. Therefore a great number of approximations are necessary, and it is to be expected that the various proposed theories may turn out different results which are not always reconcilable. In order to clarify many obscure points in the theories, and to display in a simple manner the essential physical features governing boundary layer flow, it seems worthwhile to outline the main approaches of the analytical treatments, and especially to elucidate the bases and assumptions underlying the theories. Where possible the theoretical results will be compared with existing experimental results.

First the fundamental hydrodynamic equations, as developed earlier, will be simplified in Art. 8 under the special conditions of the boundary layer. Consequently some simple relations between pressure, temperature, and velocity can be derived in Art. 9. These will at once show some features of heat transfer in the boundary layer, and especially of the recovery factor, without going into the turbulent transport processes. For a deeper understanding of the problems, some statistical methods of transport phenomena become necessary. Existing theories make extensive use of the concept of mixing length as a parameter of the turbulent exchange of properties. Since several fundamental questions arise in connection with the application of mixing length to various types of transport (mass, momentum, and heat) governing the boundary layer, and in the analogy theories between heat transfer and skin friction (the so-called Reynolds analogy), the statistical foundation of the transport processes will be studied in Art. 10. As an immediate application, the Reynolds analogy can be better understood and will be treated in Art. 11.

Theories relating to velocity profiles in a compressible turbulent boundary layer do not seem to differ much from the corresponding theories for the incompressible boundary layer, especially concerning their basis and method of attack. Therefore we shall reserve these for Chap. 4 where incompressibility is assumed, and be content here to give only some experimental data on the velocity distribution.

The skin friction in a compressible boundary layer deserves special attention, because of its important compressibility effect and its practical significance. The basis of the theories will be described in Art. 12; the empirical formulas illustrating the essential behavior of skin friction will be given in Art. 13; and finally the comparison between theories and

experiments will be given in Art. 14. Since no unique theory has evolved, the emphasis will be placed on the description and discussion of the bases and assumptions underlying the theoretical treatments rather than their detailed analysis. Experimental data will be compared with theories. This method of approach seems best to show the present state of the subject and to serve as a guide to future theoretical and experimental investigations.

B.8. Fundamental Equations of Motion of a Compressible Boundary Layer. When applying the hydrodynamic equations of Art. 4, 5, and 6 to the boundary layer developed on a flat plate with steady free stream velocity, certain simplifying approximations may be made. First of all, the mean flow is assumed two-dimensional with mean velocities denoted by U and V in the x and y directions respectively, where x is the coordinate parallel to the plate, measured from the leading edge, and y is normal to the wall. The turbulence is still three-dimensional, with components u , v , and w in the x , y , and z directions.

We now consider the order of magnitude of terms involved in the hydrodynamic equations. If U is taken as a magnitude of standard order $O(1)$, and the thickness of the boundary layer δ is small compared to the distance x , it follows that $\partial/\partial t$, $\partial/\partial x$, $\partial^2/\partial x^2 \sim O(1)$, and $\partial/\partial y \sim O(\delta^{-1})$, $\partial^2/\partial y^2 \sim O(\delta^{-2})$. Also we assume that $V \sim O(\delta)$, the mean density $\bar{\rho}$ is $O(1)$, and the total energy content per unit mass \bar{E} is $O(1)$. If the viscous term of Eq. 4-5 is to be at most of the same order as the remaining terms, then it follows that μ is at most of the order of δ^2 . By the same reasoning, the correlations involving u , v , ρ' , T' , such as \bar{uv} , $\bar{uT'}$; $\bar{vT'}$; $\bar{\rho'u}$, $\bar{\rho'v}$, $\bar{\rho'T'}$, are at most of the order of δ , while the triple correlation $\rho'uv$ will be at most of the order of δ^2 .

Retaining the predominant terms of the same order of magnitude, we can easily reduce the dynamic equations (Eq. 4-5, 4-6, and 6-4a) respectively to the following forms:

$$\frac{\partial}{\partial t} (\bar{\rho} U) + \frac{\partial}{\partial x} (\bar{\rho} U^2) + \frac{\partial}{\partial y} (\bar{\rho} UV) = - \frac{\partial \bar{p}}{\partial x} + \frac{\partial}{\partial y} \left(\mu \frac{\partial U}{\partial y} - \bar{\rho} \bar{uv} - U \bar{\rho}'v \right) \quad (8-1)$$

$$- \frac{\partial \bar{p}}{\partial y} - \frac{\partial}{\partial y} (\bar{\rho} v^2) = 0 \quad (8-2)$$

$$\frac{\partial \bar{\rho}}{\partial t} + \frac{\partial}{\partial x} (\bar{\rho} U) + \frac{\partial}{\partial y} (\bar{\rho} V) + \frac{\partial}{\partial y} (\bar{\rho}'v) = 0 \quad (8-3)$$

$$\begin{aligned} \frac{\partial}{\partial t} (\bar{\rho} \bar{E}) + \frac{\partial}{\partial x} (\bar{\rho} \bar{E} U) + \frac{\partial}{\partial y} (\bar{\rho} \bar{E} V) \\ = \frac{\partial}{\partial y} \left(\frac{\partial \bar{E}}{\partial y} - \bar{\rho} v \bar{E}' - \bar{\rho}' v \bar{E} \right) + \frac{\partial}{\partial y} \left[\left(\frac{1}{Pr} - 1 \right) \mu \frac{\partial (c_p T)}{\partial y} \right] \end{aligned} \quad (8-4)$$

B · TURBULENT FLOW

Similarly from Eq. 6-3a with the same order of approximations we obtain

$$\begin{aligned}\frac{\partial}{\partial t} (\bar{\rho} E^0) + \frac{\partial}{\partial x} (\bar{\rho} E^0 U) + \frac{\partial}{\partial y} (\bar{\rho} E^0 V) &= \frac{\partial}{\partial y} \left(\mu \frac{\partial E^0}{\partial y} - \bar{\rho} v \bar{E}' - \bar{\rho}' v E^0 \right) \\ &\quad + \frac{\partial}{\partial y} \left[\left(\frac{1}{Pr} - 1 \right) \mu \frac{\partial}{\partial y} (c_p \bar{T}) \right] + \bar{\rho} \bar{u} \bar{v} \frac{\partial U}{\partial y} \quad (8-5)\end{aligned}$$

Except for the production term $\bar{\rho} \bar{u} \bar{v} \partial U / \partial y$, Eq. 8-4 and 8-5 have the same form. In the following we shall be concerned with Eq. 8-4 rather than Eq. 8-5.

Eq. 8-1, 8-2, 8-3, 8-4, and 8-5 form a system of basic equations of the compressible boundary layer. The effects of the density fluctuation are to contribute an additional Reynolds stress, an apparent source, and an additional eddy conductivity respectively in the equations of momentum, continuity, and energy.

B,9. Relationships between Velocity, Pressure, and Temperature Distributions. Some simple relations are now derived for velocity, pressure, and temperature by integrating the momentum and energy equations. This is done here without entering into the mechanism of turbulence in the boundary layer. We consider a steady boundary layer, with strictly parallel flow (all average quantities depend only on the coordinate y).

First by integrating the momentum equation (Eq. 8-2) from y to δ , where δ is the thickness of the boundary layer, we obtain

$$\begin{aligned}\bar{p} &= \bar{p}_* + \bar{\rho} \bar{v}^2 \\ &= \bar{p}_* \left(1 + \gamma M_*^2 \frac{\bar{\rho} \bar{v}^2}{\bar{\rho}_* \bar{U}_*^2} \right) \quad (9-1)\end{aligned}$$

since $M_*^2 = \rho_* U_*^2 / \gamma \bar{p}_*$. Here quantities without subscript are taken at the coordinate y , while subscript $*$ denotes the quantity at the edge of the boundary layer. For future reference, superscript 0 denotes the total or stagnation value, and subscript w denotes the value at the wall ($y = 0$). The assumption of a constant pressure within the boundary layer is valid if the free stream Mach number is of the order of $O(1)$, and if the previous assumption of small turbulence level ($\bar{v}^2 / U^2 \ll 1$) is made.

For the derivation of energy relations, the following conventional boundary conditions are used:

$$\text{At } y = 0: \quad U = 0, V = 0, u = 0, v = 0, w = 0, \bar{T} = T_w \quad (9-2a)$$

$$\text{At } y = \delta: \quad U = U_*, \bar{T} = T_* \quad (9-2b)$$

If $Pr = 1$ is assumed, the energy equation (Eq. 8-4) takes the form

$$\frac{\partial}{\partial y} \left(\mu \frac{\partial \bar{E}}{\partial y} - \bar{\rho} \bar{E}' v - \bar{E} \bar{\rho}' v \right) = 0 \quad (9-3a)$$

This is similar to the momentum equation (Eq. 8-1), rewritten as follows:

$$\frac{\partial}{\partial y} \left(\mu \frac{\partial \bar{U}}{\partial y} - \bar{\rho} \bar{u} \bar{v} - \bar{U} \bar{\rho}' \bar{v} \right) = 0 \quad (9-3b)$$

Further from the equation of continuity, Eq. 8-3, we have $\bar{\rho}' \bar{v} = \text{const}$. Therefore a comparison between Eq. 9-3a and 9-3b leads to the following linear relationship between \bar{E} and \bar{U} :

$$\bar{E} = c_p \bar{T} + \frac{1}{2} \bar{U}^2 + \frac{1}{2} (\bar{u}^2 + \bar{v}^2 + \bar{w}^2) = c_p T_*^0 \left[(1 - \eta) \frac{\bar{U}}{U_*} + \eta \right] \quad (9-4)$$

where the constant T_*^0 and η , as determined by the boundary conditions (Eq. 9-2a and 9-2b), are

$$\begin{aligned} \eta &= T_* / T_*^0 \\ c_p T_*^0 &= c_p T_* + \frac{1}{2} U_*^2 \end{aligned}$$

T_*^0 is the stagnation temperature at $y = \delta$. If we neglect as usual the turbulent intensity in Eq. 9-4, we obtain the approximate relation

$$c_p \bar{T} + \frac{1}{2} \bar{U}^2 = c_p T_*^0 \left[(1 - \eta) \frac{\bar{U}}{U_*} + \eta \right] \quad (9-5)$$

Eq. 9-5 gives a relation between \bar{T} and \bar{U} on the basis that the *laminar* Prandtl number is unity. Some authors have derived the same relation requiring that the turbulent Prandtl number should also be unity (see e.g. [8]), but the latter condition is superfluous according to the above considerations.

Eq. 9-5 gives the temperature-velocity relationship including heat transfer. If the wall is insulated, we must have

$$\left(\frac{\partial \bar{T}}{\partial y} \right)_w = 0 \quad (9-2c)$$

but, according to Eq. 9-5,

$$\frac{\partial \bar{T}}{\partial y} + \frac{U}{c_p} \frac{\partial \bar{U}}{\partial y} = \frac{T_*^0}{U_*} (1 - \eta) \frac{\partial \bar{U}}{\partial y} \quad (9-6)$$

and since in general $(\partial \bar{U} / \partial y)_w \neq 0$, the condition (Eq. 9-2c) imposed upon Eq. 9-6 requires that

$$\eta = 1$$

hence Eq. 9-5 simplifies to the following form:

$$c_p \bar{T} + \frac{1}{2} \bar{U}^2 = c_p T_* \quad (= \text{const}) \quad (9-7)$$

Bereitgestellt von | Technische Universität Braunschweig

Angemeldet

Heruntergeladen am | 10.02.18 10:00

Heute (19.)

B · TURBULENT FLOW

with an insulated wall. We conclude that for $Pr = 1$, the relationships between temperature and velocity in the turbulent boundary layer are the same as those in the laminar boundary layer, which were first obtained by Crocco [9].

In an insulated boundary layer at low speeds, Squire [10] and Ackerman [11] have independently deduced the formula

$$c_p T_w = c_p T_\infty + \frac{1}{2} Pr^{\frac{1}{2}} U_\infty^2 \quad (9-8)$$

for $Pr \neq 1$ or $Pr = 1$. Here T_w is the temperature at the wall. When there is no heat transfer, T_w is sometimes called equilibrium temperature. This formula may be expected to be not seriously in error at high speeds, and includes Eq. 9-7 as a special case with $Pr = 1$. As $Pr < 1$ in general, the temperature at the wall is accordingly smaller than the total free stream temperature.

In the light of Eq. 9-4, a more general formula for the case of $Pr \neq 1$ can be written as follows:

$$c_p T_w = c_p T_\infty + \frac{1}{2} r_e U_\infty^2 \quad (9-9a)$$

by introducing a factor r_e , called the *recovery factor*. The recovery factor can then be considered as defined by Eq. 9-9a, and it then becomes

$$r_e = \frac{T_w - T_\infty}{T_\infty^0 - T_\infty} \quad (9-9b)$$

Using the adiabatic relation $T_\infty^0/T_\infty = 1 + (\gamma - 1)M_\infty^2/2$,

$$r_e = \frac{\left(\frac{T_w}{T_\infty^0}\right)\left(1 + \frac{\gamma - 1}{2} M_\infty^2\right) - 1}{\frac{\gamma - 1}{2} M_\infty^2} \quad (9-9c)$$

Here M_∞ is the Mach number at the edge of the boundary layer, and γ is the ratio of specific heats. According to Eq. 9-8 and 9-9, the recovery factor should not differ very much from the value

$$r_e = Pr^{\frac{1}{2}} \quad (9-10)$$

The turbulent recovery factor, which shows a close agreement with Eq. 9-10, has been measured by Mack [12] over the surface of a cone, in the range of free stream Mach number from 1.33 to 4.50, to be 0.88 ± 0.01 , as compared with the calculated value of $Pr^{\frac{1}{2}} = 0.89$, based on the recovery temperature. Experiments for a flat plate have been made by Stalder, Rubesin, and Tendeland [13] ($r_e = 0.89 \pm 0.01$) at Mach number 2.4. Also the measurements of the laminar recovery factor show a close agreement with the theoretical value of $Pr^{\frac{1}{2}}$. The experimental results of various investigations are summarized in Fig. B,9a and B,9b.

In general the recovery factor depends on the Reynolds number. In

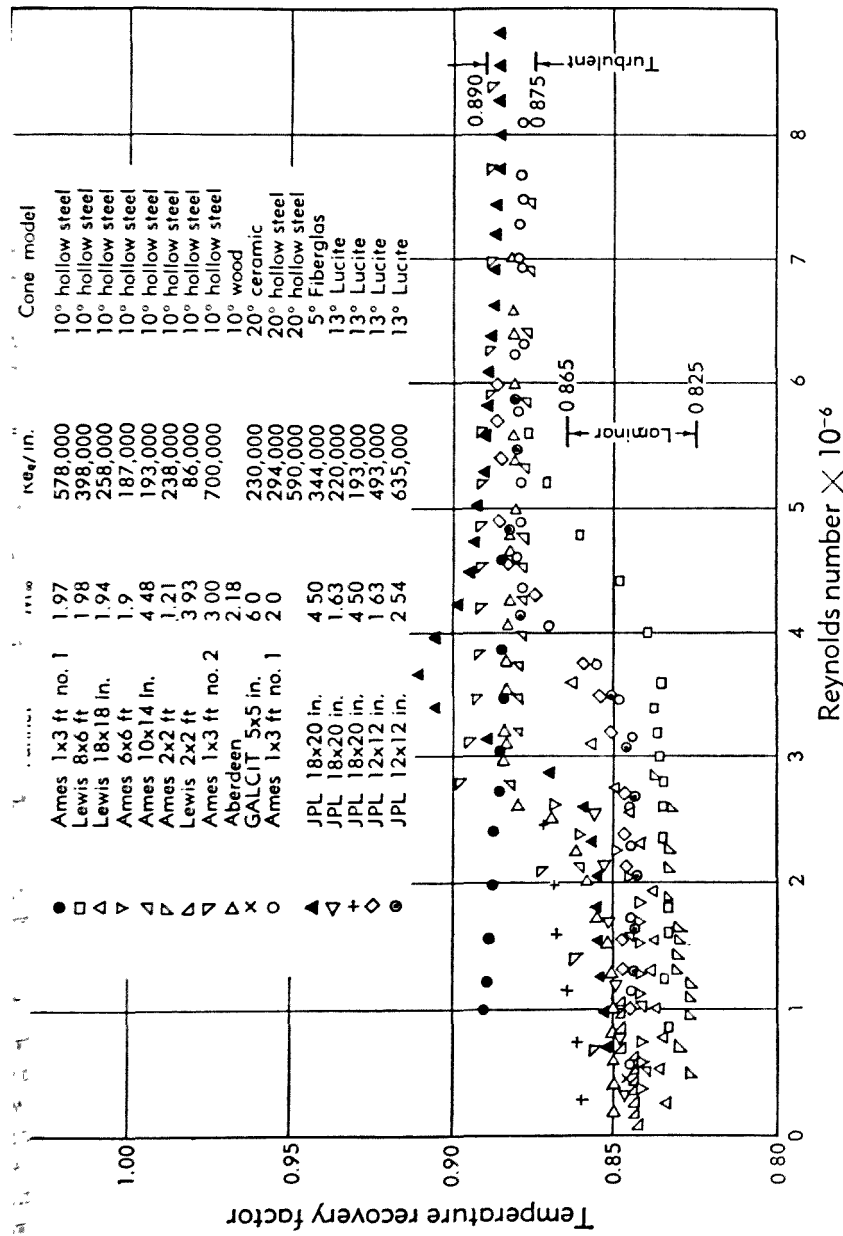


Fig. B.9a. Variation of the temperature recovery factor of cones with the Reynolds number, after Mack [12]. The Reynolds number R is based upon the distance from the cone tip and on the conditions at the edge of the boundary layer.

B · TURBULENT FLOW

in the transition region, the recovery factor varies from the lower laminar value to the higher turbulent value. An increase of the turbulent recovery factor with the Reynolds number in the fully turbulent region predicted by the theoretical formula of Seban [14],

$$r_* = 1 - (4.71 - 4.11B - 0.601Pr)Re^{-0.2}$$

$$B = \frac{Pr}{2} \frac{5Pr + 7}{5Pr + 1}$$

and the theoretical formula of Shirokow [15],

$$r_* = 1 - 4.55(1 - Pr)Re^{-0.2}$$

is not systematically detectable from the experimental results of Fig. B.9a and B.9b. Here Re is the Reynolds number based on the distance

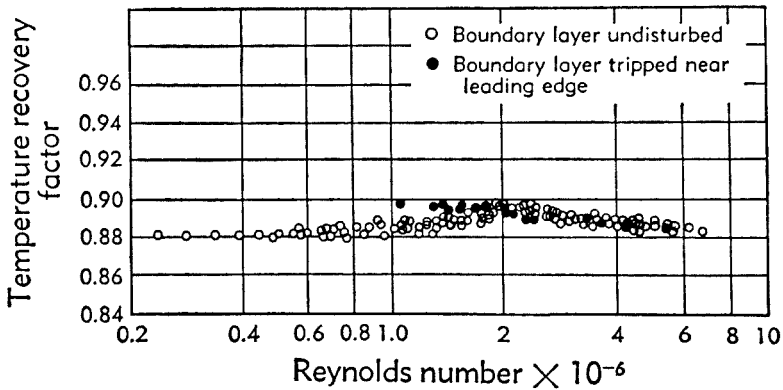


Fig. B.9b. Variation of the temperature recovery factor with the Reynolds number in the case of a flat plate, after Stalder, Rubesin, and Tendeland [13], $M_\infty = 2.4$. The Reynolds number xU_∞/ν_∞ is based on the conditions at the edge of the boundary layer and on the distance from the leading edge.

from a leading edge. There is probably also some slight variation of the recovery factor with the Mach number. The measurements of Mack [12] show a slight increase of the recovery factor with the Mach number, while those of Stine and Scherrer [16] show no variation. The Mach number effect predicted by the theoretical formula of Tucker and Maslen [17],

$$r_* = Pr^m$$

$$m = \frac{N + 1 + 0.528M^2}{3N + 1 + M^2}$$

$$N = 2.6 Re^{1/4}$$

is not yet verified by experiments. According to Fig. B.9a and B.9b, the turbulent recovery factors on cones and flat plates are of the same order,

while the laminar recovery factors on plates are higher than those on cones and other models. These high values of the recovery factor can be attributed to heat conduction effects in the leading edge region of the flat plate.

The foregoing relations between temperature and velocity will be referred to in Art. 12 in connection with the relation between the temperature profile and the velocity profile. If $Pr = 1$, the relations become especially simple, as shown by Eq. 9-5 with heat transfer and by Eq. 9-7 without heat transfer. If $Pr \neq 1$, the viscous dissipation and the heat conduction render such a general relationship between temperature and

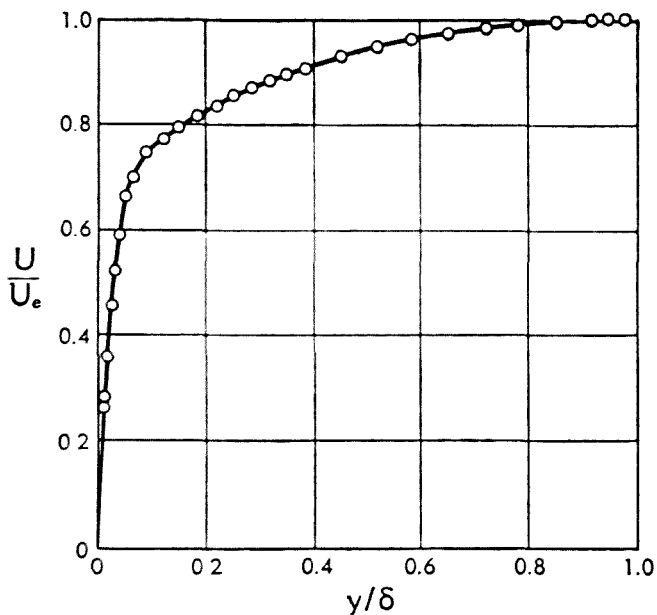


Fig. B,9c. Velocity profile across turbulent boundary layer. The free stream Mach number is 4.93 and there is no heat transfer. The data are drawn after Lobb, Winkler, and Persh [18] and private communications.

velocity very difficult, and a basic approach to the problem must involve the detailed mechanism of turbulence. However, without turning to this approach a relation between the temperature at the wall and the velocity and temperature at $y = \delta$ was made possible by introducing a recovery factor r_s . For no heat transfer such a relation was found to be that of Eq. 9-9a, and this agreed rather well with measurements. The question may be asked as to what form the relation might take if it were generalized to include the heat transfer and to cover all positions in the boundary layer. To this end and by similar reasoning, we could introduce a variable recovery factor $r(y)$ which satisfies Eq. 9-9a at the limit and becomes $r(y) = 1$ for $Pr = 1$. It is expected that a relation between T^0 and T_w

B · TURBULENT FLOW

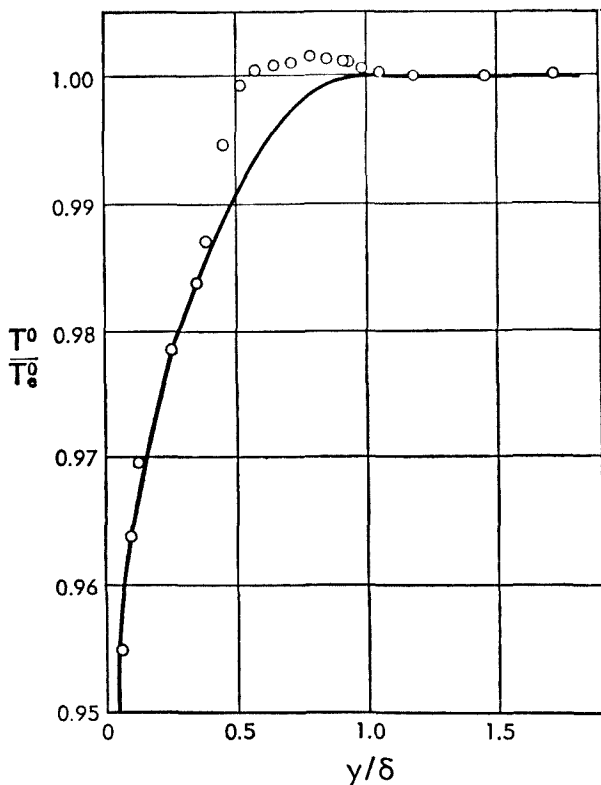


Fig. B.9d. Total temperature profile across turbulent boundary layer. The free stream Mach number is 4.93 and there is no heat transfer. The experimental data in circles are drawn after Lobb, Winkler, and Persh [18] and private communications. The curve is drawn according to Eq. 9-12, by assuming equal thickness of boundary layers for U and T .

could then be formulated predicting that T^0/T_e^0 increases as $(U/U_e)^2$ increases. With this in view we shall introduce a variable recovery factor $r(y)$ and write by analogy to Eq. 9-7,

$$c_p \bar{T} + \frac{1}{2}r(y)U^2 = c_p T_e + \frac{1}{2}r_e U_e^2 \equiv c_p T_w \quad (9-11)$$

Here it is assumed that the heat conduction through the wall is absent, i.e. $(\partial \bar{T} / \partial y)_w = 0$, but Pr may be arbitrary. Eq. 9-11 gives $T^0(y)$ in terms of $U(y)$ as follows:

$$\frac{T^0}{T_e^0} = \frac{T_w}{T_e^0} + \left(1 - \frac{T_w}{T_e^0}\right) \alpha \left(\frac{U}{U_e}\right)^2 \quad (9-12)$$

with

$$\alpha = \frac{r(y) - 1}{r_e - 1}$$

For a velocity distribution given by Fig. B,9c, the curve in Fig. B,9d shows the distribution of T^0/T_e^0 given by Eq. 9-12 when it is assumed as a rough approximation that $\alpha = 1$. On the same figure are shown the measurements of Lobb, Winkler, and Persh [18]. Fig. B,9e shows the measurements of van Driest [19] and Spivack [20]. Both figures suggest that T^0/T_e^0 passes through a maximum value in excess of unity, the indication of this being most pronounced in Fig. B,9e. This phenomenon cannot be explained from the above considerations unless a proper distribution of $r(y)$ is taken into account.

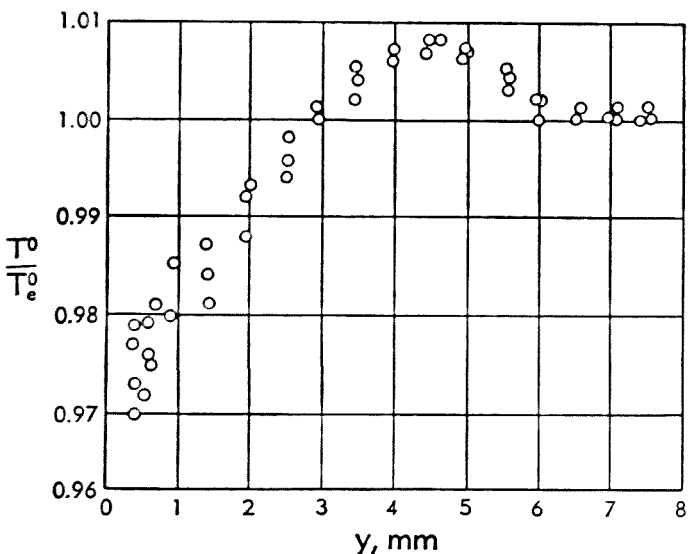


Fig. B,9e. Total temperature profile across turbulent boundary layer at free stream Mach number 2.8. The data are from Spivack [20] with an axial distance from throat of 12.96 inches.

B,10. Phenomena of Transport of Properties in a Turbulent Fluid. Up to the present we have dealt with the mean turbulent flow and certain simple relationships between mean quantities. For the latter, analogies were employed rather than procedures based on a mechanism of turbulence. Since the superficial nature of this approach is apparent, it becomes advisable to look into the physical transport processes of turbulence which are embodied in transport terms like \bar{w} , $\bar{\rho}v$, $\bar{T'v}$, etc., of the fundamental equations obtained in Art. 8. They represent the mean rate of transfer of u , ρ' , and T' respectively, across a unit area perpendicular to y . One of the major aims of turbulent theory is to find a method of calculating these transport terms directly from the hydrodynamic equations governing the turbulent motion (Eq. 4-3, 4-4, and 6-1). At present the difficulties of the theories make such a program not yet possible.

B · TURBULENT FLOW

The other approach is to regard the statistical effect of turbulence on the mean flow as being similar to that of molecular viscosity or heat conduction, so that the turbulent transport terms can be treated by the same statistical methods as those applied to transport processes in non-turbulent motions. To this end, and as a basis of the statistical theory of transport processes by molecular motions in a gas, we use the Boltzmann equation

$$\frac{\partial f}{\partial t} + \xi_i \frac{\partial f}{\partial x_i} + X_i \frac{\partial f}{\partial \xi_i} = \frac{\delta f}{\delta t} \quad (10-1)$$

where $\delta f / \delta t$ is a symbol representing the collision integral, $f(t, \mathbf{x}; \boldsymbol{\xi}) d\mathbf{x}d\boldsymbol{\xi}$ is the number of particles in the space and velocity elements $d\mathbf{x}d\boldsymbol{\xi}$ at the instant t ; \mathbf{x} and $\boldsymbol{\xi}$ are the vectors of position and velocity, \mathbf{X} is the external force per unit mass. The left-hand side of Eq. 10-1 represents the rate of increase in time of the number of particles in the phase element $d\mathbf{x}d\boldsymbol{\xi}$ when we move together with the particles in the phase space $\mathbf{x}, \boldsymbol{\xi}$. The right-hand side represents the effect of restoring and direct collisions which throw the particles respectively in and out of the phase element.

A consequence of the Boltzmann equation is the equation of evolution of a transferable property $\Phi(t, \mathbf{x})$ defined by

$$\Phi(t, \mathbf{x}) = \frac{\int d\boldsymbol{\xi} \phi(\boldsymbol{\xi}) f}{\int d\boldsymbol{\xi} f} \quad (10-2)$$

where $\phi(\boldsymbol{\xi})$ is a function of the random velocity $\boldsymbol{\xi}$. As special cases it is interesting to put $\phi = 1, \xi_i, \frac{1}{2}\xi_i^2$, thus obtaining from Eq. 10-1 and 10-2 the general hydrodynamic equations

$$\left. \begin{aligned} \frac{\partial \bar{\rho}}{\partial t} + \frac{\partial}{\partial x_i} (\bar{\rho} U_i) &= 0 \\ \bar{\rho} \frac{D U_i}{D t} \equiv \bar{\rho} \left(\frac{\partial U_i}{\partial t} + U_j \frac{\partial U_i}{\partial x_j} \right) &= \bar{\rho} X_i + \frac{\partial \sigma_{ij}}{\partial x_j} \\ \bar{\rho} \frac{D I}{D t} - \frac{\partial q_i}{\partial x_i} &= \sigma_{ij} \epsilon_{ij} - \bar{\rho} U_i X_i \end{aligned} \right\} \quad (10-3)$$

Here the density $\bar{\rho}$, the speed U_i , and the internal thermal energy per unit volume I are defined by the mean values

$$\bar{\rho} = m \int f d\boldsymbol{\xi} = mn$$

$$U_i = \frac{1}{n} \int \xi_i f d\boldsymbol{\xi} = \xi_i$$

$$I = \frac{1}{2} \bar{C}_i^2$$

where $C_i = \xi_i - U_i$ is the thermal velocity and m is mass. The mean values of high powers of C_i are

$$\sigma_{ij} = -\bar{\rho} \bar{C}_i \bar{C}_j = \text{stress tensor}$$

$$q_i = -\frac{1}{2} \bar{\rho} \bar{C}_i \bar{C}_j^2 = \text{thermal flux}$$

I is the internal energy, which is equal to $C_i \bar{T}$ for an ideal gas, and finally

$$\epsilon_{ij} = \frac{1}{2} \left(\frac{\partial U_i}{\partial x_j} + \frac{\partial U_j}{\partial x_i} \right)$$

Eq. 10-3 express the conservation of mass, momentum, and energy respectively. In order to express the quantities σ_{ij} and q_i in terms of the macroscopic quantities $\bar{\rho}$, U_i , and \bar{T} (or I) we have to investigate further the Boltzmann equation (Eq. 10-1). Because it is nonlinear in character, it can only be solved by approximations. For the detailed calculations, reference may be made to the textbook of Chapman and Cowling [21]. As a first approximation it is found that

$$\begin{aligned} \sigma_{ij} &= -p \delta_{ij} + 2\mu(\epsilon_{ij} - \frac{1}{3}\epsilon_{kk}\delta_{ij}) \\ q_i &= k \frac{\partial \bar{T}}{\partial x_i} \end{aligned} \quad (10-4)$$

where μ and k are found as functions of T and depend on the collision cross section. With this approximation, the second equation of Eq. 10-3 becomes the Navier-Stokes equation of motion.

In particular, for a transport in the y direction of a property which either is a scalar, or has a component in the x direction, Eq. 10-4 reduce to

$$\begin{aligned} \sigma_{xy} &= -\bar{\rho} \bar{\xi}_x \bar{C}_y = \mu \frac{\partial U}{\partial y} \\ q_x &= -\bar{\rho} \frac{1}{2} \bar{C}_x^2 \bar{C}_y = \frac{k}{c_p} \frac{\partial I}{\partial y} \end{aligned} \quad (10-5)$$

or, in general, the laminar flux of the transport J of a transferable property Φ , which is the momentum or temperature in Eq. 10-5, can be written in the following form:

$$J_{lam} = D_{lam} \frac{\partial \Phi}{\partial y} \quad (10-6)$$

where D_{lam} is a laminar phenomenological coefficient equal to the coefficient of viscosity in the case of transport of momentum, and to the coefficient of heat conduction in the case of the transport of heat.

When we deal with turbulent transport, it is necessary to replace the concept of the molecular collisions by the turbulent exchanges between uid elements. Similarly the thermal velocity C_i is replaced by the velocity u_i of turbulent motions. If the property Φ is to be transferred by

B · TURBULENT FLOW

these motions, then it is to be expected, by analogy with Eq. 10-5 and 10-6, that a turbulent flux will result in the form

$$J = -\bar{\rho}\Phi v = D \frac{\partial \Phi}{\partial y}$$

where J is turbulent flux, v is the turbulent velocity in the direction y , and D is turbulent coefficient of transport. In general the transport coefficient D may depend upon a number of unknown factors among which are the property to be transferred, and the intensity and scale of the turbulent motion. For example, its value may vary according to whether we have a transport of momentum, heat, or matter. A knowledge of its structure necessitates a detailed investigation of the basis of the turbulent exchange term by a procedure analogous to that which yielded the exchange coefficients μ and k of Eq. 10-4 from the solution of the complete Boltzmann equation including the collision term. It is hoped that some insight into the essential structure of the turbulent transport can be gained by proceeding in this way on a somewhat simplified basis made possible by adopting an approximate form of the Boltzmann equation. When applied to turbulent motion, the right-hand side of Eq. 10-1 represents the effects of the turbulent exchanges on the distribution function. It can be regarded as a forcing term which distorts the distribution from its equilibrium. Therefore we can write Eq. 10-1 approximately as follows:

$$\frac{Df}{Dt} = -\kappa(f - f_{eq}) \quad (10-7)$$

where f is the nonequilibrium distribution, f_{eq} is the equilibrium distribution, and κ depends on the efficiency of the turbulent mixing. The idea of writing such a simple relaxation type of exchange term in Eq. 10-7 in the place of the complete collision integral in Eq. 10-1 is not new. Lorentz [22], Van Vleck and Weisskopf [23] had initiated such a simplification in their study of microwave line shapes. Later Bhatnagar, Gross, and Krook [24] applied an essentially similar simplification for studying the collision processes in gases. According to Eq. 10-2 and 10-7, we can write

$$\frac{d\Phi}{dt} = -\kappa(\Phi - \bar{\Phi}) \quad (10-8)$$

Here $\Phi - \bar{\Phi}$ is the fluctuation of the transferable property. Eq. 10-8 can be used to find the evolution of the property Φ carried by a lump of fluid when the latter moves and mixes with its surroundings.

Being given $\bar{\Phi}$, the value of Φ at any instant t is given by the integral of Eq. 10-8 as follows:

$$\Phi(t) = \kappa \int_0^\infty d\tau e^{-\kappa\tau} \bar{\Phi}(t - \tau) \quad (10-9a)$$

where $\Phi(t - \tau)$ is the mean value of the property Φ when the lump of fluid carrying Φ found itself at the instant $t - \tau$. It can be expanded into series as follows:

$$\Phi(t - \tau) = \Phi(t) - \frac{\partial \Phi(t)}{\partial y} \int_{t-\tau}^t dt' v(t') \quad (10-9b)$$

where the integral term is the displacement of the lump of fluid in the interval of time τ . The expansion is valid when the lump of fluid makes only *small displacements* and when it is assumed that Φ is stationary, but nonuniform.

After substitution for $\Phi(t - \tau)$, Eq. 10-9a becomes

$$\Phi(t) = \Phi - \frac{\partial \Phi}{\partial y} \kappa \int_0^\infty d\tau e^{-\kappa\tau} \int_{t-\tau}^t dt' v(t')$$

The double integral is

$$\begin{aligned} \kappa \int_0^\infty d\tau e^{-\kappa\tau} \int_{t-\tau}^t dt' v(t') &= \kappa \int_0^\infty d\tau e^{-\kappa\tau} \int_0^\tau dt'' v(t - t'') \\ &= \kappa \int_0^\infty dt'' v(t - t'') \int_{t''}^\infty d\tau e^{-\kappa\tau} \\ &= \int_0^\infty dt'' e^{-\kappa t''} v(t - t'') \end{aligned}$$

Thus

$$\Phi(t) = \Phi(t) - \frac{\partial \Phi(t)}{\partial y} \int_0^\infty dt'' e^{-\kappa t''} v(t - t'')$$

Hence the flux for the transport of Φ is:

$$J \equiv -\bar{\rho} \bar{\Phi} v = \bar{\rho} \frac{\partial \Phi(t)}{\partial y} \int_0^\infty dt'' e^{-\kappa t''} \overline{v(t - t'')} v(t) \quad (10-10a)$$

Consequently the turbulent coefficient of transport D is found as follows:

$$D = \int_0^\infty dt'' e^{-\kappa t''} \overline{v(t - t'')} v(t) \quad (10-10b)$$

The transport coefficient D in Eq. 10-10 depends on the autocorrelation function of velocities $\overline{v(t - t'')} v(t)$ and on κ . In its turn κ depends on a number of factors among which is the property to be transferred. This entails that D may differ according to the nature of properties to be transferred, i.e. heat, momentum, particles, etc.

Now we shall compare this result with the concept of mixing length, so often used in the study of the turbulent motion. By analogy with the kinetic theory of gases one may suppose that there is a length l , which represents the distance traveled by the lump of fluid between the instant when it was freed from its surroundings carrying with it the mean property of these surroundings, and the instant when it arrives in a

B · TURBULENT FLOW

new layer where it is supposed to mix with the new surrounding fluid. In this case, the transport coefficient is $\bar{v}l$, which can be written in the integral form

$$\bar{v}l = \int_0^{\infty} dt'' \overline{v(t-t'')} v(t) \quad (10-11)$$

if the correlation of velocities converges. Eq. 10-11, based on the mixing length, does not distinguish between the transport of heat, momentum, and matter, because the same length is intrinsically implied in all cases.

As an illustration, Eq. 10-10 may be applied to the special case of transport of momentum and heat along the y direction. We then obtain

$$\tau = -\bar{\rho}\overline{uv} = \bar{\rho}D_u \frac{\partial U}{\partial y} \quad (10-12)$$

$$q = -\bar{\rho}c_p\overline{T'v} = \bar{\rho}c_p D_h \frac{\partial \bar{T}}{\partial y}$$

where τ is the turbulent shear stress, q is the rate of turbulent transport of heat, and D_u and D_h are respectively the transport coefficients of momentum and heat defined by Eq. 10-10b. The coefficients are commonly termed "turbulent exchange coefficients."

The results (Eq. 10-12) can be compared with the Boussinesq formulas of turbulent transport of momentum and heat, written usually in the following form:

$$\begin{aligned} \tau &= \epsilon_\mu \frac{\partial U}{\partial y} \\ q &= \epsilon_k \frac{\partial \bar{T}}{\partial y} \end{aligned} \quad (10-13)$$

where ϵ_μ is the eddy viscosity and ϵ_k is the eddy heat conductivity, introduced by formal analogy to the corresponding laminar viscosity and heat conductivity of the Navier-Stokes and Fourier equations. Eq. 10-13 give neither the structure of the exchange coefficients nor the basis of the transfer. However, they can be made completely identical in form with Eq. 10-12, if the following expressions are assigned to ϵ_μ and ϵ_k

$$\epsilon_\mu = \bar{\rho}D_u$$

$$\epsilon_k = \bar{\rho}c_p D_h$$

The ratio

$$\frac{D_u}{D_h} = \frac{\epsilon_\mu c_p}{\epsilon_k} \equiv Pr_t$$

is called the turbulent Prandtl number by analogy to the laminar Prandtl number introduced in Eq. 6-4b. We see that the mixing length theory

(Eq. 10-11), which implies $D_u = D_k$, predicts a turbulent Prandtl number of unity. However, experiments show that Pr_t is about 0.7, a value very close, incidently, to the laminar Prandtl number for air.

The fact that the turbulent Prandtl number, as given by the ratio D_u/D_k , is different from unity is interesting and indicates that Eq. 10-10b, rather than the mixing length formula (Eq. 10-11), should be more correct. However, due to the simplification introduced in the transport equation (Eq. 10-7), the parameter κ is not determined in terms of the transferable property, so that the numerical value of the ratio of the two exchange coefficients cannot be computed from Eq. 10-10b alone. An auxiliary equation is needed to determine the transfer of property, for example, heat or particles, under the action of a turbulent fluid. In the case of the transfer of particles, such an equation may govern the motion of a small spherical particle suspended in a turbulent fluid. On the basis of it, the velocity correlation for the particles can be computed in terms of the velocity correlation of the ambient fluid or vice versa, and hence the ratio of the two exchange coefficients can be obtained. This has been done by Tchen [25], and, for the case of $\kappa = 0$, it has been found that the exchange coefficient of particles is equal to that of the fluid (Eq. 10-11). This case is not surprising, since consistently the relaxation is neither involved in the motion of the fluid nor in the motion of the particles, and no difference in exchange coefficients should exist, as already revealed by the simple theory of Eq. 10-10b. The ratio of the two exchange coefficients for the case of $\kappa \neq 0$ has not yet been studied on this basis. Several authors are concerned with such difficulties of diffusion phenomena, see e.g. [25] and the Burgers lecture on the turbulent fluid motion [26].

In the integrand of Eq. 10-10b, the exponential term can be considered as a retarding effect of the relaxation between the equilibrium and nonequilibrium distribution in the transport phenomena (Eq. 10-8). Hence the complete integrand of Eq. 10-10b can be considered as a correlation corrected for the relaxation by means of the exponential factor. In the diffusion problem based on the model of a random walk, such an effect has been considered by Tchen [27] in the form of a more general memory, which could be either negative or positive, so that the corrected correlation will contain a factor respectively smaller or larger than unity.

Before leaving the discussion, it is important to remark that the diffusion phenomena, described by the above transport phenomena, are only valid for irregular movements of small scales, since we have used in Eq. 10-9b a series expansion in terms of a length and some gradient of the transferable property. Such a diffusion can be called diffusion of the gradient type. On the other hand, when the irregular movements are of coarse scales, the bulk property rather than its local gradient must be the governing factor. The latter diffusion can be called diffusion of the

bulk convective type, and will be discussed in Art. 29 in connection with the coarse eddies of free turbulent flow.

The structure of the transport coefficients can be determined by means of kinetic equations more general than the Boltzmann equation. This attempt has been made in an article by Tchen published in the Proceedings of the International Symposium on Atmospheric Diffusion (1958).

B.11. Reynolds Analogy between Heat Transfer and Skin Friction. As an application of the transport processes treated in Art. 10, let us study the Reynolds analogy between heat transfer and momentum transfer. Let $q = -\bar{\rho}c_p\bar{vT}'$ be the rate of turbulent heat transfer in the y direction across the unit area normal to this axis, and $\tau = -\bar{\rho}\bar{uv}$ be the rate of momentum transfer or turbulent shear stress. According to Eq. 10-6 we have

$$q = -\bar{\rho}c_p\bar{vT}' = \bar{\rho}c_pD_h \frac{\partial \bar{T}}{\partial y}$$

$$\tau = -\bar{\rho}\bar{uv} = \bar{\rho}D_u \frac{\partial U}{\partial y}$$

The following expressions written in nondimensional form may be compared:

$$-\frac{q}{\bar{\rho}c_p(U - U_*)(T - T_*)} \text{ and } \frac{\tau}{\bar{\rho}(U - U_*)^2} \quad (11-1)$$

Here U_* and T_* are the velocity and temperature at a reference plane, which, in the present discussion, is taken at the edge of the boundary layer. The Reynolds analogy is a statement of equality of the two expressions of Eq. 11-1. Let us investigate this analogy in some detail. Of special interest are the heat and momentum transfers at the wall, where the two expressions of Eq. 11-1 become

$$St = \frac{q_w}{\bar{\rho}_w c_p U_*(T_w - T_*)}; \quad \frac{1}{2} c_f = \frac{\tau_w}{\bar{\rho}_w U_*^2} \quad (11-2)$$

where the subscript w denotes the value at the wall, St is the coefficient of heat transfer or Stanton number, and c_f the coefficient of skin friction. Then the Reynolds analogy leads to

$$St = \frac{1}{2} c_f \quad (11-3)$$

This result was first obtained by Reynolds [28] and is also given by Squire [7, p. 819] and Goldstein [6, p. 654] in their study of heat transfer.

It is easy to see that Eq. 11-3 cannot be valid in general because, in the compressible case of an insulated boundary layer, we must have $St = 0$ and $c_f \neq 0$, which obviously violate Eq. 11-3. Therefore it is worthwhile to derive a more general relationship between the heat transfer and skin friction. For this purpose we make use of the relation (Eq.

B.11 · REYNOLDS ANALOGY

9-5) between the temperature and velocity for the case of $Pr = 1$. By differentiating with respect to y , we obtain

$$\left(\frac{\partial T}{\partial y} \right)_w = (T_*^0 - T_w) \frac{1}{U_*} \left(\frac{\partial U}{\partial y} \right)_w$$

Thus in terms of $(\partial U / \partial y)_w$, we can write St and c_f as defined by Eq. 11-2 in the following form:

$$St = D_h \frac{T_*^0 - T_w}{T_* - T_w} \frac{1}{U_*^2} \left(\frac{\partial U}{\partial y} \right)_w$$

$$\frac{1}{2} c_f = D_w \frac{1}{U_*^2} \left(\frac{\partial U}{\partial y} \right)_w$$

so that

$$\frac{St}{\frac{1}{2} c_f} = \frac{D_h}{D_w} \frac{T_*^0 - T_w}{T_* - T_w} = \frac{D_h}{D_w} \left[1 - \frac{\frac{\gamma - 1}{2} M_*^2}{\eta \left(1 + \frac{\gamma - 1}{2} M_*^2 \right) - 1} \right] \quad (11-4)$$

where $\eta = T_w/T_*^0$, M_* is the Mach number of the stream at $y = \delta$, and γ is the ratio of specific heats. Eq. 11-4 can be considered as a generalization of the Reynolds analogy to include the effects of the heat transfer, compressibility, and the difference in the transport of heat and momentum. As $M_* > 0$, $\eta \neq 1$, and $D_h \neq D_w$ according to Art. 10, the right-hand side of Eq. 11-4 is in general not unity, and the Reynolds relation (Eq. 11-3) is not obtained. However, if we neglect the effect of compressibility, for example at low speeds, and if the transports of heat and momentum are similar ($D_h = D_w$), the right-hand side of Eq. 11-4 is approximately unity, and the Reynolds analogy (Eq. 11-3) is then found to be valid. In general those restrictive conditions are not present, and the Reynolds analogy will not hold. For example, in the case of a heated plate ($\eta > 1$), the factor between brackets in Eq. 11-4 is smaller than unity, so that in many circumstances we have

$$St < \frac{1}{2} c_f, \quad (11-5a)$$

This inequality is verified by experiments. On the other hand, with intense cooling of the plate ($\eta < 1$) the term between brackets in Eq. 11-4 may become larger than unity so that we may get

$$St > \frac{1}{2} c_f, \quad (11-5b)$$

In spite of its defects, the Reynolds analogy (Eq. 11-3) is often used in theories of boundary layers with heat transfer because of its simplicity, and sometimes the experiments show that the analogy is a surprisingly good approximation.

Instead of defining the shear stress and heat transfer on the basis of

B · TURBULENT FLOW

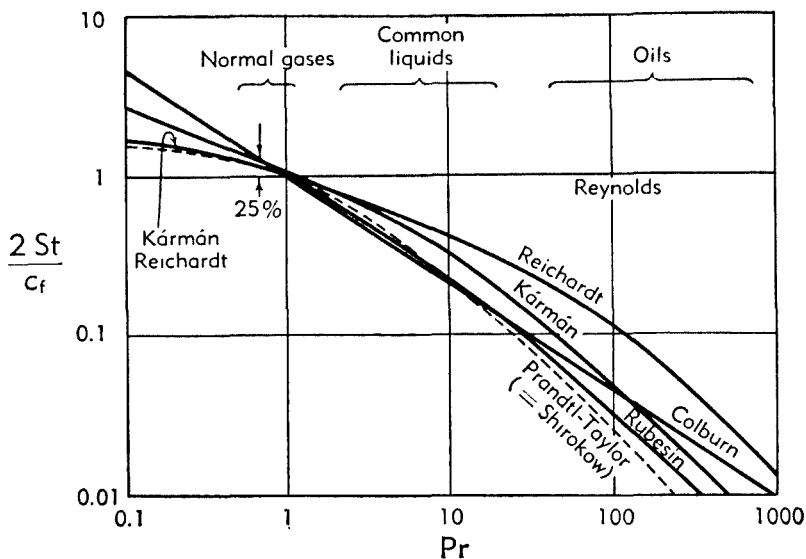


Fig. B.11a. Analogy theories of turbulent heat transfer;
 $M_e = 0, R_e = 10^7$ after Chapman and Kester [29].

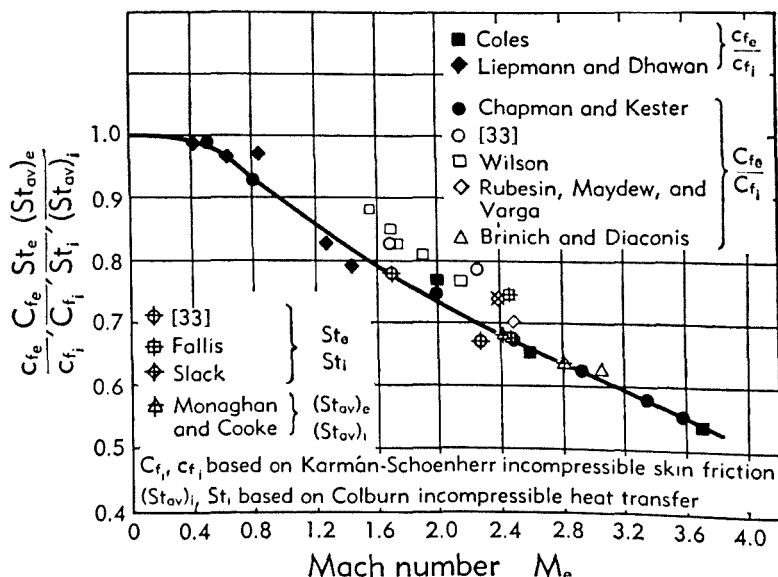


Fig. B.11b. Variation of skin friction and heat transfer
 coefficients with Mach number, after Pappas [33].

Bereitgestellt von | Technische Universität Braunschweig

the elementary and fundamental transport phenomena by turbulence, as was done in Eq. 10-12, one could consider a more general shear stress and heat transfer, by defining them by the right-hand side of the boundary layer equations, Eq. 8-1 and 8-4 respectively. Then a new coefficient of skin friction and a new Stanton number are obtained with a rather complicated ratio between them. Such an analogy between shear stress and heat transfer is called in the literature "Modified Reynolds Analogy" [8]. While it is already hard to express a satisfactory analogy between two elementary transfers, one wonders sometimes whether an analogy between a complex transfer of different nature (turbulent and laminar combined) could be expected in a reasonably simple form. The results of some of those analogy theories and the effects of the Prandtl number are shown in Fig. B,11a, after Chapman and Kester [29]. The data mentioned in Fig. B,11a are found in [15,30,31,32]. Fig. B,11b, after Pappas [33] shows how the skin friction coefficient and the heat transfer coefficient vary with the Mach number. The data of Fig. B,11b refer to [29,32,33,34,35,36,37,38,39,40,41,42,43].

B,12. Basis of Skin Friction Theories. For the analysis of the stresses acting on a body moving at high speeds, a study of the skin friction in a compressible fluid becomes important. Not only is it necessary for drag calculations, but it is useful for estimating heat transfer by means of the Reynolds analogy discussed in Art. 11.

Before discussing experimental results and their comparison with theories, it appears desirable to review in a simple and general way the main steps, concepts, and approximations underlying the theories which have been proposed.

According to Eq. 8-1, the turbulent shear stress for a compressible flow is

$$\tau = -\bar{\rho} \bar{w} - U \bar{\rho}' v \quad (12-1a)$$

The first term of the right-hand side of Eq. 12-1a represents a momentum transfer, and the second a mass transfer. The ratio of the second term to the first is estimated to be proportional to the square of the local Mach number. Now the theories of skin friction assume, as a first approximation, a value of $\tau = \tau_*$ for Eq. 12-1a, where τ_* is the total shear stress at the wall. Any variation of τ through the boundary layer is taken into account only in the higher order of approximations. Since the local Mach number is small near the wall, the second term of the right-hand side of Eq. 12-1a can be neglected, and we obtain

$$\tau = -\bar{\rho} \bar{w} \quad (12-1b)$$

The next step is to express the fluctuating quantities in terms of the

B · TURBULENT FLOW

mean quantities in accordance with the relations (Eq. 10-11 and 10-12) as follows:

$$\tau = \bar{\rho} \bar{v} l \frac{\partial U}{\partial y} \quad (12-2a)$$

where, following Prandtl, $\bar{v}l$ is expressed by

$$\bar{v}l = l^2 \frac{\partial U}{\partial y} \quad (12-2b)$$

The mixing length l is now to be expressed in terms of the local mean flow parameters. This can be done [6, Chap. 8] either by means of the Kármán similarity hypothesis

$$l = \kappa_1 \frac{\partial U / \partial y}{\partial^2 U / \partial y^2} \quad (12-3)$$

or by means of the Prandtl hypothesis

$$l = \kappa_2 y \quad (12-4)$$

where κ_1 and κ_2 are numerical constants. With the Kármán hypothesis, Eq. 12-2a can be written as follows:

$$\tau = \kappa_1^2 \bar{\rho} \frac{(\partial U / \partial y)^4}{(\partial^2 U / \partial y^2)^2} \quad (12-5)$$

In boundary layer theories the equations are usually rendered dimensionless by introducing a reference velocity

$$U_\tau = \sqrt{\frac{\tau_w}{\rho_w}} \quad (12-6a)$$

and a reference length

$$\frac{\mu_w}{\rho_w U_\tau} = \frac{\mu_w}{\sqrt{\rho_w \tau_w}} \quad (12-6b)$$

where the subscript w denotes the value at the wall.

Using the reference velocity and length, as defined by Eq. 12-6, we can write the following dimensionless quantities:

$$y^* = \frac{\rho_w U_\tau y}{\mu_w} = \frac{y \rho_w U_\tau}{\mu_w} \sqrt{\frac{c_{f_w}}{2}} \quad (12-7a)$$

$$U^* = \frac{U}{U_\tau} = \frac{U}{U_\tau} \sqrt{\frac{2}{c_{f_w}}} \quad (12-7b)$$

$$\rho^* = \frac{\bar{\rho}}{\rho_w} = \frac{T_w}{T} \quad (12-7c)$$

and rewrite Eq. 12-5 in the dimensionless form as follows:

$$\kappa_1^2 \rho^* = \frac{(\partial^2 U^* / \partial y^{*2})^2}{(\partial U^* / \partial y^*)^4} \quad (12-8)$$

(36)

where c_{f_w} is the skin friction coefficient at the wall, defined by

$$c_{f_w} = \frac{\tau_w}{\frac{1}{2}\rho_w U_*^2} \quad (12-9a)$$

The expression (Eq. 12-7c) is based on the equation of state of a perfect gas and the constancy of pressure across a boundary layer (compare the assumptions underlying Eq. 9-1).

In order to formulate the differential equation for U^* , it is necessary to express ρ^* in terms of U^* . This is possible by using relations between the temperature and velocity, such as those discussed in Art. 9. However, it is more proper to regard the boundary layer as a composite layer, consisting of a laminar sublayer very close to the wall with a superposed fully developed turbulent layer. Obviously the computation for such a condition becomes more elaborate, requiring matching of flow conditions at the interface and consideration of the heat transfer through it. But the final result of the temperature-velocity relation turns out to be rather simple and is of the form

$$\rho^{*-1} \equiv \frac{T}{T_*} = A_0 + A_1 U^* + A_2 U^{*2} \quad (12-10)$$

as could be expected from the elementary considerations of Art. 9, although the coefficients A_0 , A_1 , and A_2 are more complicated functions of Pr , c_{f_w} , T_*^0/T_* , and M_* . For the details of the analysis by which these are found the reader is referred to [44,45].

When ρ^* in Eq. 12-8 is replaced by Eq. 12-10 there is obtained an ordinary nonlinear differential equation of second order for $U^*(y^*)$, with Pr , c_{f_w} , T_*^0/T_* , M_* as parameters. The integration gives two constants to be determined by two boundary conditions taken at the interface between the laminar sublayer and the turbulent layer. According to experimental data for incompressible flow [46], these are

$$\begin{aligned} U^* &= y^* = 11.5 \\ \frac{\partial U^*}{\partial y^*} &= 0.218 \end{aligned} \quad (12-11)$$

In principle, Eq. 12-8 and 12-10 with the boundary conditions (Eq. 12-11) can be solved, with the solutions of the following general form:

$$U^* = U^* \left(y^*; Pr, c_{f_w}, \frac{T_*^0}{T_*}, M_* \right) \quad (12-12)$$

In practice the solution is very elaborate and various numerical and approximate methods must be used.

Now we assume that all the parameters in Eq. 12-12 are constant, except c_{f_w} which depends on x . Thus after integration of $U^*(y^*)$ given by

B · TURBULENT FLOW

Eq. 12-12, according to the formula of momentum thickness,

$$\theta \equiv \int_0^\infty \frac{\bar{\rho}}{\rho_\infty} \frac{U}{U_\infty} \left(1 - \frac{U}{U_\infty}\right) dy \quad (12-13)$$

the momentum thickness $\theta(c_{f_w})$ must be a function of x . Since the solution (Eq. 12-12) is valid only in the turbulent boundary layer and not in the laminar sublayer, some error will be introduced in the integration of Eq. 12-13 by using Eq. 12-12. However, since the laminar sublayer is thin, the error must be very small.

We recall that the coefficient of skin friction c_{f_w} is defined by Eq. 12-9a in terms of density ρ_w , and that the momentum equation in the integral form, for a flat plate with zero pressure gradient, is

$$c_{f_w} \equiv \frac{\tau}{\frac{1}{2} \rho_\infty U_\infty^2} = 2 \frac{d\theta}{dx} \quad (12-9b)$$

where c_{f_w} is the skin friction coefficient referred to ρ_∞ , which will be frequently used later on. It is to be noted that $c_{f_w}/c_{f_\infty} = T_\infty/T_w$. After integration with respect to x , Eq. 12-9b can be rewritten as follows:

$$\begin{aligned} x &= 2 \frac{T_w}{T_\infty} \int_\infty^{c_{f_w}} \frac{d\theta(c_{f_w})}{dc_{f_w}} \frac{1}{c_{f_w}} dc_{f_w} \\ &= 2 \left(1 + \frac{\gamma - 1}{2} M_*^2\right) \frac{T_w}{T_\infty^0} \int_\infty^{c_{f_w}} \frac{d\theta(c_{f_w})}{dc_{f_w}} \frac{1}{c_{f_w}} dc_{f_w} \end{aligned} \quad (12-14)$$

The value of the integrand of Eq. 12-14 is given by the differentiation of Eq. 12-13. In Eq. 12-14, the limits of integration are (∞, c_{f_w}) for c_{f_w} , corresponding to $(0, x)$ for x , because at $x = 0$ the boundary is so thin that the velocity gradient and the skin friction become infinite. If we write x in terms of the Reynolds number $\rho_w U_\infty x / \mu_w$, the integration of Eq. 12-14 gives a relation between the skin friction coefficient and the Reynolds number of the following form:

$$c_{f_w} = c_{f_\infty} \left(\frac{\rho_w U_\infty x}{\mu_w}, Pr, \frac{T_\infty^0}{T_w}, M_* \right) \quad (12-15)$$

Further the heat transfer coefficient may be found on the basis of the skin friction coefficient by means of the Reynolds analogy as examined in Art. 11.

Instead of using the Kármán similarity hypothesis (Eq. 12-3), which serves as the foundation of the differential equation (Eq. 12-5), we can use the Prandtl hypothesis (Eq. 12-4) so that Eq. 12-2a now becomes

$$y \frac{\partial U}{\partial y} = \frac{1}{\kappa_2} \sqrt{\frac{\tau_w}{\bar{\rho}}} \quad (12-16a)$$

Again by introducing the dimensionless quantities (Eq. 12-7), we can rewrite Eq. 12-16a in the following dimensionless form:

$$y^* \frac{\partial U^*}{dy^*} = \frac{1}{\kappa_2} \rho^{*-4} \quad (12-16b)$$

In Eq. 12-16 the assumption is again made that τ is constant across the boundary layer with the value τ_w . For ρ^* , the expression given by Eq. 12-10 is again used, and all further steps to compute U^* and the skin friction coefficient are similar to the treatment given above for the Kármán hypothesis. It is remarked that the differential equation (Eq.

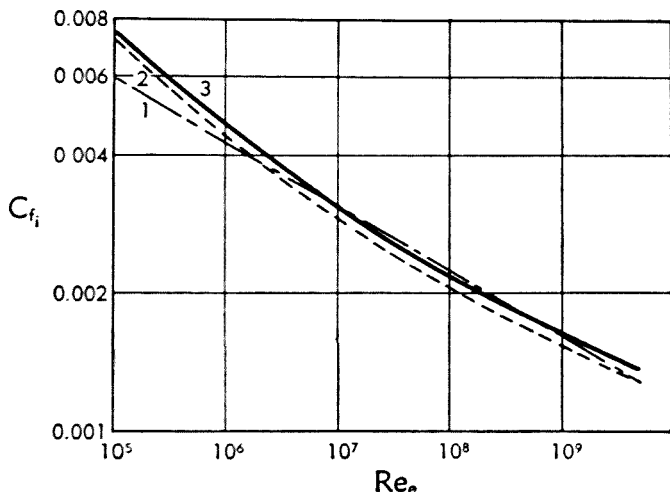


Fig. B,12a. Comparison of the mixing length and similarity hypotheses of skin friction. Curve 1 illustrates the Falkner law according to Eq. 13-15, curve 2 illustrates the Kármán law (Eq. 12-17), based on the similarity hypothesis, and curve 3 is the Prandtl law (Eq. 12-18) drawn with a coefficient 0.472, based on the mixing length hypothesis.

12-16b) from the Prandtl hypothesis corresponds to the differential equation (Eq. 12-8) from the Kármán hypothesis. However, Eq. 12-16b is of the first order and needs only one boundary condition, namely the interface condition

$$U^* = 11.5 \quad \text{at} \quad y^* = 11.5$$

It is interesting to compare the effect of the two hypotheses (Eq. 12-3 and 12-4) on the skin friction. For the sake of simplicity and in order to avoid as much as possible other assumptions which may obscure the issue, the comparison is made for skin friction coefficients of incompressible flow. Fig. B,12a shows that the Kármán and Prandtl hypotheses do not lead to an appreciable difference in skin friction coefficients. The curves are drawn according to the following formulas:

Kármán hypothesis [47],

$$\frac{0.242}{\sqrt{C_{f_1}}} = \log (C_{f_1} Re) \quad (12-17)$$

Prandtl hypothesis [48],

$$C_{f_1} = 0.472(\log Re)^{-2.68} \quad (12-18)$$

As an additional comparison, the power law of Falkner according to Eq. 13-5 with $A = 0.0262$, $n = \frac{1}{7}$ is also plotted, and agrees well with the

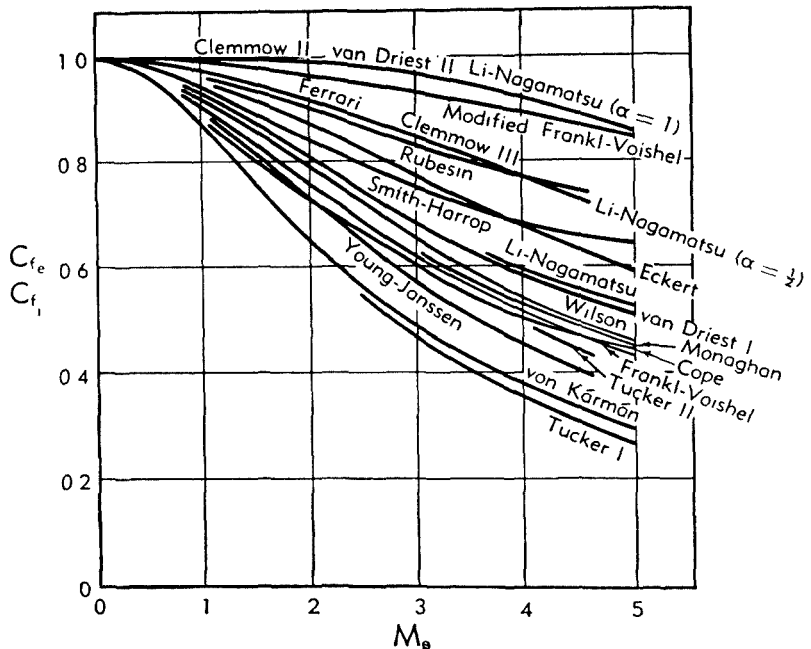


Fig. B.12b. Compressibility effect on skin friction (theories), after Chapman and Kester [29].

Kármán and Prandtl hypotheses. The Prandtl law has originally the coefficient 0.472 but Schlichting adopts a coefficient 0.455. Eq. 12-17 is sometimes called the Kármán-Schoenherr formula, and Eq. 12-18 the Prandtl-Schlichting formula.

Although the skin friction coefficient at low speeds does not depend very much on the Kármán or Prandtl hypotheses, with the application of those hypotheses to high speeds there arise many uncertainties. Now consideration must be given to new exchanges, such as density mixing and heat transfer, and to the variation of fluid properties across the boundary layer. An investigation of the theoretical basis of skin friction as given above will reveal many passages which are uncertain and arbi-

trary. Therefore it is not surprising that they yield a great number of different predictions of skin friction at high speeds. Fig. B.12b shows that the various theories differ appreciably at large M_∞ . They are based on the recovery factor $r_\infty = 1$, with the exception of the theory of Wilson which is based on $r_\infty = 0.89$. The viscosity-temperature exponent α covers the range of $\alpha = 0.75$ to 1, and the Reynolds number covers the range of $Re = 7$ to 10×10^6 . The discrepancies between the values of skin friction predicted by the various theories increase as the Mach number increases. At a Mach number of 5, the theoretical values of the skin friction differ by a factor greater than 3. Only a small portion of the discrepancies can be attributed to the different values of Re , r_∞ , and α used in the various theories. Because of their uncertainties, we shall not enter into the detail of the theories, and the readers who are interested in such details are referred to [19, 38, 49, 50, 51, 52, 53, 54, 55, 56, 57, 58, 59, 60]. In view of the difficulties of such theories of the skin friction coefficient, some empirical formula of skin friction coefficient may often be more useful in practice. These will be treated in Art. 13.

B.13. Empirical Laws of Skin Friction. Let us define again the various skin friction coefficients used in the theories and experiments. The local skin friction coefficient is defined in its general form by

$$c_f = \frac{2\tau_w}{\rho_w U_\infty^2} \quad (13-1a)$$

The wall and free stream values are obtained by writing in Eq. 13-1a, respectively, $\rho = \rho_w$ and $\rho = \rho_\infty$:

$$c_{f_w} = \frac{2\tau_w}{\rho_w U_\infty^2} \quad (13-1b)$$

$$c_{f_\infty} = \frac{2\tau_\infty}{\rho_\infty U_\infty^2} \quad (13-1c)$$

which have already been introduced in Eq. 12-13. The local skin friction coefficient c_f is a function of x . Its average value is called the "average skin friction coefficient" C_f ,

$$C_f = \frac{1}{x} \int_0^x c_f(x) dx \quad (13-2)$$

or inversely

$$c_f(x) = C_f(x) + x \frac{\partial C_f}{\partial x} \quad (13-3)$$

Corresponding to c_{f_w} and c_{f_∞} , we can write their average values C_{f_w} and C_{f_∞} . In the dimensionless form x can be replaced by the Reynolds numbers

$$Re = \frac{\rho_w U_\infty x}{\mu_w}, \quad Re_w = \frac{\rho_w U_\infty x}{\mu_w}, \quad \text{or} \quad Re_\infty = \frac{\rho_\infty U_\infty x}{\mu_\infty} \quad (13-4)$$

in respective cases.

B · TURBULENT FLOW

The empirical laws of the skin friction coefficient for a compressible fluid start from incompressible laws, and the compressibility effects are incorporated by comparison with experiments. The power law

$$c_{f_i} = A Re^{-n} \quad (13-5)$$

is an example. Here c_{f_i} is the skin friction coefficient for the incompressible boundary layer, Re is defined by Eq. 13-4, A and n are numbers ($A = 0.0262$, $n = \frac{1}{7}$, according to Falkner [61]). In order to estimate the compressible skin friction coefficient (for example c_{f_r}), we assume that a reference temperature T_r can be found so that the compressible skin friction coefficient c_{f_r} , defined by putting $\rho_r = \rho(T_r)$ into Eq. 13-1, satisfies the incompressible formula (Eq. 13-5). Then we can write

$$\begin{aligned} c_{f_r} &= c_{f_i}(Re_r) \\ &= c_{f_i} \left(Re_e \frac{\mu_e \rho_e}{\mu_r \rho_r} \right) \\ &= c_{f_i} \left[Re_e \left(\frac{T_e}{T_r} \right)^{1+\alpha} \right] \end{aligned} \quad (13-6)$$

with $\rho_r/\rho_e = T_e/T_r$ and $\mu_e/\mu_r = (T_e/T_r)^\alpha$. Since c_{f_i} follows the power law (Eq. 13-5), Eq. 13-6 can be rewritten in the following form:

$$c_{f_r} = c_{f_i}(Re_e) \left(\frac{T_e}{T_r} \right)^{-(1+\alpha)n}$$

Further, c_{f_r} can be expressed in terms of c_{f_e} by means of the definitions (Eq. 13-1) which can be rewritten as follows:

$$c_{f_r} = c_{f_e} \frac{\rho_e}{\rho_r} = c_{f_e} \left(\frac{T_e}{T_r} \right)^{-1}$$

so that Eq. 13-6 becomes

$$\frac{c_{f_e}(Re_e)}{c_{f_i}(Re_e)} = \left(\frac{T_e}{T_r} \right)^{1-(1+\alpha)n} \quad (13-7a)$$

The right-hand side of Eq. 13-7a gives the effect of compressibility (or M_e). In a compressible boundary layer T varies between T_e and T_w . It can be assumed that the compressibility effect is covered on the average, if the average temperature

$$T_r = \frac{1}{2}(T_e + T_w) \quad (13-8)$$

is taken as the reference temperature. Then $T_e/2T_r$ or $T_e/(T_e + T_w)$ can be computed in terms of M_e on the basis of Eq. 9-9, so that finally Eq. 13-7a becomes

$$\frac{c_{f_e}(Re_e)}{c_{f_i}(Re_e)} = \beta^{1-(1+\alpha)n} \quad (13-7b)$$

where

$$\beta = \left(1 + r_* \frac{\gamma - 1}{4} M_*^2 \right)^{-1} \quad (13-9)$$

r_* is the recovery factor defined by Eq. 9-9b, M_* is the free stream Mach number, and γ is the ratio of specific heats.

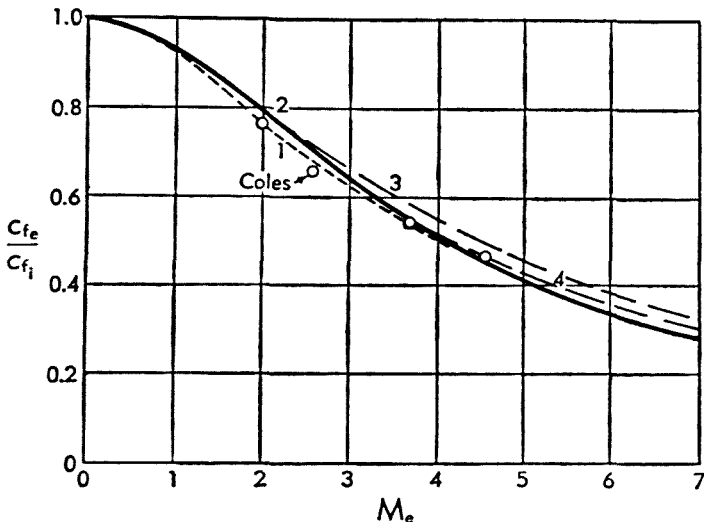


Fig. B.13. Compressibility effect on skin friction (empirical laws). $C_{f,e}/C_{f,i}$ is the ratio of average skin friction coefficients respectively at free stream Mach numbers $M_* \neq 0$ and $M_* = 0$. Curve 1 represents the theory of Frankl-Voishel [44,45]. Curves 2 and 3 represent Eq. 13-7b and 13-11, based respectively on the power law and the logarithmic law of incompressible skin friction coefficient. The experimental results of Coles [34] are shown in circles for comparison. A viscosity-temperature exponent $\alpha = 1$ is used in plotting curves 1, 2, and 3. Curve 4 is plotted with $\alpha = 0.75$, according to Eq. 13-11.

Instead of selecting the power law (Eq. 13-5) on which to base compressibility effect, we may take as an alternative example a logarithmic law of the form (decimal basis):

$$C_{f,i}(r) = A (\log Re)^{-\alpha} \quad (13-10)$$

Then by the procedures of Eq. 13-6, 13-7, and 13-8 we find the following compressibility effect:

$$\frac{C_{f,*}(Re_*)}{C_{f,i}(Re_*)} = \left[1 + \frac{(1 + \alpha) \log \beta}{\log Re_*} \right]^{-\alpha} \beta \quad (13-11)$$

where $\beta = T_*/T$, is given by Eq. 13-9, when T_* assumes the value given by Eq. 13-8.

It is interesting to note that the compressibility effect as given by Eq. 13-7b, on the basis of the power law (Eq. 13-5), is separated from the

B · TURBULENT FLOW

Reynolds number effect, while the compressibility effect (Eq. 13-11), on the basis of logarithmic law (Eq. 13-10), includes a Reynolds number effect.

The two formulas (Eq. 13-7b and 13-11) are illustrated in Fig. B,13, by taking $\alpha = 1$, $r_\infty = 1$. The Falkner constants [61]

$$A = 0.0262, \quad n = \frac{1}{7}$$

have been used in Eq. 13-5 and 13-7b, and the Prandtl constants [48]

$$A = 0.455, \quad n = 2.58$$

in Eq. 13-10 and 13-11. It is seen that they are in quite good agreement. Also plotted are the theoretical results of Frankl and Voishel [44,45], originally in tabulated form, and the experimental results of Coles and Goddard [35]. It seems that the empirical formulas (Eq. 13-7b and 13-11) agree rather well with the theory of Frankl-Voishel and with the experiments of Coles. Although the experiments of Coles are run with a slightly different Reynolds number ($Re_\infty = 8 \times 10^6$) than the Reynolds number of the theoretical curves ($Re_\infty = 7 \times 10^6$), the correction for such a discrepancy is not significant. The viscosity-temperature coefficient α has the value between 0.75 and 1.

Eq. 13-11 is also plotted in Fig. B,14b with C_{f_0} vs. Re_∞ , to be compared with experiments, by taking $\alpha = 0.75$, $n = 2.58$. C_{f_0} is based on Eq. 13-10 with $A = 0.455$. It is seen that the theoretical formula (Eq. 13-11) is in good agreement with experiments.

B,14. Comparison between Experiments and Theories. There exists an extensive history of experiments on skin friction. Because of the importance of skin friction to naval architecture, experiments on skin friction were started as early as 1793 by Beaufoy. Schoenherr [47] gives a good review of experiments prior to 1932.

In Fig. B,14a are plotted the experimental values of skin friction in compressible flow. The ratio C_{f_0}/C_{f_1} or c_{f_0}/c_{f_1} is illustrated. Except for the measurements of Chapman-Kester and Liepmann-Dhawan, wherein the incompressible skin friction values are deduced experimentally, all data points shown are based on the incompressible skin friction formula (Eq. 12-17) of Kármán-Schoenherr. There are two methods of determining the skin friction coefficient. Liepmann-Dhawan, Coles, and Chapman-Kester determine the skin friction coefficient by direct force measurements. Others determine it by surveying the boundary layer and then calculating the friction coefficient by the usual momentum method. At the Mach number of 5, the two methods yield a discrepancy of about 5 per cent.

Since the empirical theories, as given in Art. 13, do not differ very much according to Fig. B,13, we have plotted the theoretical formula

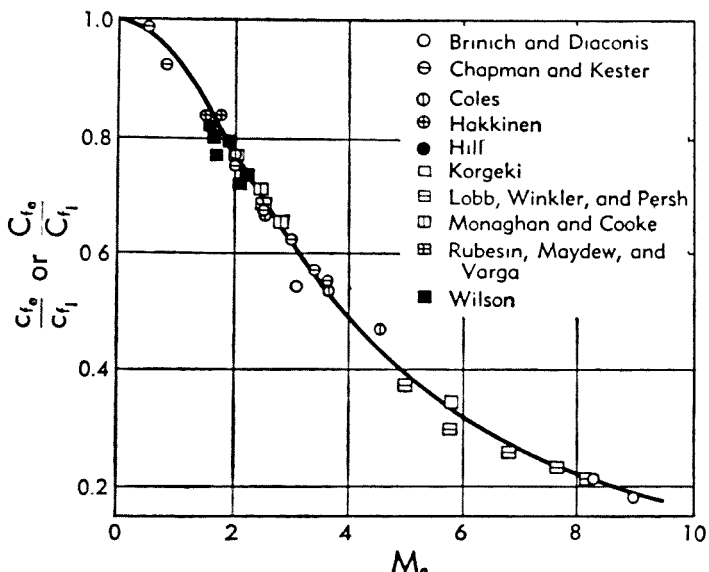


Fig. B.14a. Compressibility effect on turbulent skin friction (experimental). The experimental data are plotted according to [18, 29, 32, 34, 38, 39, 42, 62, 63]. The curve is drawn according to Eq. 13-9, with a viscosity-temperature coefficient of 0.75.

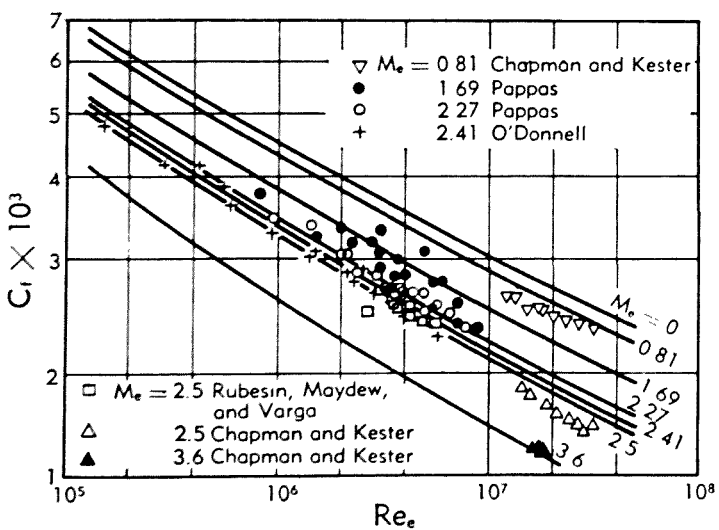


Fig. B.14b. Variation of skin friction with Reynolds number. C_f = average skin friction coefficient. $Re_e = \rho_e U_\infty / \mu_e$, Reynolds number based on the free stream. The experimental data are drawn from [29, 32, 33, 65] for the free stream Mach number $M_e = 0.81 - 3.6$. The theoretical curves ($M_e = 0 - 3.6$) are plotted according to Eq. 13-11, for $n = 2.58$, $A = 0.455$, $\alpha = 0.75$.

B · TURBULENT FLOW

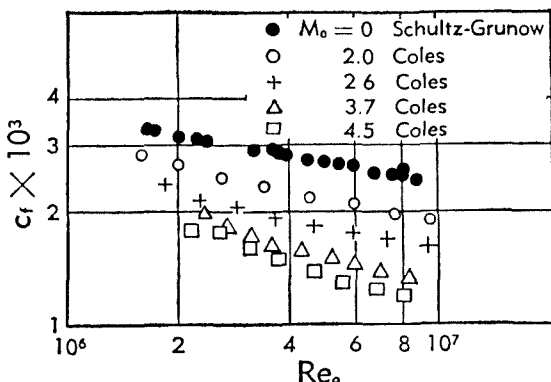


Fig. B.14c. Variation of skin friction with Reynolds number. c_f = local skin friction coefficient, Re_e = Reynolds number based on the free stream conditions. The data are drawn from [66,67].

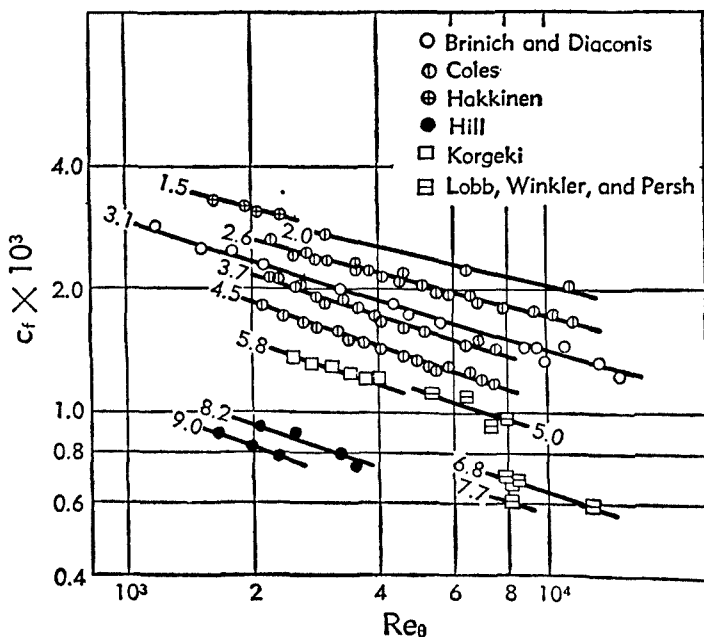


Fig. B.14d. Variation of skin friction with Reynolds number. c_f = local skin friction coefficient, Re_θ = Reynolds number based on the momentum thickness. The experimental data are drawn from [18,39,63,64,66] for the free stream Mach number $M_\infty = 1.5 - 9.0$.

(Eq. 13-9) with $\alpha = 0.75$, and $n = \frac{1}{7}$ based on the power law of incompressible skin friction to compare with experiments. It is seen that more experiments at higher Mach numbers are needed in order to understand skin friction better and to formulate better theories. The data of Fig. B.14a are plotted according to [18,29,32,34,38,39,42,62,63,64].

Fig. B.14b, B.14c, and B.14d illustrate the variations of the experimental skin friction coefficients c_f and C_f with the Reynolds numbers, based on the free stream conditions and the momentum thickness. It is interesting to see whether the experiments would follow some semi-empirical laws of skin friction. For this purpose, Eq. 13-11 is plotted for $n = 2.58$, $A = 0.455$, and $\alpha = 0.75$ in Fig. B.14b, and we see that Eq. 13-11 is in quite good agreement with experiments.

CHAPTER 4. GENERAL TREATMENT OF INCOMPRESSIBLE MEAN FLOW ALONG WALLS

B.15. Power Laws. In attempting to deal with turbulent flows confined within pipes and channels or bounded on one side by a wall, much attention was given in the older literature to power laws. These were found to be very useful in that they could be made to approximate observed mean velocity distributions and to yield resistance laws that were reasonably correct over a limited Reynolds number range. These laws are, of course, purely empirical, but they have not lost their usefulness when one wishes to express the general character of a velocity profile in a pipe or boundary layer, or wishes to make an estimate of skin friction. We should, however, be mindful of their limitations.

The power laws stem from the Blasius resistance formula for smooth straight pipes of circular cross section [68]. They were found, however, to be transferable to two-dimensional channels with parallel walls and two-dimensional boundary layers, if the radius of a pipe, the half-width of a channel, and the thickness of a boundary layer were regarded as equivalent dimensions, and if velocities were referred to those at the center or free stream. In all cases the walls are assumed to be smooth. Since the detailed development is available elsewhere [69], only the main steps are given here. Because the condition of incompressibility has been imposed, the physical properties of the fluid are independent of the flow and constant for any set of conditions. Hence we may simply denote the density by ρ , the viscosity by μ , and the kinematic viscosity by ν .

Since it is not necessary to distinguish among the flows in pipes, channels, and boundary layers in bringing out the elemental aspects of power formulas, the distance from the wall is expressed by y , the velocity at the center or in the free stream by U_* , and the value of y where the velocity is U_* by δ . The only constraint on the flow considered is the

(Eq. 13-9) with $\alpha = 0.75$, and $n = \frac{1}{7}$ based on the power law of incompressible skin friction to compare with experiments. It is seen that more experiments at higher Mach numbers are needed in order to understand skin friction better and to formulate better theories. The data of Fig. B.14a are plotted according to [18,29,32,34,38,39,42,62,63,64].

Fig. B.14b, B.14c, and B.14d illustrate the variations of the experimental skin friction coefficients c_f and C_f with the Reynolds numbers, based on the free stream conditions and the momentum thickness. It is interesting to see whether the experiments would follow some semi-empirical laws of skin friction. For this purpose, Eq. 13-11 is plotted for $n = 2.58$, $A = 0.455$, and $\alpha = 0.75$ in Fig. B.14b, and we see that Eq. 13-11 is in quite good agreement with experiments.

CHAPTER 4. GENERAL TREATMENT OF INCOMPRESSIBLE MEAN FLOW ALONG WALLS

B.15. Power Laws. In attempting to deal with turbulent flows confined within pipes and channels or bounded on one side by a wall, much attention was given in the older literature to power laws. These were found to be very useful in that they could be made to approximate observed mean velocity distributions and to yield resistance laws that were reasonably correct over a limited Reynolds number range. These laws are, of course, purely empirical, but they have not lost their usefulness when one wishes to express the general character of a velocity profile in a pipe or boundary layer, or wishes to make an estimate of skin friction. We should, however, be mindful of their limitations.

The power laws stem from the Blasius resistance formula for smooth straight pipes of circular cross section [68]. They were found, however, to be transferable to two-dimensional channels with parallel walls and two-dimensional boundary layers, if the radius of a pipe, the half-width of a channel, and the thickness of a boundary layer were regarded as equivalent dimensions, and if velocities were referred to those at the center or free stream. In all cases the walls are assumed to be smooth. Since the detailed development is available elsewhere [69], only the main steps are given here. Because the condition of incompressibility has been imposed, the physical properties of the fluid are independent of the flow and constant for any set of conditions. Hence we may simply denote the density by ρ , the viscosity by μ , and the kinematic viscosity by ν .

Since it is not necessary to distinguish among the flows in pipes, channels, and boundary layers in bringing out the elemental aspects of power formulas, the distance from the wall is expressed by y , the velocity at the center or in the free stream by U_* , and the value of y where the velocity is U_* by δ . The only constraint on the flow considered is the

B · TURBULENT FLOW

shear stress at the wall τ_w . This means, of course, that the effect of a pressure gradient is neglected, and we must limit ourselves to cases where the pressure is constant or changing so slowly in the stream direction that its effect is minor compared to the effect of τ_w . The coefficients involved are accordingly:

$$\text{The local friction coefficient } \frac{\tau_w}{\frac{1}{2} \rho U_*^2} = c_f \quad (15-1)$$

$$\text{The friction velocity } \sqrt{\frac{\tau_w}{\rho}} = U_r \quad (15-2)$$

Assuming that the local friction coefficient depends on the Reynolds number and may be expressed in powers of the Reynolds number, the relation may be written

$$c_f = \frac{\text{const}}{\left(\frac{U_* \delta}{\nu}\right)^m} \quad (15-3)$$

where $U_* \delta / \nu$ is a Reynolds number based on the maximum velocity and the distance from the wall to the point of maximum velocity. It follows from Eq. 15-3 and the definitions (Eq. 15-1 and 15-2) that

$$\frac{U_*}{U_r} = \text{const} \left(\frac{U_r \delta}{\nu} \right)^{\frac{m}{2-m}} \quad (15-4)$$

where $U_* \delta / \nu$ is a Reynolds number based on the friction velocity and δ . Eq. 15-3 and 15-4 are both expressions for conditions near the wall. However, it may be argued that a formula similar to Eq. 15-4 may be used to express the velocity at any distance from the wall without appreciable error because the main increase in velocity takes place near the wall. Assuming this, the velocity distribution is written

$$\frac{U}{U_r} = \text{const} \left(\frac{U_r y}{\nu} \right)^{\frac{m}{2-m}} \quad (15-5)$$

where U is the mean velocity at the distance y from the wall.

We assume now that all mean velocity profiles are similar, and accordingly that U/U_r is a function of y/δ . While this assumption is exactly true for laminar flow, it is only an approximation for turbulent flow. The appropriate power-law form of the function is indicated by Eq. 15-5 and is written

$$\frac{U}{U_r} = \left(\frac{y}{\delta} \right)^{\frac{m}{2-m}} \quad (15-6)$$

By taking $m = \frac{1}{4}$ it is found that Eq. 15-3 expresses the variation of friction coefficients in pipes over the range $3000 < U_* \delta / \nu < 70,000$. With

the constants also determined from pipe tests, Eq. 15-3, 15-4, 15-5, and 15-6 become

$$c_f = 0.0466 \left(\frac{U_* \delta}{\nu} \right)^{-1} \quad (15-3a)$$

$$\frac{U_*}{U_r} = 8.74 \left(\frac{U_r \delta}{\nu} \right)^{\frac{1}{4}} \quad (15-4a)$$

$$\frac{U}{U_r} = 8.74 \left(\frac{U_r y}{\nu} \right)^{\frac{1}{4}} \quad (15-5a)$$

$$\frac{U}{U_*} = \left(\frac{y}{\delta} \right)^{\frac{1}{4}} \quad (15-6a)$$

The foregoing formulas for pipes would not be expected to apply to other cases. However, they do apply to two-dimensional channels and flat plates over a limited range of Reynolds number for particular coefficients and exponents. Power-law velocity distributions fit the observed distributions in an over-all way but not in all detail.

When applied to the flat plate, Eq. 15-3a and 15-6a may be used to calculate δ and c_f as functions of x and of a Reynolds number based on x , provided the boundary layer begins as a turbulent layer at the leading edge. The loss of momentum flux through any section of the boundary layer is given by

$$\int_0^{\delta} \rho U (U_* - U) dy$$

The momentum thickness θ , which when multiplied by ρU_*^2 gives this quantity, is accordingly defined by

$$\theta = \frac{1}{\rho U_*^2} \int_0^{\delta} \rho U (U_* - U) dy = \int_0^{\delta} \frac{U}{U_*} \left(1 - \frac{U}{U_*} \right) dy \quad (15-7)$$

Since τ_w alone accounts for the loss of momentum, it follows that

$$\frac{d\theta}{dx} = \frac{\tau_w}{\rho U_*^2} = \frac{1}{2} c_f \quad (15-8)$$

With the velocity distribution given by Eq. 15-6a, $\theta = 7\delta/72$. By substituting this and Eq. 15-3a into Eq. 15-8, and integrating with the boundary condition $\delta = 0$ when $x = 0$, the result is

$$= 0.381x \left(\frac{U_* x}{\nu} \right)^{-\frac{1}{4}} \quad (15-9)$$

where x is the distance from the leading edge and $U_* x / \nu$ is a Reynolds number based on x and the velocity of the free stream. From Eq. 15-3a and 15-9 it follows that

$$c_f = 0.0592 \left(\frac{U_* x}{\nu} \right)^{-\frac{1}{4}} \quad (15-10)$$

(49)

B · TURBULENT FLOW

Again taking $\theta = 7\delta/72$ and using Eq. 15-9,

$$C_f = 0.074 \left(\frac{U_\infty x}{\nu} \right)^{-\frac{1}{7}} \quad (15-11)$$

where C_f is the mean friction coefficient from the leading edge to the point x . Eq. 15-11 checks the tests on smooth plates for $U_\infty x/\nu$ up to about 3×10^6 .

Power formulas should be regarded as interpolation formulas, useful over a limited range of Reynolds number. For $U_\infty \delta/\nu$ over 100,000, Eq. 15-6a agrees better with measurements when the exponent $-\frac{1}{7}$ is replaced by $-\frac{1}{8}$, and even $-\frac{1}{9}$ when the Reynolds number is sufficiently high. Skin friction formulas may likewise be improved for agreement with measurement over a greater range of Reynolds number by adjusting the exponent. For example, as we have seen in Art. 13, Falkner [61] uses an exponent of $-\frac{1}{7}$ instead of $-\frac{1}{8}$ and gives

$$c_f = 0.0262 \left(\frac{U_\infty x}{\nu} \right)^{-\frac{1}{7}} \quad (15-12)$$

$$C_f = 0.0306 \left(\frac{U_\infty x}{\nu} \right)^{-\frac{1}{7}} \quad (15-13)$$

It must be remembered that the foregoing considerations apply only to smooth walls. Except for Art. 23, where the effect of roughness is considered, and elsewhere where roughness is mentioned, the smooth-wall condition is implied throughout this chapter.

B,16. Wall Law and Velocity-Defect Law. Two laws that have gone far toward giving order and meaning to the seemingly confusing and conflicting data on flows bounded or partially bounded by walls are the “law of the wall” attributed to Prandtl (for example [70]) and the “velocity-defect law” introduced by von Kármán [71]. The first pertains to the region close to the wall where the effect of viscosity is directly felt and the second pertains to the bulk of the shear layer where viscous forces become negligible.

The law of the wall is based on the logical premise that the tangential stress at the wall τ_w must depend on the velocity U at the distance y from the wall and on the viscosity μ and density ρ . Assuming that the stress at the wall is the only constraint on the flow, we may write

$$F(\tau_w, U, y, \mu, \rho) = 0$$

This may be expressed in dimensionless form by

$$\frac{U}{U_\tau} = f \left(\frac{U_\tau y}{\nu} \right) \quad (16-1)$$

in terms of the characteristic friction velocity U_τ and the characteristic length ν/U_τ . The functional equation (Eq. 16-1) is the law of the wall. In the laminar sublayer it takes the special form

$$\frac{U}{U_\tau} = \frac{U_\tau y}{\nu} \quad (16-2)$$

which arises from the circumstance that the sublayer is so thin that τ therein is constant and equal to τ_w . In Eq. 16-2 the density included in the terms automatically cancels out.

The range of y over which Eq. 16-1 is valid must be established by experiment. It might be supposed that the range would be severely limited by pressure gradient effects when these are present, since, as we have seen, the pressure acting across an area of unit width and height y has been neglected. Recent data, to be discussed in Art. 19, show that there remains a considerable range over which the law is valid for both rising and falling pressures and that the law is not so restricted as to be useless until conditions of near-separated flow are reached. Thus there is a range, even though possibly short, beyond the laminar sublayer, where the functional relation (Eq. 16-1) is universally of the same form. This is true only when there is a laminar sublayer, and therefore true only when the wall is aerodynamically smooth.

The argument leading to the velocity-defect law is that the reduction in velocity ($U_* - U$) at distance y is the result of a tangential stress at the wall, independent of how this stress arises but dependent on the distance δ to which the effect has diffused from the wall. We may then write

$$U_* - U = G(U_\tau, y, \delta)$$

and in terms of dimensionless ratios

$$\frac{U_* - U}{U_\tau} = g\left(\frac{y}{\delta}\right) \quad (16-3)$$

This is the velocity-defect law.

The law (Eq. 16-3), unlike Eq. 16-1, holds true for rough as well as smooth walls, provided the roughness elements are not so large that y becomes indeterminate. Data for boundary layers with constant pressure are found to fall on a single curve within the precision fixed by the experimental scatter. This is shown by Fig. B,16 which presents various data collected by Clauser [72] for different Reynolds numbers and for smooth and rough walls. Aside from the fact that the law cannot apply in the vicinity of the laminar sublayer nor at distances comparable to the height of roughness elements, it appears to exhibit a universality for constant pressure boundary layers. Clauser has shown, however, by a formal argument that the law is fundamentally not universal when U , varies from one set of data to another, but that the dispersion will gener-

ally be small and scarcely outside the usual random scattering due to observational errors.

The function g is affected to degrees that are far from negligible by conditions imposed on the flow from without. The effect of the pressure gradient, which will be considered in Art. 19, is of most importance. It is also affected by free stream turbulence and is therefore different in pipes and channels than in boundary layers. This sensitivity of the velocity-defect law to outer conditions stands in sharp contrast to the law of the wall which is remarkably insensitive in this respect.

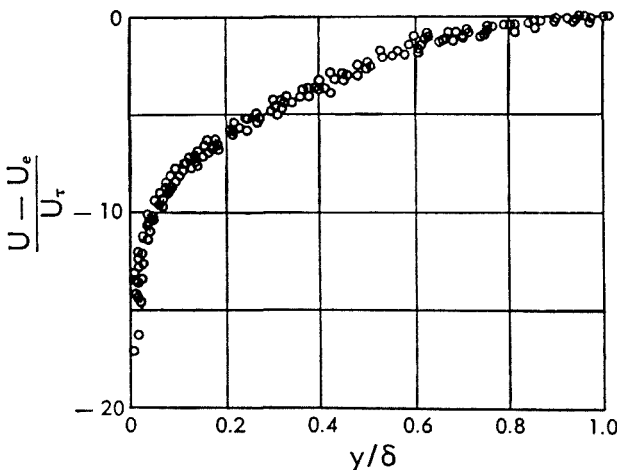


Fig. B,16. Data for smooth and rough walls plotted on basis of velocity-defect law. (Taken from Clauser [72] omitting data source and designation.)

B,17. Logarithmic Formulas. From time to time it has been inferred in the literature that the two laws, Eq. 16-1 and 16-3, are empirical laws, and in the sense that their adoption has depended on experimental confirmation, they are empirical. Certainly they draw but little on any knowledge of turbulent structure. About their only connection with the behavior of turbulence is the justification of the assumption that transfer processes are affected by viscosity very near a wall, but are independent of viscosity and dependent on the scale of the shear layer in the bulk of the flow. The principal empirical fact about these laws is that their regions of validity overlap one another. There is nothing in their makeup that requires an overlap, and the only apparent reason for it is a gradual change from wall conditions to outer-flow conditions.

Millikan [73] has shown that if there is any region of overlap, no matter how limited, in which both laws are valid, then the functions f and g must be logarithms. Since this is the same form which results from mixing length considerations, but which is arrived at without re-

course to a physical model, the authors feel that this deduction must be ranked among the major contributions to the subject. A simple way of arriving at this result is to reexamine Eq. 16-1 and 16-3, written in the following forms:

$$\frac{U}{U_r} = f \left[\left(\frac{y}{\delta} \right) \left(\frac{U_r \delta}{\nu} \right) \right] \quad (17-1)$$

$$\frac{U}{U_r} = \frac{U_*}{U_r} - g \left(\frac{y}{\delta} \right) \quad (17-2)$$

Since these are two expressions for the same quantity, and since a multiplying factor inside a function must have the same effect as an additive factor outside a function, the functions f and g must be logarithms.

The two formulas are usually written in the form

$$\frac{U}{U_r} = \frac{2.3}{K} \log \left(\frac{U_r y}{\nu} \right) + c_1 \quad (17-3)$$

$$\frac{U_* - U}{U_r} = c_2 - \frac{2.3}{K} \log \frac{y}{\delta} \quad (17-4)$$

where K , c_1 , and c_2 are experimentally determined constants. It follows from Eq. 17-1 and 17-2, when f and g are expressed as logarithms, that K must be common to both Eq. 17-3 and 17-4. The constant K is universal and the logarithmic form of the functions do fit the observations, but only over a limited range of the variables. More specifically they have the logarithmic form where they overlap, but not necessarily much beyond this region. This may be taken as evidence that the empirically established overlap is not a basic condition and therefore not a sufficiently strong one to impel a long range validity for the laws deduced from it. The extent to which these laws fit the data and are influenced by various conditions will be taken up in Art. 19, 20, and 21.

For the present we direct our attention to Eq. 17-4 in order to call attention to the fact that the constant c_2 is found to be the same for pipes and channels, but that it has a different value for boundary layers of flat plates. This is shown in Fig. B,17a in which pipe data have been omitted. The data are taken from [67,74,75,76,77]. The Reynolds number Re_s is in all cases $U_r \delta / \nu$. The constant 5.75, corresponding to $K = 0.40$, is common to both, provided the curves are fitted near the wall. It is seen that the log law does not fit well for the full range of y/δ . This means only that the logarithmic form of the defect law is at fault, not the functional form of the law itself. More significant is the fact that the function g in Eq. 16-3 is different in boundary layers from that in channels. This difference is evidently due mostly to a sensitivity to conditions at the outer limit $y = \delta$ rather than to the presence of a small falling

B · TURBULENT FLOW

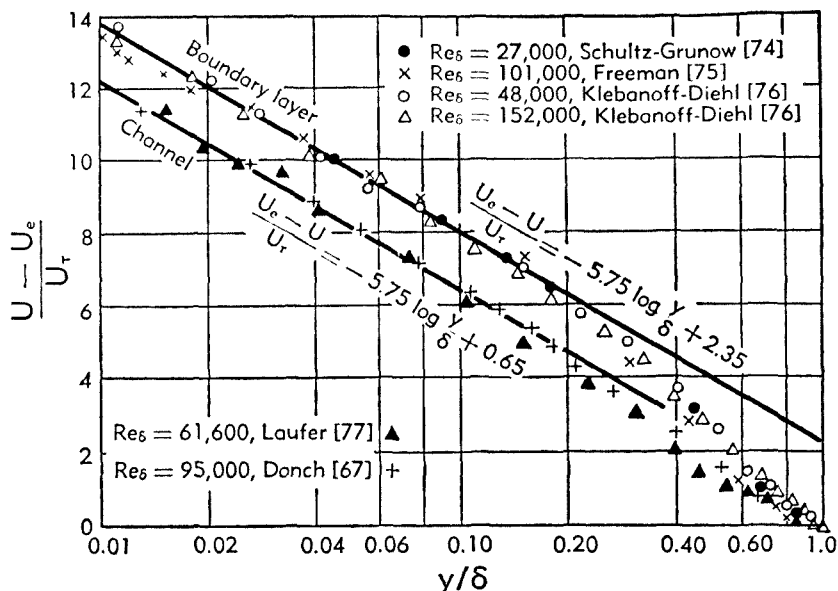


Fig. B,17a. Logarithmic law, comparison for channel and boundary layer of flat plate.

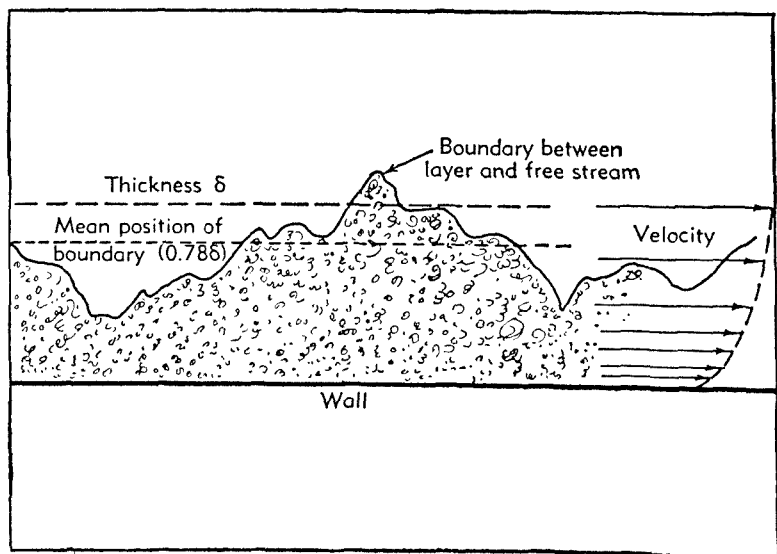


Fig. B,17b. Schematic diagram of boundary layer.

pressure in the case of a channel, and a constant pressure in the case of a boundary layer.

The boundary layer bounded by a free stream of negligible turbulence is known to have a sharp but very irregular outer limit. This is illustrated schematically in Fig. B,17b. The phenomenon is common to all turbulent shear flows which are limited only by the extent to which they have diffused into nonturbulent fluid. There is no such limit for fully developed turbulent flow in pipes and channels where turbulent motions may freely cross the center. To a limited extent a similar condition can be produced in boundary layer flows by introducing turbulence into the free stream by means of a grid. It has been noted that the profiles then deviate toward those for the pipe and channel.

B,18. Smooth Wall Incompressible Skin Friction Laws. So far our laws have been so general that pipes and channels on the one hand and boundary layers on the other could be treated as one subject. We may continue in this vein in expressing the general form of the skin friction law, but shortly it will be necessary to make a distinction.

Since skin friction depends on conditions near the wall, Eq. 17-3 and 17-4 are used to derive a formula for skin friction, as was first done by von Kármán [71]. If these equations are added, the result is

$$\frac{U_s}{U_r} = \frac{2.3}{K} \log \left(\frac{U_s \delta}{\nu} \right) + \text{const} \quad (18-1)$$

By using Eq. 15-1 and 15-2 and introducing $Re_s = U_s \delta / \nu$, Eq. 18-1 becomes

$$\sqrt{\frac{2}{c_f}} = \frac{2.3}{K} \log (Re_s \sqrt{c_f}) + \text{const} \quad (18-2)$$

Eq. 18-2 has been verified by a number of reliable measurements in pipes. With the constants for pipe flow as given by von Kármán [78], Eq. 18-2 becomes

$$\sqrt{\frac{2}{c_f}} = 4.15 \log (Re_s \sqrt{c_f}) + 3.60 \quad (18-3)$$

where Re_s is based on the velocity at the center U_s and the radius of the pipe. The constant 4.15 corresponds to $K = 0.39$, this value having been chosen to give the best all-around agreement.

The Kármán skin friction formula for flat plates [78,79] results from conversion of Eq. 18-3 into terms involving x , where x is the distance from the leading edge and the assumed beginning of the turbulent boundary layer. It is expressed as

$$\sqrt{\frac{2}{c_f}} = \frac{2.3}{K} \log (Re c_f) + \text{const} \quad (18-4)$$

where $Re = U_\infty x / \nu$ and c_f is again the local friction coefficient defined by Eq. 15-1. With the constants evaluated from Kempf's measurements on a flat plate [80], Eq. 18-4 becomes

$$\frac{1}{\sqrt{c_f}} = 4.15 \log (Re c_f) + 1.7 \quad (18-5)$$

Schoenherr [47] found the coefficient of mean friction over the distance x to be given by

$$\frac{0.242}{\sqrt{C_f}} = \log (Re C_f) \quad (12-17)$$

and the relation between the local and the mean friction coefficients to be

$$c_f = \frac{0.558 C_f}{0.558 + 2 \sqrt{C_f}} \quad (18-6)$$

Eq. 12-17 is one of the most widely used formulas for incompressible flow and, as previously mentioned in Art. 12 and 14, is sometimes called the Kármán-Schoenherr formula.

As reported by Prandtl [48], Schlichting proposed an interpolation formula of the form

$$C_f = 0.455 (\log Re)^{-2.58} \quad (12-18)$$

The comparison between Eq. 12-17 and 12-18 is shown in Fig. B.12a. The corresponding interpolation formula for c_f , also given by Schlichting [80], is

$$c_f = (2 \log Re - 0.65)^{-2.3} \quad (18-7)$$

Schultz-Grunow [74] adopted the Prandtl law with constants as follows:

$$c_f = 0.370 (\log Re)^{-2.584} \quad (18-8)$$

While the foregoing formulas are expressed in the form usually desired for engineering purposes, they suffer from the drawback that the boundary layer is often laminar for a significant distance before transition occurs. In such cases formulas based on Re cannot be applied without assuming some fictitious origin for x . A formula like Eq. 18-3, based on the local parameter Re_θ , does not involve this difficulty. Because of the indefiniteness of the outer limit of the boundary layer, the momentum thickness θ is commonly used in place of δ , and $Re_\theta = U_\infty \theta / \nu$ takes the place of Re_δ . Squire and Young [81] obtained from Eq. 18-4 the approximate relation

$$\frac{1}{\sqrt{c_f}} = A \log Re_\theta + B \quad (18-9)$$

with the constants A and B chosen to give the best agreement with Eq.

12-18. Their final expression, written in the form most commonly used, is

$$\frac{2}{c_f} = [5.890 \log (4.075 Re_\theta)]^2 \quad (18-10)$$

On the experimental side, measurements using the floating-element technique, wherein the shear stress on an element of the wall is determined from a direct force measurement, are now believed to be the most reliable. The best known examples of results employing this technique

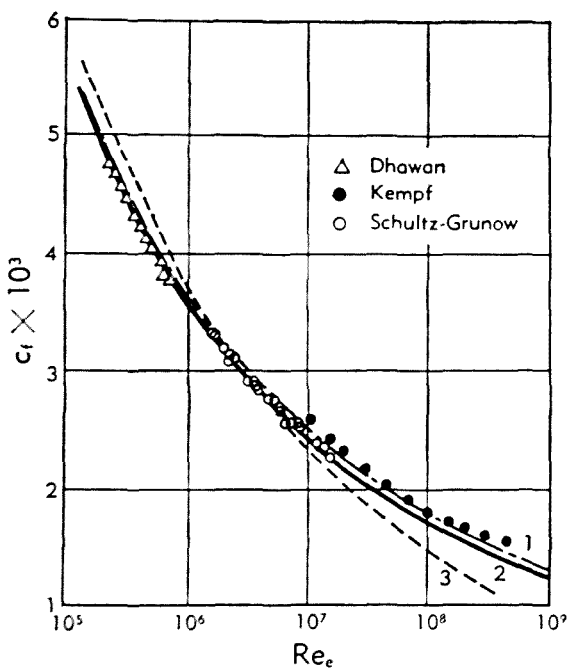


Fig. B,18. Local skin friction coefficient for smooth wall, zero pressure gradient. Experimental values represented by points. Curve 1: Eq. 18-5; curve 2: Eq. 18-8; curve 3: Eq. 15-10.

are those of Kempf [82] and the more recent results of Schultz-Grunow [74] and Dhawan [37]. These are given in Fig. B,18. Represented for comparison are the curves corresponding to the power formula (Eq. 15-10) and the logarithmic formulas (Eq. 18-5 and 18-8).

B,19. Effect of Pressure Gradient. When a body moves through a fluid, the pressure in the neighborhood of the body is different from that in the undisturbed fluid in ways that are too well known to be recounted here. It suffices merely to point out that pressure gradients are the rule rather than the exception. The present discussion will be limited to two-

dimensional flow where pressure gradients in the x and y directions are encountered.

Boundary layers are usually so thin compared to the relatively large distances over which pressure changes occur that the changes across the layer are so small that they have insignificant effects. The pressure may change even more gradually in the x direction, but here the boundary layer extends over the full range of the pressure changes, and cumulative effects become important. The thickness of the layer is always affected, and the mean velocity profile will change form as the flow progresses unless conditions are so arranged that it is held in equilibrium by the balance between inertial, pressure, and friction forces. Pipe and channel flows are examples of equilibrium flows in which the pressure drop is exactly balanced by wall friction. As shown by Clauser [83], a balance is possible in boundary layer flows under certain conditions, and his contributions to this subject will be taken up in Art. 20. In general, mean velocity distributions undergo progressive changes when subjected to pressure gradients—the less so when the flow proceeds toward lower pressures, and the more so when the flow proceeds toward higher pressures. The latter therefore deserves, and usually receives, the greater attention.

The importance of flow to higher pressures is emphasized by the possibility, and often the occurrence, of flow separation. Separation is the result of flow reversal and an accumulation of stagnant fluid over which the moving fluid passes without having to follow the contour of a body. An adverse pressure gradient opposes motion in the direction of the main flow and can set up motion in the reverse direction when the fluid has lost sufficient momentum through friction with a wall. Since the momentum approaches zero at a wall, only the shear stresses between the faster- and slower-moving fluids can prevent flow reversal. Whether or not reversal will occur depends on an interplay between the shear stresses and the pressure gradient. In any case the fluid movement is retarded, and shear stresses are expended against internal forces on the fluid arising from the pressure gradient. The maximum shear stress is no longer at the wall, as it is for constant pressure, but now occurs some fraction of the boundary layer thickness away from the wall depending on the state of retardation of the layer. These effects reduce skin friction and the momentum losses from this source, but only in exchange for even greater internal momentum losses resulting from shear stresses applied to pressure-retarded flow.

A classic example of the typical evolution of velocity profiles occurring when a boundary layer is subjected to a monotonically increasing pressure sufficient to bring about eventual flow separation is the set of curves compiled by von Doenhoff and Tetrovin [84] shown in Fig. B,19a. Here U_∞ is the local free stream velocity just outside the boundary layer, and

B.19 · EFFECT OF PRESSURE GRADIENT

θ is the momentum thickness. Each curve of the set is characterized by a constant value of the form parameter H , where $H = \delta^*/\theta$ and in accordance with the usual definitions

$$\delta^* = \text{displacement thickness} = \int_0^\delta \left(1 - \frac{U}{U_\infty}\right) dy$$

$$\theta = \text{momentum thickness} = \int_0^\delta \frac{U}{U_\infty} \left(1 - \frac{U}{U_\infty}\right) dy$$

On the grounds that all suitable boundary layer data available up to 1943 could be made to fit one or another of these curves, von Doenhoff and

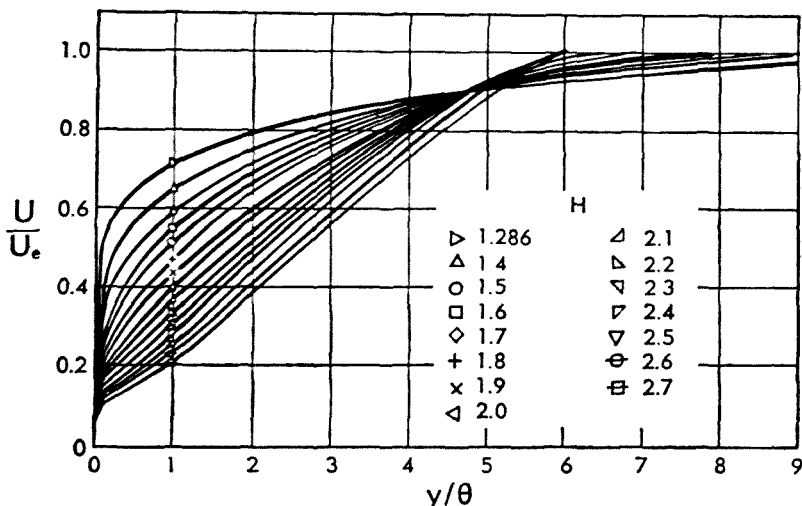


Fig. B.19a. Velocity profiles corresponding to various values of H , after von Doenhoff and Teterivin [84].

Teterivin concluded that H was a suitable form parameter. When the pressure increases with increasing x and the gradient is sufficient to bring about eventual separation, H steadily increases, and each successive profile takes a shape similar to one of those in the figure. Separation is imminent when H is above 2 and is likely to occur when H is 2.6 or 2.7. Apparently this family characteristic is only true of nonequilibrium profiles, for Clauser has recently shown that equilibrium profiles, for which H remains nearly constant with increasing x , do not align themselves with the typical forms of this family (see Art. 20). However, the general features are preserved.

There has been a great deal of speculation about the abrupt rise of the curves of Fig. B.19a near the origin. It will be noted that even when the flow is about to separate the steep initial rise is present. Thanks to the recent contributions of Coles [85], to be considered in Art. 21, and to facts

pointed out earlier by Clauser about the law of the wall, this feature now has a simple explanation. If we regard the phenomenon as a sharp drop in velocity to zero at the wall instead of a rise from the wall outward, we see that this is simply the region where wall friction becomes predominant over the pressure effect. In other words, this is the region governed by the law of the wall. Typical of the agreement with the law of the wall and of the manner of departing from it are the examples shown in Fig. B,19b taken from Coles' paper [85]. When the Reynolds number is high and the pressure is either constant or the adverse gradients are not excessive, the agreement is more as shown in Fig. B,19c given by Clauser [83].

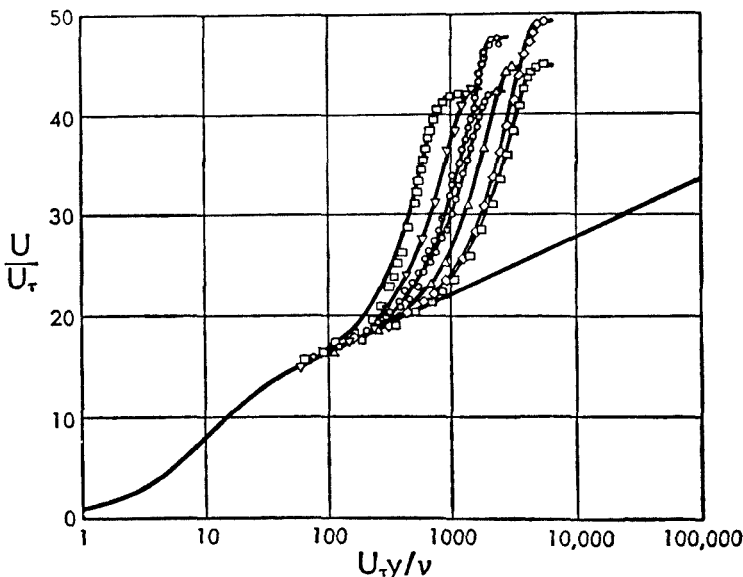


Fig. B,19b. Agreement and departures from the law of the wall, after Coles [85].

The region of the wall is a region for which we have a unique relationship between the velocity and the shear stress at the wall. Sometimes, slightly different working formulas evolve from the fitting to experimental data. We find, for example:

$$\text{According to Clauser } \frac{U}{U_r} = 5.6 \log \left(\frac{U_r y}{v} \right) + 4.9 \quad (19-1)$$

$$\text{According to Coles } \frac{U}{U_r} = 5.75 \log \left(\frac{U_r y}{v} \right) + 5.10 \quad (19-2)$$

It is difficult to specify where departures from the law occur, because this depends both on the Reynolds number and the pressure gradient. Departures occur at lower values of $U_r y/v$ and are greater as the effect of

the adverse pressure gradient on the profile becomes more marked, i.e. as H is greater. They also occur at lower values of $U_\tau y/v$ as the Reynolds number decreases. Landweber [86] has shown that the logarithmic part no longer exists if $U_\tau \delta^*/v$ is less than 725. At the wall side the law begins to merge into Eq. 16-2 somewhere around $U_\tau y/v = 50$. The outer limit of the laminar sublayer is usually taken as 11.5, representing the point where the curve of Eq. 16-2 and the logarithmic law intersect.

For a number of years there was considerable uncertainty about the effect of the adverse pressure gradient on the skin friction, and most methods of treating turbulent boundary layers assumed that the gradient had no effect. Estimates by means of the momentum equation were unreliable and in some cases showed an apparent increase in the skin friction

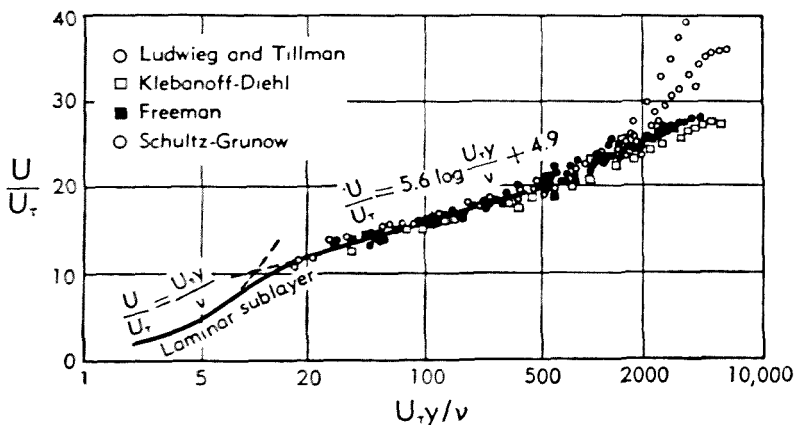


Fig. B.19c. Test of the law of the wall, after Clauser [83].

coefficient in regions of strongly rising pressure. When data based on more direct methods became available, such as those of Schubauer and Klebanoff [87] and Newman [88], based on hot wire measurements of shear stress, and those of Ludwig and Tillmann [89], based on the heated-element method, it became clearly evident that c_f was decreased by an adverse pressure gradient, and was steadily reduced toward zero as separation was approached, as logic dictates that it should be. The whole question has been considerably clarified by the universal character of the law of the wall which establishes a unique relation between velocity near the wall and skin friction without explicitly involving the pressure gradient. The effect of the pressure gradient on the skin friction is thereby seen to result from its reduction of velocity near the wall.

The relation between the integral characteristics of a two-dimensional boundary layer and the pressure gradient is obtained by integrating the equation of motion from $y = 0$ to $y = \delta$. The commonly used form,

obtained from the equation of motion with only first order terms in the boundary layer approximation, is known as the Kármán momentum equation, and is expressed as

$$\frac{d\theta}{dx} = \frac{c_f}{2} + \frac{(H+2)}{2} \frac{\theta}{q} \frac{dp}{dx} \quad (19-3)$$

where q is the dynamic pressure in the free stream where the pressure is p . This equation gives a synoptic description of boundary layer development and is independent of detailed processes. The relation between the various quantities in the equation does, however, depend on the mechanics of the turbulent diffusion process.

When the pressure gradient is positive (adverse) and large, the second term on the right-hand side of Eq. 19-3 may, and usually does, become large compared to $c_f/2$. For this condition the growth of θ with x depends primarily on internal momentum losses resulting from the expenditure of tangential forces against those portions of the stream which are retarded by pressure gradient and which, by the action of the force, progress to higher pressures but do not gain momentum equivalent to the forces expended. When a boundary layer exists, a pressure rise can be negotiated only by the loss of momentum. A reduction of c_f by pressure gradient is not an indication that drag is reduced.

When $d\theta/dx$ in Eq. 19-3 is due largely to the pressure gradient term, it is obvious that c_f cannot be accurately determined from measurements of $d\theta/dx$. It is now generally recognized that Eq. 19-3 is unsuited for this purpose when pressure gradients assume appreciable values. Not only is the accuracy poor but totally unrealistic values of c_f have been indicated. Several explanations have been offered having to do with the neglected terms in the equation of motion, but it now appears in the light of Clauser's experience [83] that departures of the flow from two-dimensionality are largely responsible.

The universal character of the law of the wall has suggested itself as a useful and reliable means of obtaining local skin friction coefficients from measured velocity distributions. It seems that the first published recognition of this occurs in the paper by Clauser [83], who devised the following procedure and used it in the analysis of his experimental results.

Using $U_r = U_* \sqrt{c_f/2}$, the following expressions are written:

$$\frac{U}{U_r} \equiv \frac{U}{U_*} \sqrt{\frac{2}{c_f}} \quad \text{and} \quad \frac{U_r y}{\nu} \equiv \frac{U_* y}{\nu} \sqrt{\frac{c_f}{2}}$$

With these and Eq. 19-1 he obtained the family of curves shown in Fig. B,19d having c_f as the parameter. Application of the figure to a determination of c_f merely requires the placing of a measured velocity distribution thereon and reading off the value of c_f , interpolating where necessary. It is still necessary to measure velocities within a short distance of a

wall, but the requirement of nearness is considerably relaxed over that required to derive c_f from the initial slope of a velocity distribution.

Ludwieg and Tillmann [89], who first confirmed the validity of the law of the wall in a region of adverse pressure gradient by means of their heated-element measurements of c_f , deduced the following formula for c_f :

$$c_f = \frac{0.246}{10^{0.678H} Re_s^{0.265}} \quad (19-4)$$

where H is the form parameter and $Re_s = U_s \theta / \nu$. This formula gives c_f reasonably well where the velocity profiles conform to the H -parameter family of Fig. B,19a.

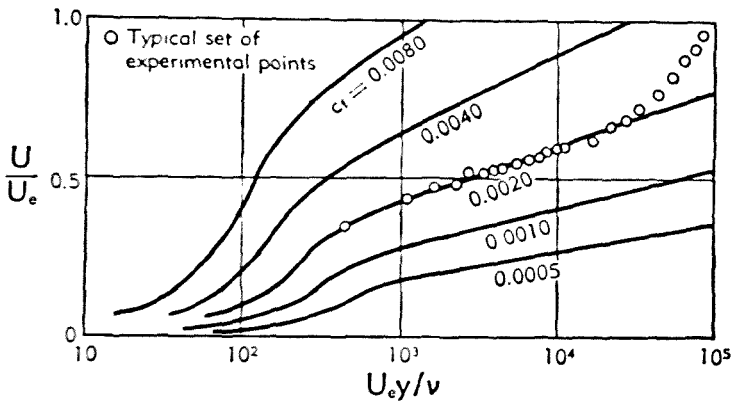


Fig. B,19d. Chart for experimental determination of turbulent skin friction coefficient, after Clauser [83].

B,20. Equilibrium Boundary Layers According to Clauser. Since the velocity profile beyond the immediate region of the wall is affected by the pressure gradient, a universal representation on the basis of the velocity-defect law, as shown by Fig. B,16, is not in general obtained. However, by means of an experiment in which long lengths of two-dimensional turbulent boundary layer could be subjected to various adverse pressure gradients, Clauser [83] showed that the pressure distribution could be adjusted to give similar boundary layer profiles when plotted on the basis of the defect law. The form of the function was different from that for constant pressure flow and also different for each separate pressure distribution, but the significant fact was that the same functional relation applied over an essentially arbitrary number of cross sections for any one pressure distribution. He termed the resulting boundary layer an "equilibrium boundary layer" on the grounds that the sameness of the function g in the case of a pressure gradient implied the same similarity of major flow characteristics as was maintained in constant

pressure flow. Constant pressure flows are then just one member of a family of flows developed under specific kinds of pressure distributions.

With regard to the kind of pressure distribution required to produce an equilibrium flow, Clauser points out that a gradient parameter like $(\delta'/\tau_w)dp/dx$, where δ' represents some effective face area over which the pressure acts, represents the ratio of forces acting on the layer; and if this is held constant, the flow should have a constant history and therefore be in equilibrium. The choice of the proper quantity, δ' , was not known when the experiments were performed, and the attainment of equilibrium

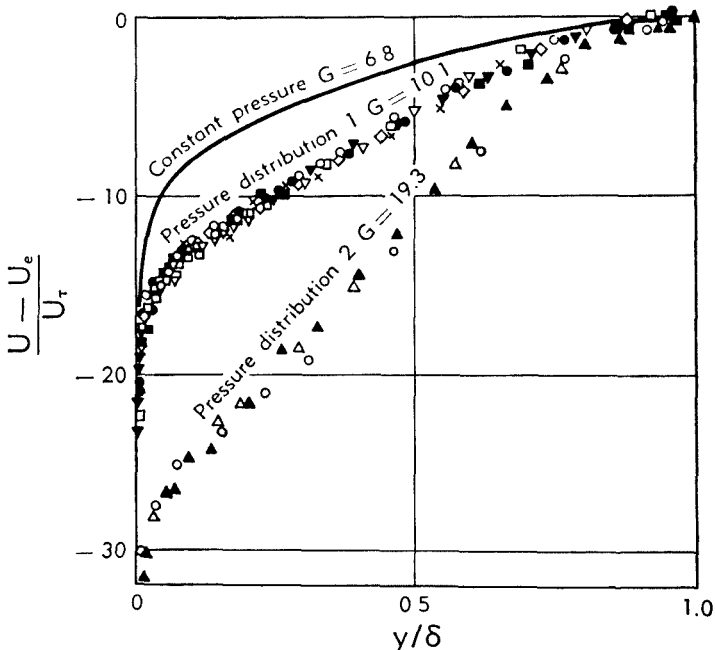


Fig. B,20a. Equilibrium boundary layer profiles on the basis of the velocity-defect law, after Clauser [72].

conditions proceeded on a cut-and-try basis. In a later article [72] Clauser concluded that the proper parameter was $(\delta^*/\tau_w)dp/dx$. Studies were conducted for two pressure distributions, designated as pressure distribution 1, corresponding to a mild adverse gradient, and pressure distribution 2, corresponding to a considerably stronger adverse gradient but not sufficient to cause separation. The resulting mean velocity profiles are shown in Fig. B,20a compared to a constant pressure profile.

Due to the uncertainty in defining δ , Clauser sought a more suitable thickness parameter. Obviously it was required that this be proportional to δ , since equilibrium profiles correlate on the basis of y/δ . The customary δ^* and θ were not suitable because their ratio to δ could be shown to

depend on c_f . Similarly the customary shape parameter H was found to be unsuited to equilibrium profiles. He therefore adopted as the thickness parameter

$$\Delta = \int_0^\infty \frac{U_\infty - U}{U_\infty} dy \quad (20-1)$$

and as integral shape parameter

$$G = \int_0^\infty \left(\frac{U_\infty - U}{U_\infty} \right)^2 dy / \int_0^\infty \frac{U_\infty - U}{U_\infty} dy = \int_0^\infty \left(\frac{U_\infty - U}{U_\infty} \right)^2 d\left(\frac{y}{\Delta}\right) \quad (20-2)$$

Their relations δ^* , θ , and H are

$$\delta^* = \sqrt{\frac{c_f}{2}} \Delta \quad (20-3)$$

$$\theta = \sqrt{\frac{c_f}{2}} \left(1 - G \sqrt{\frac{c_f}{2}} \Delta \right) \quad (20-4)$$

$$H = \frac{1}{(1 - G \sqrt{c_f/2})} \quad (20-5)$$

The reader is referred to the original paper for a more detailed discussion of these parameters. The logarithmic plot of the data in terms of

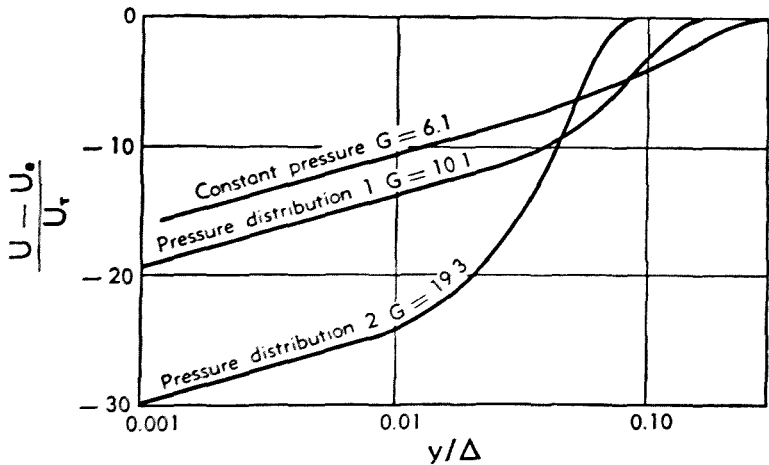


Fig. B,20b. Logarithmic plot of equilibrium velocity profiles using the Clauser thickness parameter Δ , after Clauser [83].

y/Δ is given here in Fig. B,20b. It is seen that near the wall the defect law conforms to the logarithmic law, as it must according to the arguments of Art. 17 if it overlaps the region in which the law of the wall is valid. This would be true, however, whether equilibrium existed or not, but

B · TURBULENT FLOW

without equilibrium a family of curves instead of a single curve would be obtained for any one pressure distribution. The parameters for these curves are:

	G	Δ/δ
Constant pressure	6.1	3.6
Pressure distribution 1	10.1	6.4
Pressure distribution 2	19.3	12.0

We shall return to Fig. B,20b in Art. 23 in connection with the universal skin friction law proposed by Clauser for equilibrium flows.

Another interesting fact brought out by Clauser's investigation is that equilibrium profiles do not conform to the H -parameter family of profiles shown in Fig. B,19a. Comparisons at two values of H are shown in Fig. B,20c. It will be seen that nonequilibrium profiles are considerably more

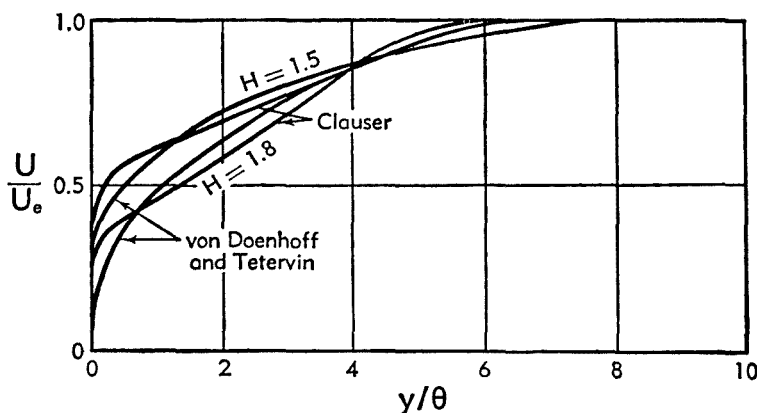


Fig. B,20c. Comparison of equilibrium profiles and von Doenhoff-Tetervin one-parameter profiles, after Clauser [83].

rounded than equilibrium profiles. Furthermore H remained nearly constant with downstream distance for equilibrium profiles, whereas H increases progressively for nonequilibrium profiles. This suggests that the increase in δ^* is slower and therefore that mixing is more thorough when equilibrium exists. This may merely mean that the imposed changes from section to section are now slow enough for the turbulent mixing to better keep pace. It may also mean that the mixing rates are higher for equilibrium than for nonequilibrium flow. In this connection information on turbulent structure is needed. A start in this direction was made by Ruetenik and Corrsin [90] who investigated equilibrium turbulent flow in a channel with a 1-degree half angle of divergence. Even for this small divergence, the average turbulent energy was found to be greater than that for a parallel channel by a factor of about 3. However, what is still needed is information of this sort to compare equilibrium and non-equilibrium flows.

The reader is referred to Clauser's paper [83] for a number of significant facts brought to light in his investigation. One of these concerned the downstream instability of a turbulent boundary layer with a large adverse pressure gradient. When the pressure gradient was small, no difficulty was experienced in adjusting the pressure distribution to obtain a desired equilibrium profile; but when it was large, great difficulty was experienced. He attributes the condition for large pressure gradients to a downstream instability, meaning that a change, say in the local gradient or in θ , made at one point would produce further changes downstream as the layer developed, rather than become damped out. This is an instability in x , not in time.

B,21. Law of the Wake According to Coles. In the short space of this article it is impossible to cover adequately the careful and extensive study which led Coles [85] to propose the law of the wake as an extension to the law of the wall. After having examined practically all available experimental data on turbulent boundary layers in terms of the logarithmic form of the law of the wall, expressed by Eq. 19-2, and noting the universal agreement with the law near the wall and the characteristic departure from it away from the wall, he concluded that the flow had a wakelike character, modified in various degrees by wall constraints. He concluded further that the wakelike form could be reduced to a second universal similarity law which he called the "law of the wake." A linear combination with the law of the wall was then proposed as an over-all similarity law representing the complete profile for equilibrium and non-equilibrium flows alike.

Attempts to generalize the law of the wall and the defect law so as to fit experimental results are not new. Millikan [73], for example, proposed forms to fit the distribution in pipes and channels. Others have expressed and employed ideas bearing certain similarities to the present one, those known being Lees and Crocco [91], Ross and Robertson [93], and Rotta [93]. Coles, however, appears to have been the first to show evidence of a universal wake law and to give it a rational physical explanation.

In general form the mean velocity profile in turbulent shear flow may be expressed as

$$\frac{U}{U_\tau} = f\left(\frac{U_\tau y}{\nu}\right) + h(x, y) \quad (21-1)$$

For equilibrium flows it is found experimentally that Eq. 21-1 may be written

$$\frac{U}{U_\tau} = f\left(\frac{U_\tau y}{\nu}\right) + g\left(\pi, \frac{y}{\delta}\right) \quad (21-2)$$

where π is a parameter which is independent of x and y for a specific

B · TURBULENT FLOW

situation and pressure distribution. The defect law is correspondingly expressed as

$$\frac{U_e - U}{U_r} = F\left(\pi, \frac{y}{\delta}\right) \quad (21-3)$$

Coles concluded from his survey of existing data that the central problem was not so much a study of the defect function F as a study of the original function $g(\pi, y/\delta)$ which gives the departure of the mean velocity profile from the logarithmic law of the wall. Since the characteristic departure was obviously not confined to equilibrium flows, the mean-velocity profile was expressed in the form

$$\frac{U}{U_r} = f\left(\frac{U_r y}{\nu}\right) + \frac{\pi(x)}{K} \omega\left(\frac{y}{\delta}\right) \quad (21-4)$$

where K is a constant, $\pi(x)$ denotes that π is now in general a function of x , and $\omega(y/\delta)$ is a universal wake function common to all two-dimensional turbulent boundary layer flows.

The term

$$\frac{\pi(x)}{K} \omega\left(\frac{y}{\delta}\right)$$

in Eq. 21-4 gives the departure from the logarithmic law of the wall, i.e. from

$$\frac{U}{U_r} = \frac{1}{K} \ln\left(\frac{U_r y}{\nu}\right) + c$$

where, according to Coles, $K = 0.4$ and $c = 5.10$ (Eq. 19-2).

From an analysis of experimental data, Coles found the form of $\omega(y/\delta)$ as given in Fig. B.21a, in which $\omega(y/\delta)$ has been subjected to the normalizing conditions $\omega(0) = 0$, $\omega(1) = 2$, and $\int_0^1 \omega(y/\delta) dy = 1$. When plotted against y/δ these curves have a nearly symmetrical S shape; and, due to the normalization, have the maximum value of 2 at $y/\delta = 1$. The curves obtained from Clauser's equilibrium profiles and the one obtained from Wieghardt's data, which Coles finds to be also an equilibrium flow, are plotted against the parameter $yU_r/(\delta^* U_e)$, which is equal to y/Δ in Clauser's notation. Included in this set are data from nonequilibrium profiles and the data of Liepmann and Laufer [94] for a region of turbulent mixing between a uniform flow and a fluid at rest.

The general working form of Eq. 21-4 may be written

$$\frac{U}{U_r} = \frac{1}{K} \ln\left(\frac{U_r y}{\nu}\right) + c + \frac{\pi(x)}{K} \omega\left(\frac{y}{\delta}\right) \quad (21-5)$$

where the constants K and c have the numerical values as given above. In order to use this formula, $\pi(x)$ must be known. It follows from Eq

21-5, using the normalizing condition $\omega(1) = 2$, that

$$\frac{U_*}{U_r} = \frac{1}{K} \ln \left(\frac{U_r \delta}{\nu} \right) + c + \frac{2\pi(x)}{K} \quad (21-6)$$

where

$$\frac{U_*}{U_r} = \sqrt{\frac{2}{c_f}}$$

Thus Eq. 21-6 is an expression for $\pi(x)$ in terms of the skin friction coefficient c_f . For other relationships and a tabulation of $\omega(y/\delta)$ and related functions the reader is referred to Coles' original paper [85].

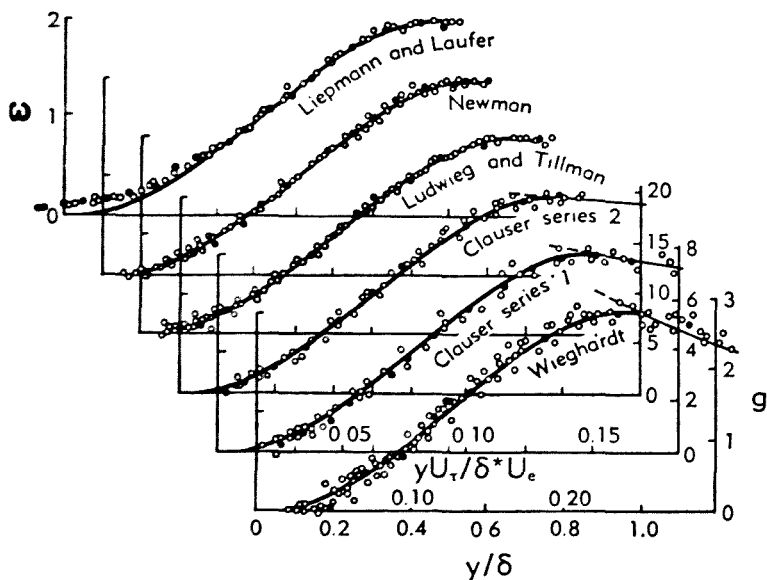


Fig. B,21a. The law of the wake, after Coles [85].

Coles found that in most cases (Eq. 21-5) fitted available experimental data on velocity distributions well and concluded, for unseparated flows at least, that the wake hypothesis appeared to be a useful concept. The analytic character of the method enabled him to express also the distribution of shear stress across the boundary layer. Computed distributions represented observations, except where the adverse pressure gradients were large. Here there were large discrepancies, reminiscent of those obtained by using the momentum equation.

The general success of the method led Coles to suggest that yawed or three-dimensional flows might be usefully represented by universal functions considered as vector rather than scalar quantities. For further discussions along these lines the reader is again referred to the original paper.

It is, of course, not uncommon to find empirical formulas with enough adjustable constants to fit experimental results. In the present case, however, the formula, with a specified function $\omega(y/\delta)$ and constants previously specified in the law of the wall, stands the test of a wide variety of conditions. In addition the present similarity law appears to be based on meaningful physical concepts, which may be described as follows.

It is easily seen that a wake is a natural consequence of earlier frictional constraints no matter how they may have arisen. There is therefore coming from upstream a flow of wakelike character, modified obviously by the remnant of upstream effects which caused it and by the local effects which distort the profile so that the velocity approaches zero at the wall. The remarkable thing was that Coles could extract S-shaped profiles typical of the pure wake component.

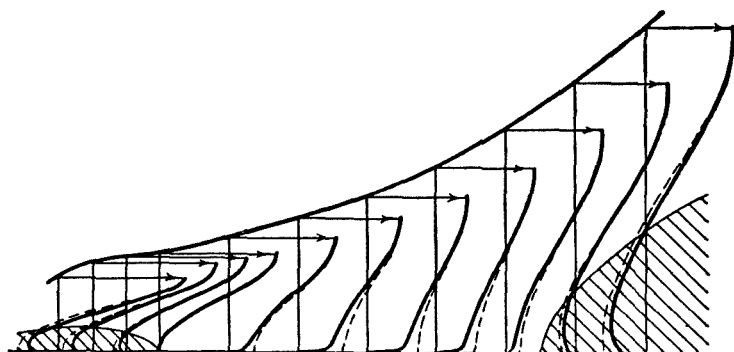


Fig. B,21b. Mean velocity profiles of hypothetical boundary layer, after Coles [85].

No claim is made that the turbulent structure is the same as that of a real wake. From the limited information available it appears that wake structure is coarser (has larger eddies) than boundary layer structure. However, the law of the wake may be interpreted as a manifestation of a large scale mixing process in which stress-controlling motions are independent of viscous effects. The wall effect, as we already know, superposes a viscous effect which increases in magnitude as the wall is approached.

The concept is best illustrated by the diagram of a hypothetical boundary layer used by Coles, reproduced here in Fig. B,21b. The figure shows velocity profiles for various values of x in a flow proceeding from separation to separation through a region of attached flow. The dashed lines denote the wakelike component represented by the function $\omega(y/\delta)$. At points of separation or reattachment we find the wake component only. In regions of attachment we see the effect of the wall friction, and the requirement of vanishing velocity at the wall being met by a sharp drop to zero at the wall.

B,22. Mixing Length and Eddy Viscosity in Boundary Layer Flows. As mentioned in Art. 3 and 10, the transport of momentum by turbulent motions may be regarded as involving an eddy viscosity. We shall briefly reexamine the associated concepts in the light of certain known facts about the flow in various parts of the boundary layer.

In turbulent boundary layers three fairly distinct regions are easily recognized. First there is the laminar sublayer which is typically 0.01 to 0.001 of the total thickness of the layer. Beyond this is a turbulent region which extends to 0.1 to 0.2 of δ and comprises the inner part of the layer where the logarithmic law is valid and the mean flow is virtually unaffected by pressure gradient. A short time response and rapid adjustment to local conditions are also characteristic of this region (see discussion by Clauser [72]). Finally, there is the outer 0.8 to 0.9 of the layer where the eddies are limited in lateral extent only by the confines of the layer and mixing is relatively free. In the laminar sublayer molecular diffusion predominates, being exclusively this at the wall. Turbulent diffusion progressively increases as we enter the logarithmic region from the wall side and soon predominates over molecular diffusion. For virtually everything except the laminar sublayer the transfer processes should be governed by a property of the motion. We wish to see whether this property may be legitimately and usefully expressed in terms of an eddy viscosity, ϵ_μ .

Dimensionally, ϵ_μ is a product of density, velocity, and length. According to the mixing length theory

$$\epsilon_\mu = \rho \bar{v} l \quad (22-1)$$

where v is the y component of turbulent velocity and l is the reach of a turbulent motion while it has the velocity v and is called the mixing length. Prandtl's assumption is that $v = l dU/dy$ and $l = c_2 y$ (see Art. 10). It is implied in this assumption that the correlation between v and l is absorbed into the value of l .

Using these assumptions and assuming further that τ is independent of y and equal to τ_w , the value at the wall, we find the well-known expression

$$\frac{\tau_w}{\rho} = c_2^2 y^2 \left(\frac{dU}{dy} \right)^2$$

or using $U_*^2 = \tau_w/\rho$

$$U_* = c_2 y \frac{dU}{dy} \quad (22-2)$$

This expression may be integrated to give the velocity distribution if we know the lower limits of y and U . These are their values at the edge of the sublayer, which may be found from Eq. 16-2 and written in terms of

B · TURBULENT FLOW

a free constant: $y_t = cv/U_\tau$ and $U_t = cU_\tau$. If we now integrate Eq. 22-2 as follows:

$$\frac{1}{c_2} \int_{y_t}^y \frac{dy}{y} = \frac{1}{U_\tau} \int_{U_t}^U du$$

we obtain exactly the law of the wall

$$\frac{U}{U_\tau} = \frac{1}{c_2} \ln \frac{U_\tau y}{v} + \text{const}$$

where c_2 has the same numerical value as K .

If we assume at the outset, as Prandtl did also, that $v = U_\tau$, and again take $l = c_2 y$, we again obtain

$$U_\tau = c_2 y \frac{dU}{dy}$$

This is identical to Eq. 22-2 and again yields exactly the law of the wall.

It is time to examine the consequences of these results. Since the law of the wall is well founded and is one of the most universal features of turbulent flow, we cannot escape the conclusion that the above assumptions are valid for the region in which the logarithmic law is obeyed. We know, of course, that we must stay near the wall, if for no other reason than that τ changes with y . More specifically we may express the eddy viscosity

$$\frac{\epsilon_\mu}{\rho} = c_2 y U_\tau \quad (22-3)$$

in the region where the logarithmic law of the wall is valid.

Turning our attention to the outer 80 to 90 per cent of the layer, we find that both Townsend [1] and Clauser [72] have explored the possibility that ϵ_μ is constant in this region. Townsend employed the rather straightforward procedure of solving the boundary layer approximation of the equation of mean motion, considering both constant pressure flow and equilibrium flow with pressure gradient. We call attention here only to his treatment of the constant pressure case. When the constants involving ϵ_μ were chosen for the best fit of experimental results, fair agreement was found for $y/\delta > 0.05$. The principal defect was the usual one, namely that a constant ϵ_μ yielded too slow an approach to the free stream velocity. Evidently ϵ_μ effectively decreases near the outer edge, due no doubt to intermittency of turbulent flow. The extent and quality of the over-all agreement was, however, sufficiently good to show that an essentially constant and valid ϵ_μ is a physical reality in the turbulent parts of the flow beyond the logarithmic region.

Clauser employed the novel approach of making laminar profiles resemble the outer portion of the constant pressure turbulent profile when the laminar profiles were reduced to the basis of $(U - U_\infty)/U$, vs. y/δ .

He noted that the principal difference in appearance between constant pressure laminar profiles and turbulent profiles was that the turbulent profiles dropped so abruptly at the wall as to appear to extrapolate to a nonzero velocity at the wall, whereas laminar profiles went to zero much more gradually and did not give this impression. The characteristic shape of the turbulent profile arises from the circumstance that the laminar sublayer next to the wall and the flow adjacent to it has a lower viscosity than the eddy viscosity prevailing in the main body of the turbulent flow. Consequently a large part of the velocity change from the wall to the free stream occurs in this low viscosity region. If the same situation were made to prevail in a laminar layer, say by placing a layer of fluid of lower viscosity next to the wall, a laminar profile could be made to resemble a turbulent profile. Clauser therefore proceeded to simulate this condition in a family of laminar profiles obtained by solving the Blasius equation for slip velocities U_s at the wall, U_s/U_∞ amounting to 0, 0.2, 0.4, 0.5, 0.6, 0.7, and 0.8. He then attempted to collapse the family to a single curve by dividing $(U - U_s)/U_\infty$ and y/δ by suitable factors. Leaving details to the original paper [72], we merely point out the significant fact that exact coincidence proved to be impossible, but that two procedures each resulted in a narrow band of curves. Clauser concluded that the same basic dissimilarity would prevent turbulent profiles, which pertain to different values of U_s , from collapsing to a single curve on the basis of the velocity-defect law. Accordingly there is an almost-but-not-quite universal curve.

The next step was to relate the laminar profiles to turbulent profiles on a velocity-defect-law basis by an appropriate eddy viscosity, ϵ_μ . The appropriate velocity and length were chosen by the same reasoning process that leads to a reference velocity U_∞ and a reference length δ in the velocity-defect law, and ϵ_μ was expressed by

$$\frac{\epsilon_\mu}{\rho} = \alpha U_\infty \Delta$$

where α is a constant of proportionality to be determined. Since Δ is equal to $U_\infty \delta^*/U_\infty$ (see Art. 20)

$$\frac{\epsilon_\mu}{\rho} = \alpha U_\infty \delta^* \quad (22-4)$$

which is an expression for ϵ_μ in readily available quantities.

The original article must be consulted for the details of the fitting process and the curves showing comparisons with data of Fig. B,16. Best agreement was obtained with $\alpha = 0.018$. Considering that a narrow band of laminar curves is obtained rather than a single curve and that experimental data are expected to show a similar dispersion, the agreement is excellent for the outer 80 to 90 per cent of the layer. The method pro-

B · TURBULENT FLOW

posed for connecting the outer and inner portions is left to the original article.

A treatment of the same character was applied to equilibrium flows involving adverse pressure gradients. Again a good fit was obtained by assuming a constant eddy viscosity given by Eq. 22-4 even for near-separation profiles. Some of the more significant results of this work were: (1) that $(\delta^*/\tau_w)dp/dx$ proved to be the proper pressure gradient parameter which must be constant throughout an equilibrium layer, (2) that α turned out to be practically independent of pressure gradient (independent of the parameter $(\delta^*/\tau_w)dp/dx$) and to have the value of approximately 0.018 in all cases tested.

An interesting outcome of a constant α is a constant eddy Reynolds number. If such a Reynolds number is defined by

$$Re_\epsilon = \frac{\rho U_\infty \delta^*}{\epsilon_\mu}$$

we find from Eq. 22-4 that $Re_\epsilon = 1/\alpha$. Taking $\alpha = 0.018$, $Re_\epsilon = 56$. A constant eddy Reynolds number is just another way of expressing the behavior trend of all turbulent shear flows, namely a tendency for the transferring agents to be proportional to the length and velocity scales of the flow.

Most important of all is the evidence from these sources that ϵ_μ behaves in equilibrium flows toward mean-velocity distributions beyond the range of the logarithmic law as though it were constant. This cannot be taken as a sweeping generalization, but it furnishes good evidence that ϵ_μ is likely to have a strong leaning in this direction generally and therefore will have only a weak dependence on local conditions. This being so, there is little foundation for a mixing length theory in such regions, and it renders of little significance the various arguments about how mixing length should be expressed. The degree to which ϵ_μ is constant and the exactness with which a gradient type of diffusion is obeyed for coarse mixing are probably not sufficient to represent more sensitive quantities like shear stress distributions.

Near the wall the mixing length theory may be applied, and we see that a valid procedure starts with an expression for ϵ_μ that has a striking resemblance to that for the outer flow. The comparison is:

Inner flow $\frac{\epsilon_\mu}{\rho} = c_2 y U_\tau; \quad c_2 = 0.4$

Outer flow $\frac{\epsilon_\mu}{\rho} = \alpha U_\infty \Delta; \quad \alpha = 0.018$

In the first case the mixing scale is proportional to the distance from the wall; in the second case it is proportional to the thickness of the shear layer.

The foregoing considerations regarding a constant eddy viscosity are given more for the physical ideas that they embody than for any possible expediency in methods of computation.

B,23. Effect of Roughness. The treatment of roughness and its effects is rendered difficult and somewhat inexact by the varied geometrical forms of roughness and the variety of ways in which it may be distributed. Again we are confronted with a subject that cannot be treated adequately in a short space, and the reader can profit by consulting additional sources of information, such as [95,78,6,96,97].

The pattern of roughness studies was set largely by the extensive work of Nikuradse [95] on sand-grain roughness in tubes. Sand-grain roughness has been adopted as a standard in skin friction studies, and is taken to mean roughness elements consisting of grains, either being sand or like grains of sand, of nearly uniform size but generally of irregular shape spread with maximum density on a plain surface. The significant dimensions then reduce to one, this one being the mean height of the roughness element, denoted by k . It is customary to express the effect of an arbitrary type of roughness in terms of an equivalent sand-grain roughness. For example, the effect of a given distribution of rivets of height k , is reduced to the effect of equivalent sand roughness of height k . A number of such equivalents are given by Schlichting [96].

It has been found that the onset of an effect of sand-grain roughness on skin friction and on the flow near the wall depends on k relative to the thickness of the laminar sublayer. A more precise length, avoiding the arbitrariness of the sublayer thickness, is ν/U_r . Using this, the criterion becomes a roughness Reynolds number

$$\frac{U_r k}{\nu}$$

It has been found that below some value of this number roughness has no effect. The surface is then said to be aerodynamically smooth. Above this value an effect sets in, at first as a mixture of smooth-wall and rough-wall behaviors, involving both the roughness and viscous effects. When $U_r k / \nu$ reaches a sufficiently large value, the behavior is characteristic of the roughness only, becoming independent of viscosity. The final condition is termed "fully rough." When the final condition is reached, the laminar sublayer no longer exists since the particles themselves induce turbulent mixing by the flow about them. Broadly speaking, the foregoing is true of all types of roughness but the limits are different for different types.

We shall shortly return to these limits and the importance of the parameter $U_r k / \nu$, but first we turn our attention to the fully rough condition where viscosity no longer enters explicitly into the picture. Here

B · TURBULENT FLOW

τ_w depends on the velocity U at some small distance y from the wall and on k and ρ . By dimensional reasoning similar to that leading to Eq. 16-1 we find

$$\frac{U}{U_r} = f\left(\frac{y}{k}\right) \quad (23-1)$$

As we have already noted, the velocity-defect law is unaffected by roughness. Since it again develops that there exists a region of overlap where both laws are valid, a logarithmic function is indicated in Eq. 23-1, and the law may be written

$$\frac{U}{U_r} = \frac{1}{K} \ln\left(\frac{y}{k}\right) + \text{const} \quad (23-2)$$

where K is the same as that appearing in the smooth wall law and in the velocity-defect law.

Just as in the case of the smooth wall law there is a linear relationship between U/U_r and $\ln(y/k)$ only for the region of the wall, not throughout the whole boundary layer. Obviously there is some question about a suitable reference point from which to measure y . If y is not expressed correctly, the region that should be linear becomes curved. Experimentally this is used to find the origin of y . No cases are known where the origin did not lie somewhere between the top and bottom of the roughness elements.

The well-known skin friction law for fully rough walls is obtained by adding Eq. 23-2 and the defect law (Eq. 17-4) and using the relationship $U_s/U_r = \sqrt{2/c_f}$. The result is

$$\sqrt{\frac{2}{c_f}} = \frac{1}{K} \ln\left(\frac{\delta}{k}\right) + \text{const} \quad (23-3)$$

Since the defect law is affected by the pressure gradient, Eq. 23-3 applies only to cases where the effect of the pressure gradient is negligible. The effect of the free stream conditions is also present, but this effect is small and may be absorbed in the constant.

The effect of roughness is seen to depend on its height compared to the boundary layer thickness. The effect is independent of Reynolds number. These two circumstances illustrate in a very direct way an inherent characteristic of turbulent diffusion in shear flow, namely that the length scale in eddy diffusion processes tends to remain proportional to the thickness of the shear layer. In other words, mixing tends to take place on a scale of coarseness proportional to the boundary layer thickness, or the radius of a pipe. Ordinarily this rule cannot hold true in the immediate neighborhood of a wall where the turbulent motions are influenced by the presence of the wall; but if flow about roughness elements introduces a scale of mixing proportional to the scale of the shear layer,

then the rule does hold true for the entire layer. This is true when k is proportional to δ , and at the same time $U_\tau k/\nu$ is sufficiently large to make viscous effects negligible. If we fully grasp the foregoing facts, it does not seem so strange that a small quantity like k should be associated with a much larger quantity like δ and furthermore occupy a position of equal importance.

An important characteristic of the roughness effect, first pointed out by Nikuradse [95], is a downward shift of the velocity near the wall from that corresponding to the smooth wall condition at a given value of U . This is understandable in view of the fact that the mixing action of the roughness elements increases the rate of momentum transfer, and a lower velocity near the wall is required to keep U the same. In connection with this downward shift it is necessary to recall that we now have two wall laws:

$$\text{Smooth wall} \quad \frac{U}{U_\tau} = \frac{1}{K} \ln \left(\frac{U_\tau y}{\nu} \right) + \text{const}$$

$$\text{Fully rough wall} \quad \frac{U}{U_\tau} = \frac{1}{K} \ln \left(\frac{y}{k} \right) + \text{const}$$

Both are dependent on conditions near the wall and both are independent of stream conditions, such as boundary layer thickness and pressure gradient. If we subtract the second equation from the first and call the difference $\Delta U/U_\tau$, the downward shift in velocity is found to be

$$\frac{\Delta U}{U_\tau} = \frac{1}{K} \ln \left(\frac{U_\tau k}{\nu} \right) + \text{const} \quad (23-4)$$

This equation applied only for values of $U_\tau k/\nu$ for which the surface is fully rough.

The behavior of $\Delta U/U_\tau$ over a wide range of values of $U_\tau k/\nu$ has been determined by a number of investigators. A representative summary of results given by Clauser [72] is reproduced in Fig. B,23a. This figure is very instructive. It shows the behavior of different kinds of roughness through the range smooth, partially rough, and fully rough conditions. The limits of such ranges can be judged from this figure. Where the roughness elements are of uniform size, as for example uniform sand, the limit below which the wall is smooth is reasonably definite. It appears to be $U_\tau k/\nu \approx 4$. However, when the roughness consists of a mixture of sizes or is not densely packed and a fictitious k is chosen to bring the curves into coincidence in the fully rough regime, then the lower limit cannot be specified. The lower limit for the fully rough condition is seen to be somewhere between 50 and 100.

It is interesting to interpret these limits in terms of $k/\delta_{\text{laminar}}$, where δ_{laminar} is the thickness of the laminar sublayer on a smooth wall. The sublayer is

inherently an indistinctly defined region, but taking the conventionally defined sharp limit given by

$$\delta_{lam} = 11.5 \frac{\nu}{U_r}$$

the effect of roughness begins when $k/\delta_{lam} \approx \frac{1}{3}$ and the fully rough regime sets in when k/δ_{lam} is between 4 and 8. These figures tell us little that could not be inferred, namely that the roughness elements must be well

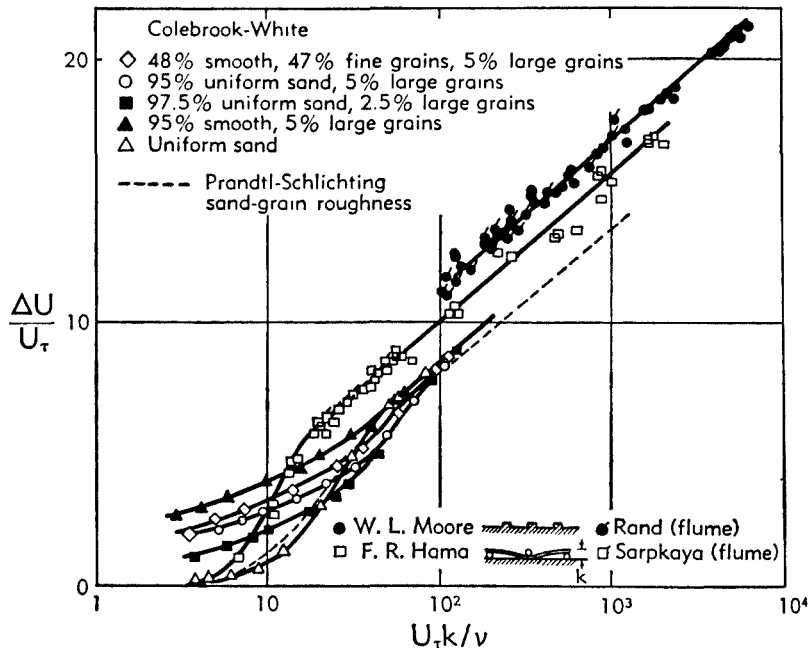


Fig. B.23a. Effect of roughness on universal turbulent velocity profile, after Clauser [72].

buried in the laminar sublayer to have no effect and must extend well above it to completely eradicate viscosity effects.

It may be shown rather simply that in order for a surface to remain aerodynamically smooth the roughness must decrease almost inversely with the free stream velocity. If the critical value is designated as k_{cr} and the limit is taken as $U_r k_{cr}/\nu = 4$, then

$$k_{cr} = 4 \frac{\nu}{U_r} = 4 \left(\frac{\nu}{U_s} \right) \sqrt{\frac{2}{c_f}}$$

where c_f is the smooth wall coefficient which varies with U_s but only slowly. It is also apparent from the slow variation of c_f that the requirements on k_{cr} are nearly as stringent on a large body as on a small one.

Returning to Fig. B.23a it is significant that the data conform to the

law (Eq. 23-4) for the fully rough condition. This means that the linear portion of the velocity distribution curve for a rough wall parallels that for a smooth wall but is stepped down by an amount $\Delta U/U_r$. With experimentally determined values of $\Delta U/U_r$, the velocity distribution for a fully rough wall may be expressed by the aid of the smooth wall formula. For this we use Eq. 19-1 containing the constants given by Clauser. The rough wall formula is then

$$\frac{U}{U_r} = 5.6 \log \left(\frac{U_r y}{\nu} \right) - \left(\frac{\Delta U}{U_r} \right) + 4.9 \quad (23-5)$$

A skin friction formula results at once by subtracting Eq. 23-5 from the logarithmic form of the velocity-defect law. Clauser [83] has obtained a universal law applicable to equilibrium flows including the effect of the pressure gradient by noting, on the basis of Fig. B,20b, that a pressure gradient also has the effect of producing a step-down in the velocity, $\Delta U_2/U_r$. Accordingly he writes the generalized defect law for equilibrium flows

$$\frac{U - U_s}{U_r} = 5.6 \log \left(\frac{y}{\Delta} \right) - \left(\frac{\Delta U_2}{U_r} \right) + 0.6 \quad (23-6)$$

Since Eq. 23-5 is unaffected by the pressure gradient, and Eq. 23-6 takes the effect of the pressure gradient into account, a universal skin friction law results by subtraction of Eq. 23-6 from Eq. 23-5. The end result may be written

$$\sqrt{\frac{2}{c_f}} = 5.6 \log Re_{t*} - \frac{\Delta U}{U_r} \left(Re_k \sqrt{\frac{c_f}{2}} \right) + \frac{\Delta U_2}{U_r} (G) + 4.3 \quad (23-7)$$

where $\sqrt{c_f/2} = U_r/U$, $\delta^* = \sqrt{c_f/2} \Delta$, $Re_k = U_* k / \nu$, $Re_{t*} = U_* \delta^* / \nu$, and $(\Delta U/U_r)(Re_k \sqrt{c_f/2})$ and $(\Delta U_2/U_r)(G)$ denote functions of the arguments. The integral shape parameter G is defined in Art. 20.

In order to put Eq. 23-7 into a more convenient form for engineering applications, Clauser proposes the introduction of two auxiliary factors

$$F_1 = 10^{\Delta U / 6.6 U_r}, \quad F_2 = 10^{\Delta U_2 / 6.6 U_r}$$

which permit Eq. 23-7 to be written

$$\sqrt{\frac{2}{c_f}} = 5.6 \log \left(Re_{t*} \frac{F_2}{F_1} \right) + 4.3 \quad (23-8)$$

Factors F_1 and F_2 have been determined by Clauser using Prandtl-Schlichting data for sand-grain roughness for the calculation of F_1 and his own data for equilibrium profiles for the calculation of F_2 . These are presented in Fig. B,23b and B,23c. A plot of Eq. 23-8 for F_1 and F_2 equal to unity is given in Fig. B,23d. If a fictitious Reynolds number, $Re_t F_2/F_1$, is first obtained, c_f may be found from this figure. Since values of F_2 are based on only two equilibrium pressure distributions, more data are to

B · TURBULENT FLOW

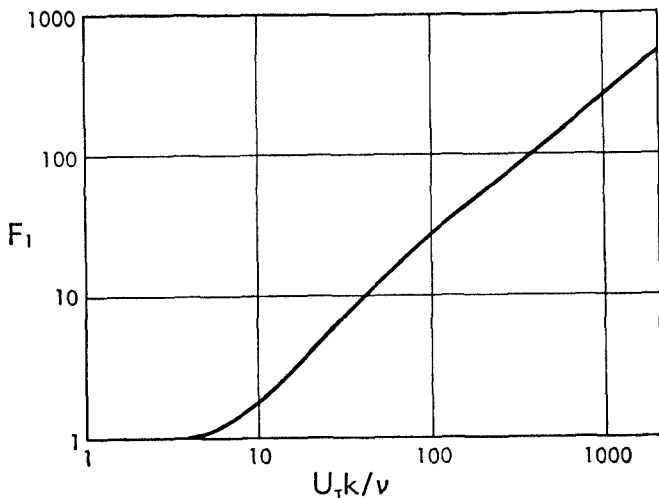


Fig. B.23b. Factor for effect of sand-grain roughness on local skin friction coefficient, after Clauser [83].

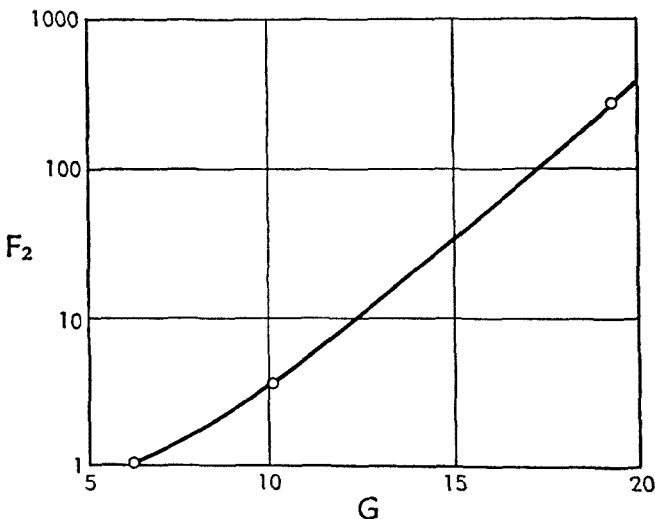


Fig. B.23c. Factor for effect of pressure gradient on local skin friction coefficient, after Clauser [83].

be desired in order to test the universality of the method. The term "universal" is here used in the restricted sense of applying only to equilibrium boundary layers.

The effect of roughness on velocity distribution is reflected in a raising of the shape parameter H . This effect has been shown by Hama [97] for a wide range of conditions. Since Clauser's integral shape parameter G is

not affected, the variation of H may be expressed as a function of c_f , by Eq. 20-5 for both smooth and rough walls.

It is worth noting before we leave the subject that experimental determinations of roughness effect in terms of $\Delta U/U_r$ vs. $U_r k/\nu$ may be made optionally in boundary layers, pipes, or channels. Application of

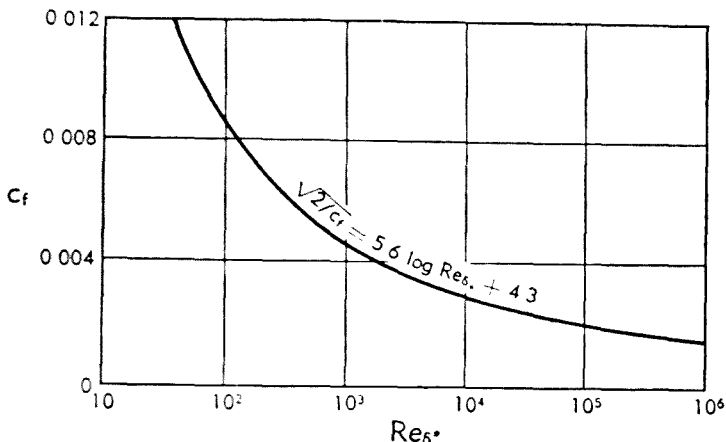


Fig. B.23d. Local skin friction coefficient for smooth plates with constant pressure, after Clauser [83].

the results then merely requires the introduction of $\Delta U/U_r$ into the appropriate smooth wall formula.

B.24. Integral Methods for Calculating Boundary Layer Development. A number of methods have been proposed for calculating boundary layer parameters and separation as functions of x for boundary layers developed on a smooth wall in the presence of pressure gradients. Most of the attention has been given to cases involving adverse pressure gradients, and the methods are mostly restricted to two-dimensional flow, although sometimes the problem is set up so as to include axially symmetric flow for the conditions where the boundary layer is thin compared to the radius of the body about its axis.

It is generally assumed that the boundary layer is so thin that pressure changes across it may be neglected. Then the equations of motion and continuity for two-dimensional flow reduce to Eq. 8-1, 8-2, and 8-3. For incompressible flow, and by neglecting viscous stress and turbulent normal stresses, these become

$$U \frac{\partial U}{\partial x} + V \frac{\partial U}{\partial y} = - \frac{1}{\rho} \frac{\partial p}{\partial x} + \frac{1}{\rho} \frac{\partial \tau}{\partial y} \quad (24-1)$$

$$\frac{\partial U}{\partial x} + \frac{\partial U}{\partial y} = 0 \quad (24-2)$$

B · TURBULENT FLOW

By integrating Eq. 24-1 from $y = 0$ to $y = \delta$, using Eq. 24-2 to eliminate V , and Bernoulli's equation to express p in terms of the local free stream velocity U_* , the Kármán integral relation is obtained. The integrals turn out to be the well-known expressions for δ^* and θ . By introducing these and their ratio H , the Kármán momentum equation is obtained. It may be written as follows by again using Bernoulli's equation to restore p :

$$\frac{d\theta}{dx} = \frac{(H + 2)}{2} \frac{\theta}{q} \frac{dp}{dx} + \frac{\tau_w}{2q} \quad (24-3)$$

where $q = \frac{1}{2}\rho U_*^2$.

Eq. 24-3 is the starting point for most known methods. These proceed on the basis of some empirically determined form parameter for the velocity profile. The earlier methods such as those of Buri [98] and Gruschwitz [99] seem now to be mainly of historical interest. Gruschwitz's method and his shape parameter,

$$\eta = 1 - \left(\frac{U}{U_*} \right)_{y=\theta}^2$$

found considerable use, but both have now been largely replaced by the method of von Doenhoff and Tetervin [84], or variations of it, employing H only.

Von Doenhoff and Tetervin [84] made what appears to be the most thorough search for a suitable form parameter. This resulted in the adoption of the parameter H and the single parameter family of profiles shown in Fig. B,19a. It is now clear from evidence previously cited that all profiles do not fit this pattern, and that any method based on such an assumption cannot be expected to give correct results under all conditions. Nevertheless the method of von Doenhoff and Tetervin has had certain successes and has appeared sufficiently promising to lead others to attempt to improve upon it.

The method is based on the assumption that it is only necessary to determine θ and H in order to establish the boundary layer characteristics. Since the momentum equation (Eq. 24-3) alone is not sufficient for this purpose, an auxiliary expression for H was set up. Recognizing that a sudden change in pressure should not produce a discontinuity in the velocity profile, it was assumed that the rate of change of H rather than H itself would depend on local forces, τ_w and dp/dx . When the ratio of these forces was expressed by

$$\frac{\theta}{q} \frac{dq}{dx} \frac{2q}{\tau_w}$$

it was found that $\theta dH/dx$ was a function of this ratio and also, to some extent, of H itself, but it was independent of Reynolds number. Using the Squire and Young formula (Eq. 18-10) for τ_w , thereby ignoring any

effect of pressure gradient on skin friction, von Doenhoff and Teterivin arrived at the following expression for $\theta dH/dx$:

$$\theta \frac{dH}{dx} = e^{4.680(H-2.975)} \left[-\frac{\theta}{q} \frac{dq}{dx} \frac{2q}{\tau_w} - 2.035(H - 1.286) \right] \quad (24-4)$$

Given dq/dx , the two equations (Eq. 24-4 and 24-3) were solved by a step-by-step procedure for θ and H as a function of x . Starting with some initial value, θ_0 and H_0 , $d\theta/dx$ and dH/dx were found. Each when multiplied by an increment of x and added to the initial values gave the next value of θ and H to repeat the process.

Garner [100] undertook to improve on the method of von Doenhoff and Teterivin by using different auxiliary expressions for skin friction and H , again disregarding the effect of pressure gradient on skin friction. The method, however, remains basically the same.

Tests of this general method have shown a closeness of agreement with observations sufficient to make it worthy of consideration when conditions are not out of the ordinary; that is, when profiles can be expected to have the form of Fig. B,19a. Since adverse pressure gradient dominates the development of the layer, the use of an incorrect expression for the skin friction apparently has minor consequences.

Teterivin and Lin [101] initiated a fresh attack on the problem, again built around the H -parameter family. They set up integral expressions for momentum, moment of momentum, and kinetic energy in a form sufficiently general to include axially symmetric flow as well as two-dimensional flow, subject to the restriction that δ is small compared to the radius of curvature about the axis of symmetry. Their principal objective was to avoid an empirical expression for H if possible. The moment of momentum equation was found to be best suited for this purpose, but it required auxiliary expressions for velocity and shear stress distributions across the layer. A power-law fitting of the H -parameter profiles was adopted as an approximate but reasonable procedure. More serious was insufficient information about the value and distribution of shear stress. While the work of Teterivin and Lin fell short of immediate success, it pointed the way to future progress.

It must be remembered that while τ_w may be reduced to small values by an adverse pressure gradient, τ may rise to large values away from the wall before falling to zero at the outer edge of the layer. Fediaevsky [102] proposed a method for calculating the distribution of τ/τ_w with y/δ employing a polynomial expression that would satisfy boundary conditions at the wall and the outer edge of the layer. Certain large discrepancies were observed between shear stress distributions calculated by this method and those directly measured by the hot wire method by Schubauer and Klebanoff [87]. Ross and Robertson [103] modified the Fediaevsky method and obtained some improvement in accuracy.

Two contributions following the general method proposed by Teterivin and Lin are those of Granville [104] and Rubert and Persh [140]. Granville's work suggested that the difficulty in using the momentum equation for H might be overcome. By examining a limited amount of experimental data he showed that the integral of the shearing stress across the layer in terms of y/δ^* was the same in adverse pressure gradients as in constant pressure flow. Rubert and Persh chose the kinetic energy equation for the determination of H and hence had to evaluate the integral of the dissipation across the layer. This they did empirically using experimental data for a variety of conditions. They also included the Reynolds normal stress in the momentum equation. Values of θ and H calculated by Rubert and Persh showed reasonably close agreement with experiment for two-dimensional boundary layers and flow in diffusers. Both of these methods draw on the work of Ludwig and Tillmann [89] for the shearing stress at the wall and the existence of the law of the wall in an adverse pressure gradient.

Two methods based on dividing the treatment between the inner part of the boundary layer and the outer part are those of Ross [141] and Spence [142]. Each uses a separate similarity for the inner and outer parts. Both use the law of the wall for the region next to the wall. Ross adopts a $\frac{1}{2}$ -power velocity-deficiency expression for the outer region with a new parameter D , thus avoiding the use of the shape parameter H . Spence retains the H -parameter for the outer region, but evaluates it by means of an expression for the velocity at the distance θ from the wall, obtained from the equation of motion formulated for the distance $y = \theta$.

The several methods here mentioned show that progress is being made on this difficult problem. In some cases more tests are needed to judge the amount of progress. There is general agreement that more information is needed on the behavior patterns of turbulent flow before a universally valid method can come within reach.

B.25. Three-Dimensional Effects. It may seem that undue attention is given to two-dimensional mean flows when in their totality all flows are three-dimensional. The justification for the convenience of avoiding the complications introduced by a third dimension is that motion in the third dimension is in many cases locally absent or so insignificant that two-dimensionality is an acceptable assumption. This fortunate circumstance comes about because boundary layers are usually thin compared to the expanse and radius of curvature of a wall.

Obviously there are many cases where the edges are too close to the region in question or the boundary layers are too thick for three-dimensional effects to be ignored even under local inspection. Common examples are flow in noncircular pipes, flow near wing tips, and flow near the

juncture between a wing and a body. Attention has already been called to the fact that three-dimensional effects are hard to avoid in regions of adverse pressure gradient. They become very pronounced in regions of flow separation. On low aspect ratio wings at large angles of attack, separation often manifests itself as a curving of the flow in a continuous fashion to form the large scale trailing vortices. Important as these cases are, we shall regard them as special problems beyond the scope of the present treatise.

Some mention will be made of a particular three-dimensionality known as yawed flow. This is the condition where the leading edge of a two-dimensional body is at an angle other than normal to the mean flow, such as might be represented by an infinitely long swept wing. In such cases deviations from the mean flow direction occur in the boundary layer. Among the first quantitative measurements to show the effects on swept wings are those of Kuethe, McKee, and Curry [105].

In the case of laminar yawed flow it is well known, and readily shown by the equations of motion, that the boundary layer development with distance normal to the leading edge and the velocity components associated with this direction are independent of yaw. In other words, boundary layer thickness and velocity profiles, based on the stream component normal to the leading edge are independent of the flow parallel to the leading edge. This is known as the "independence principle."

According to the best evidence at hand, the independence principle does not apply in turbulent flow. The experiments of Ashkenas and Riddell [106] conducted on yawed flat plates show that the thickness of the turbulent boundary layer at a given streamwise distance from the leading edge increases with the angle of yaw. A 1-inch strip of sandpaper glued to the surface near the leading edge made turbulent flow a certainty from that point on and gave an essentially fixed virtual origin for the boundary layer. In terms of distance ξ from the virtual origin parallel to the free stream direction, the displacement thickness δ^* was found to be given by

$$\delta^* = \frac{0.046\xi}{(\cos \theta)^{\frac{1}{4}}} \left(\frac{U_\infty \xi}{\nu} \right)^{-\frac{1}{4}}$$

where θ is the yaw angle. Except for the factor $(\cos \theta)^{\frac{1}{4}}$, this is the ordinary expression for δ^* in terms of wall length traversed by the flow. According to Ashkenas and Riddell, yawing would have the effect of decreasing δ^* at a given streamwise distance if the independence principle were to apply. The arguments leading to this conclusion are left to the original paper.

The above result is in disagreement with that of Young and Booth [107] who concluded that the independence principle does apply in the

turbulent boundary layer. Ashkenas and Riddell have noted this disagreement and have pointed out possible causes of error in the experiments of Young and Booth.

Even without putting this case to actual test, it may be seen that the independence principle would not be expected to apply in turbulent flow. Let us imagine a wind tunnel experiment in which we have a flat belt passing through slots in the tunnel walls and running diametrically across the stream with the stream crossing it edgewise. If the boundary layers on the two sides of the belt are laminar, running the belt has no effect on the boundary layer associated with the action of the stream, unless of course the belt is running so fast that heating effects change the viscosity and density of the air. If, on the other hand, the boundary layers are turbulent, then running the belt increases the turbulence because of the greater velocity relative to the surface. The eddy viscosity is thereby increased, and this increase affects all motions. To the flow component normal to the leading edge, the boundary layer now exhibits greater eddy viscosity. The friction to air flowing over the belt is thereby increased and the thickness of the boundary layer is increased correspondingly.

CHAPTER 5. FREE TURBULENT FLOWS

B.26. Types and General Features. The term "free turbulent flows" refers to flows which are free of confining walls and exist in shear motion relative to a surrounding fluid with which they mix freely. The flows of common technical interest are jets, wakes, and mixing zones between two uniform streams moving with different relative velocity. Problems of technical interest are the rate of spreading with distance from a source of the flow, velocity distributions, and the manner in which other transported quantities such as heat and matter are distributed and mixed with a surrounding medium.

A characteristic common to this class of flows is a lack of viscous constraints on the mean motion in all parts of the field when the Reynolds number is sufficiently high. This condition is practically always fulfilled unless the Reynolds number is so low that the turbulent regime cannot exist at all. In the case of mixing zones, jets, and two-dimensional wakes this condition never degenerates; for no matter how feeble the relative motion may become with increasing distance from the source, the Reynolds number either remains constant or increases due to the increase in size. More specifically the Reynolds number increases with distance for mixing zones and two-dimensional jets, and remains constant for axially symmetric jets and two-dimensional wakes. The axially symmetric wake is the one exception, for here the rate of decay of mean motion (and

turbulent boundary layer. Ashkenas and Riddell have noted this disagreement and have pointed out possible causes of error in the experiments of Young and Booth.

Even without putting this case to actual test, it may be seen that the independence principle would not be expected to apply in turbulent flow. Let us imagine a wind tunnel experiment in which we have a flat belt passing through slots in the tunnel walls and running diametrically across the stream with the stream crossing it edgewise. If the boundary layers on the two sides of the belt are laminar, running the belt has no effect on the boundary layer associated with the action of the stream, unless of course the belt is running so fast that heating effects change the viscosity and density of the air. If, on the other hand, the boundary layers are turbulent, then running the belt increases the turbulence because of the greater velocity relative to the surface. The eddy viscosity is thereby increased, and this increase affects all motions. To the flow component normal to the leading edge, the boundary layer now exhibits greater eddy viscosity. The friction to air flowing over the belt is thereby increased and the thickness of the boundary layer is increased correspondingly.

CHAPTER 5. FREE TURBULENT FLOWS

B,26. Types and General Features. The term "free turbulent flows" refers to flows which are free of confining walls and exist in shear motion relative to a surrounding fluid with which they mix freely. The flows of common technical interest are jets, wakes, and mixing zones between two uniform streams moving with different relative velocity. Problems of technical interest are the rate of spreading with distance from a source of the flow, velocity distributions, and the manner in which other transported quantities such as heat and matter are distributed and mixed with a surrounding medium.

A characteristic common to this class of flows is a lack of viscous constraints on the mean motion in all parts of the field when the Reynolds number is sufficiently high. This condition is practically always fulfilled unless the Reynolds number is so low that the turbulent regime cannot exist at all. In the case of mixing zones, jets, and two-dimensional wakes this condition never degenerates; for no matter how feeble the relative motion may become with increasing distance from the source, the Reynolds number either remains constant or increases due to the increase in size. More specifically the Reynolds number increases with distance for mixing zones and two-dimensional jets, and remains constant for axially symmetric jets and two-dimensional wakes. The axially symmetric wake is the one exception, for here the rate of decay of mean motion (and

turbulence) exceeds the growth in diameter, and the Reynolds number tends toward an eventual zero value.

We are therefore dealing with a class of flows in which the effects of viscosity are removed from those turbulent motions which control the mean motion and are relegated to the small scale eddies which take part in the final decay and the production of heat. In this respect the flow fields are subject to a controlling mechanism similar to that found in the outer regions of a turbulent boundary layer, but lacking the influence of a wall such as prevails to varying degrees in the boundary layer. Once the flows have attained a fully developed state, they remain similar throughout upon subsequent development, merely changing scales of length and intensive properties.

The fully developed state is an asymptotic condition reached only at some distance from a body in the case of a wake and from a nozzle in the case of a jet. Since the initial conditions in these two cases are vastly different, the distance for their effect to disappear is also different. Behind a body the flow is highly agitated by a succession of eddies comparable to the diameter of the body, and this coarse scale motion persists for a long distance. Townsend [108], in his investigation of the plane wake behind a cylinder, finds that the mean wake flow reaches similarity only after 100 cylinder diameters downstream, and that complete statistical equilibrium in the turbulent motions is not reached short of 1000 diameters. At a nozzle the initial jet consists of a potential core of relatively smooth flow, or a flow characteristic of the internal flow, bounded by a layer in which free mixing begins. Kuethe [109] finds that the potential core of a round jet is consumed between 4 and 5 nozzle diameters downstream of the plane of the nozzle, and that fully developed jet flow is established at 8 nozzle diameters.

We shall here be concerned mainly with fully developed characteristics and shall attempt to describe the principal ones, paying most attention to the plane wake (two-dimensional) and the round jet (axially symmetric) since these have been investigated in the most detail. Since little information is available on the wake of a self-propelled body, this case will not be considered. A discussion of its laws of spreading and decay may be found in [110].

B,27. Laws of Mean Spreading and Decay. A certain amount of useful information can be gathered from the equations of mean motion without requiring their actual solution. Using the condition that momentum, heat, and matter are conserved and that the flow when fully developed preserves similarity among mean motions and those turbulent motions which influence the mean motion, it is possible to obtain the laws of spreading and decay of mean properties.

The conventional procedure, which will be followed here, is to assume

B · TURBULENT FLOW

constant density. If heat is added or is generated by friction, or if another gas is added, it is assumed that the amounts are too small to affect the dynamical problem. The type of problem considered is that of fully developed rectilinear flow such as applies to the jet in a stationary surrounding medium and a wake at sufficient distance from a body.

The Reynolds equations in simple form become acceptable approximations under the conditions that (1) the viscous stresses may be neglected compared to the turbulent stresses, and (2) the mean pressure is so nearly constant that the gradients have a negligible effect on the axial motion and momentum. With regard to condition 2, it should be pointed out that the pressure in jets is slightly different from the ambient pressure [111], but this may be disregarded as far as our present interests are concerned.

Let x be measured along the axis of mean flow from some suitable origin, and U denote the mean velocity in the x direction. Let y be the lateral coordinate for two-dimensional flow and r be the radial coordinate for flow symmetrical about the x axis, and let V represent the lateral or radial component of mean velocity in each case. Then for steady mean flow the equations of motion and continuity are respectively:

$$\text{Plane jet and mixing zone} \quad \left\{ \begin{array}{l} U \frac{\partial U}{\partial x} + V \frac{\partial U}{\partial y} = \frac{1}{\rho} \frac{\partial \tau}{\partial y} \\ \frac{\partial U}{\partial x} + \frac{\partial V}{\partial y} = 0 \end{array} \right. \quad (27-1)$$

$$\left\{ \begin{array}{l} U \frac{\partial U}{\partial x} + V \frac{\partial U}{\partial r} = \frac{1}{r\rho} \frac{\partial(rU)}{\partial r} \\ \frac{\partial(rU)}{\partial x} + \frac{\partial(rV)}{\partial r} = 0 \end{array} \right. \quad (27-3)$$

$$\left\{ \begin{array}{l} U \frac{\partial U}{\partial x} + V \frac{\partial U}{\partial r} = \frac{1}{r\rho} \frac{\partial(rU)}{\partial r} \\ \frac{\partial(rU)}{\partial x} + \frac{\partial(rV)}{\partial r} = 0 \end{array} \right. \quad (27-4)$$

Here τ is the shear stress.

For wakes, equations corresponding to Eq. 27-1 and 27-3 may be further reduced because of conditions which apply at the great distances from the object necessary for similarity to exist. These are that V has become negligible, and U is nowhere much less than the free stream velocity U_* . If we express the velocity reduction by

$$\Delta U = U_* - U$$

and substitute in Eq. 27-1, at the same time dropping the term $V\partial U/\partial y$, we obtain

$$-(U_* - \Delta U) \frac{\partial \Delta U}{\partial x} = \frac{1}{\rho} \frac{\partial \tau}{\partial y}$$

To a sufficient degree of approximation this may be written

$$\text{Plane wake} \quad -U_* \frac{\partial \Delta U}{\partial x} = \frac{1}{\rho} \frac{\partial \tau}{\partial y} \quad (27-5)$$

Following a similar procedure for the round wake we obtain

$$\text{Round wake} \quad -U_* \frac{\partial \Delta U}{\partial x} = \frac{1}{r\rho} \frac{\partial(r\tau)}{\partial r} \quad (27-6)$$

The equations for the conservation of momentum are:

$$\left. \begin{array}{ll} \text{Plane jet} & \rho \int_{-\infty}^{+\infty} U^2 dy = \text{const} \\ \text{Round jet} & 2\pi\rho \int_0^{\infty} U^2 r dr = \text{const} \\ \text{Plane wake} & \rho \int_{-\infty}^{+\infty} U(U_* - U) dy = \text{const} \cong \rho U_* \int_{-\infty}^{+\infty} \Delta U dy \\ \text{Round wake} & 2\pi\rho \int_0^{\infty} U(U_* - U) r dr = \text{const} \cong 2\pi\rho U_* \int_0^{\infty} \Delta U r dr \end{array} \right\} \quad (27-7)$$

The method of employing the foregoing relations to find the laws of spreading and decay will be illustrated by carrying through the steps for the plane jet. Then the end results for all cases will be stated. If U_* is the velocity at the center of the jet and b is any convenient measure of the width (b may be the distance from the center to where U is zero or some fraction of U_*), then similarity means

$$\frac{U}{U_*} = f\left(\frac{y}{b}\right) \quad (27-8)$$

and

$$\frac{\tau}{U_*^2} = g\left(\frac{y}{b}\right) \quad (27-9)$$

where f and g are any function whose form may remain unknown. We now set $b \sim x^m$ and $U_* \sim x^{-n}$. Then the terms in the equation of motion (Eq. 27-1) become of the following order in x :

$$U \frac{\partial U}{\partial x} \sim x^{-2n-1}; \quad V \frac{\partial U}{\partial y} \sim x^{-2n-m}; \quad \frac{\partial \tau}{\partial y} \sim x^{-2n-m}$$

In order that the equation shall be independent of x , we must have $2n + 1 = 2n + m$, or $m = 1$. The momentum relation

$$\rho \int_{-\infty}^{+\infty} U^2 dy = \text{const}$$

because of order

$$x^{-2n+m}$$

and since this must be independent of x , $-2n + m = 0$. Since $m = 1$, $n = \frac{1}{2}$. Thus it is found that the plane jet spreads linearly with x and the

B · TURBULENT FLOW

velocity at the center decreases as $x^{-\frac{1}{4}}$. A similar procedure may be used for the other cases, and the results are summarized for all in Table B, 27.

Table B, 27

	Mixing zone	Plane jet	Round jet	Plane wake	Round wake
m	1	1	1	$\frac{1}{2}$	$\frac{1}{2}$
n	..	$\frac{1}{2}$	1	$\frac{1}{2}$	$\frac{1}{2}$

Width parameter x^m .

Velocity at center x^{-n} .

The same results may be obtained by setting up integral relations for the energy and using these with the momentum relations to determine m and n . This procedure is illustrated in [94].

The diffusion of heat and other scalar quantities is also of practical and theoretical interest. The equations of heat transfer, written for assumptions consistent with those made for the equations of motion, are as follows:

$$\text{Plane jet and mixing zone} \quad U \frac{\partial \bar{T}}{\partial x} + V \frac{\partial \bar{T}}{\partial y} = \frac{1}{\rho c_p} \frac{\partial q}{\partial y} \quad (27-10)$$

$$\text{Round jet} \quad U \frac{\partial \bar{T}}{\partial x} + V \frac{\partial \bar{T}}{\partial r} = \frac{1}{\rho c_p} \frac{1}{r} \frac{\partial (rq)}{\partial r} \quad (27-11)$$

$$\text{Plane wake} \quad U_* \frac{\partial \bar{T}}{\partial x} = \frac{1}{\rho c_p} \frac{\partial q}{\partial y} \quad (27-12)$$

$$\text{Round wake} \quad U_* \frac{\partial \bar{T}}{\partial x} = \frac{1}{\rho c_p} \frac{1}{r} \frac{\partial (rq)}{\partial r} \quad (27-13)$$

where \bar{T} is the mean temperature, q is the rate of heat transfer in the y or r directions per unit area (see Art. 10), and c_p is the specific heat at constant pressure. In proper terms the same equations hold for the transfer of matter. Molecular diffusion is so slow compared to turbulent diffusion that the transfer can be regarded as due entirely to turbulent motions.

Again assuming similarity, and expressing it in analogous terms, Eq. 27-10, 27-11, 27-12, and 27-13, together with the fact that the same amount of heat and matter must flow through each cross section, serve to determine the form of spreading and the decrease of center temperature or concentration as a function of x . These are the same as for the velocity, but the absolute magnitudes are different.

In all cases the origin of x is that point from which the flow appears to originate with the same law from the beginning. The point is usually found by extrapolating the experimental curves to a virtual origin. For

the round jet this is usually between 0.5 and 1.5 orifice diameters downstream from the orifice. The virtual origin appears to be less well defined for the plane wake and is different for the extrapolated center velocity than for the extrapolated width (Townsend [1]).

The foregoing relations apply as long as the Reynolds number remains sufficiently high for similarity to exist. Since the Reynolds number is proportional to x^{m-n} , it is seen from Table B,27 that, if the condition is initially satisfied, it will continue to be satisfied with ever-increasing x in all cases, with the exception of the round wake. For the latter the Reynolds number will eventually decrease to the point where the turbulent laws of spreading and decay merge into laminar laws with a new virtual origin. The distances for this change to occur can be expected to be very great, and in most cases any practical interest in the wake will have already been lost.

As already indicated, it is required in the foregoing analyses that similarity extend to the turbulent motions responsible for diffusion. The same rules must therefore apply to the scales of length and velocity entering into the diffusion process. If we adopt the concept of eddy viscosity, we may compare the behavior of a turbulent flow to that of a laminar flow in terms of the behavior of a viscosity. Denoting the mean eddy viscosity applicable to the flow by ϵ_μ , we have, since ϵ_μ is proportional to a length times a velocity,

$$\epsilon_\mu \sim x^{m-n}$$

Referring to Table B,27, we find that ϵ_μ is constant for the round jet and the plane wake. These flows should then behave as laminar flows with respect to their form of spreading and decay, as in fact they do. It must be borne in mind that we are here concerned only with the proportionality rule, not with absolute magnitudes. In the case of the plane jet, ϵ_μ increases as $x^{\frac{1}{2}}$, and we find, as we should, that the spreading and decay follow faster laws than those governing laminar flow. In this case the laminar exponents are

$$m_{lam} = \frac{2}{3}, \quad n_{lam} = \frac{1}{3}$$

In the case of the round wake, ϵ_μ decreases as $x^{-\frac{1}{2}}$, and we find, again as we should, that the spreading and decay follow slower laws than those governing laminar flow. Here the laminar exponents are

$$m_{lam} = \frac{1}{2}, \quad n_{lam} = 1$$

B,28. General Form and Structure. The boundary which separates the turbulent fluid, of say a jet or a wake, from the nonturbulent surrounding fluid is determined only by how far the motions have penetrated the surroundings. While it is self-evident that the boundary must be irregular, it was not until comparatively recent hot wire studies were

made that the highly irregular and sharply defined character of the boundary was revealed. An intermittency in the turbulence recorded from a hot wire probe in the outer regions of a round jet was first observed and studied by Corrsin [112]. It soon became apparent that this effect was due to a sharp and irregular boundary convected past the hot wire. The phenomenon was studied in considerable detail by Townsend [113,114, 115,116] in connection with his studies of the plane wake. Corrsin and Kistler [117] later made an exhaustive study of free stream boundaries, and this together with studies in the boundary layer by Klebanoff [118] has resulted in a reasonably clear understanding of the character and meaning of the free boundary.

In Art. 17 attention has already been directed to the outer boundary of a turbulent boundary layer, and the situation has been depicted schematically in Fig. B,17b. The character of the free boundary and the sharp separation between turbulent and nonturbulent fluid is shown in actual reality by the photograph of the turbulent wake of a bullet, displayed by Corrsin and Kistler, and shown here as Plate B,28. No turbulence and no other property transported by the shear flow, except some energy associated with potential motions, has penetrated the surrounding medium beyond the boundary. Moreover, the boundary is a connected surface; there are no disconnected parcels of fluid. The billows and hollows are, of course, three-dimensional. All motion in the nonturbulent fluid outside the boundary is irrotational, and the velocity there is that accompanying the potential motion of a free stream.

These phenomena are reproduced at all free boundaries, differing only in degree. An "intermittency factor" has been adopted as one of the criteria of the irregularity of the boundary. If a hot wire probe, capable of following the fluctuations, is placed so that, as the flow passes by, it is alternately in and out of the turbulent fluid, a record of the signal will show intermittently turbulent and nonturbulent sections. From such a record, or by other instrumental means, the fraction of the time that the flow is found to be turbulent may be determined. This is defined as the intermittency factor. As the probe is moved from the center of the flow outward, the intermittency factor goes from unity to zero. The customary symbol for the intermittency factor is γ . This symbol when used here is not to be confused with the same symbol for the ratio of specific heats used earlier.

It is instructive to compare γ distributions for several types of flow along with their mean velocity distributions. These are given for the boundary layer, the round jet, and the plane wake in Fig. B,28a and B,28b. In Fig. B,28a Klebanoff's data for a smooth wall and Corrsin's and Kistler's data for a very rough wall are compared. While there is considerable dispersion in the observations of intermittency, the difference between the curves for smooth and rough walls is believed to be real.

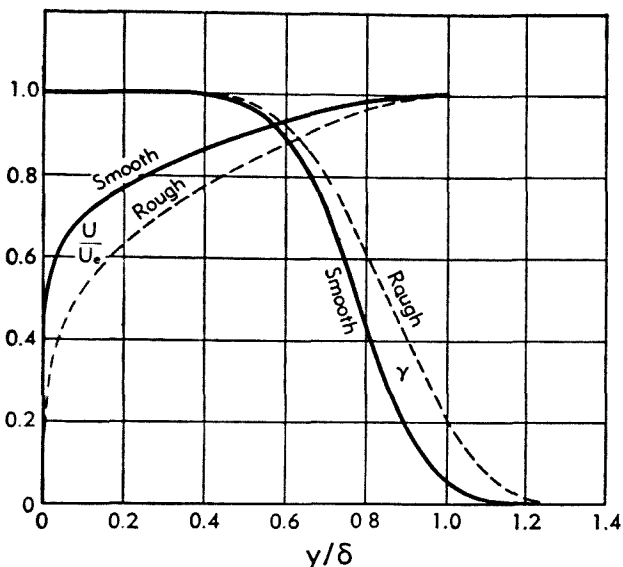


Fig. B,28a. Intermittency factor compared with velocity distribution in boundary layers for smooth and rough walls.

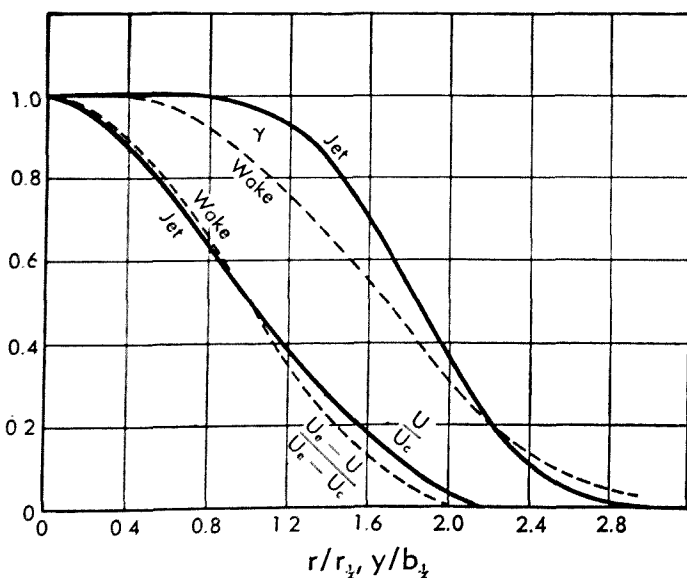


Fig. B,28b. Intermittency factor compared with velocity distribution for jet and wake. $r_{\frac{1}{2}}, b_{\frac{1}{2}}$ are distances from axis to where velocity ratios are $\frac{1}{2}$.

B · TURBULENT FLOW

Comparing the boundary layer and free flow, it is seen that the region of intermittency occurs where the velocity is not much different from that of the free stream in the case of the boundary layer, whereas it penetrates more deeply into the jet and wake flows. The range of mean velocities occurring in the region covered by the various instantaneous positions of the boundary is therefore much less for the boundary layer than for jets and wakes; and while the boundaries may appear superficially similar in all cases, the bulges and hollows involve the greater portion of the mean velocity field in free flows. This applies particularly to the wake.

According to Townsend [1] free flows contain large eddies which have a relatively small amount of energy, but which nevertheless serve to convect the fluid about in large bulks. He postulates a double structure consisting of the large eddies containing little turbulent energy and a smaller scale of eddies containing most of the turbulent energy. This would seem to be a reasonable picture in view of the freedom of motion in the absence of a wall, but, to the degree that the outer boundary of a wall flow is also free, the same picture might also apply to the outer region of a boundary layer.

A statistical measure of the width of the intermittent zone is the standard deviation of the instantaneous boundary from its mean position given by $\sqrt{[(Y - \bar{Y})^2]}$, where Y is the instantaneous position and \bar{Y} is the average position.

From Townsend's point of view the standard deviation is determined primarily by the large eddies. Corrsin and Kistler [117] were able to predict the observed behavior (not the absolute magnitude) of the standard deviation in the boundary layer, jet, and wake on the basis of Lagrangian diffusion by continuous movements (Taylor [119]). However, this required only the assumption of similarity of velocity and length scales to one another and to the main flow, and therefore does not rule out a possibly predominant part played by the large eddies. It seems evident that the contour of a marked surface completely within the turbulent region would be qualitatively like that of the free boundary, but that its coarseness would depend on the scale of the eddies in the neighborhood and on the presence of turbulence on both sides. The boundary is therefore a marker which gives us a picture of the eddy diffusion at the extreme limits.

The next question of considerable interest has to do with the mechanism by which the turbulence spreads into fluid which was originally non-turbulent. This spreading and enveloping of new fluid is the only means by which the average position of the boundary can migrate laterally. Given that the outer flow is irrotational, it must become rotational when it crosses the boundary into the turbulent region. Corrsin and Kistler have concluded that the change takes place suddenly and wholly within a very thin laminar superlayer "plastered" over the boundary. Vorticity

can be transmitted to an irrotational flow only by tangential forces due to viscosity. The layer in which this takes place is the laminar superlayer. Corrsin and Kistler have shown that this layer must be very thin, partly on the grounds that stability considerations would not permit it to be otherwise, and partly on the grounds that the turbulent stretching of vortex lines increases the vorticity and therefore sharpens up the velocity gradient. The thickness has been estimated to be less than the dissipation length λ . The presence of the laminar superlayer cannot be detected experimentally, but the observed sharp demarcation between turbulent and nonturbulent regimes tends to confirm the thinness of the layer.

The spreading of the turbulent region therefore takes place by viscous action at the immediate boundary, and the rate of encroachment depends on the steepness of the laminar gradient and on the surface area, both of which are increased by the larger-scale, eddy-diffusion process acting from within. Viscosity is the vorticity-propagating agent, but it plays no controlling role in the spread of the turbulent region. Corrsin and Kistler point out that heat and matter are transported across the boundary in exactly the same way; and if the Prandtl and Schmidt numbers are not much smaller than unity, these scalar quantities should be transported at the same rate as momentum. The processes at the immediate boundary therefore do not explain why heat and matter spread faster than momentum. We shall return to this question in Art. 29.

The phenomena just described require that the fluid everywhere beyond the boundary cannot have received any quantity by diffusion. If a jet is hot, all of the heat is confined within the sharp boundary. The same is true of all of the axial momentum. The only effect on the outer fluid is a pressure-induced flow toward the jet and pressure-induced fluctuations. Both are irrotational. The term, turbulence, cannot be applied to these fluctuations. Relatively slow, potential-type velocity fluctuations are in fact observed in the outer fluid. Jumps in mean velocity are also observed in passing from turbulent to nonturbulent regions. Apparently in some cases these are smaller than would be expected if free stream velocity prevailed in the nonturbulent regions. Townsend proposes that the fluid between two turbulent bulges is partially carried along as the bulges move downstream, but there is some disagreement on this point. Corrsin and Kistler find jumps in the intermittent region of a boundary layer of about the order to be expected if the outer fluid is not carried along.

The sharp boundary is not to be confused with the limits as usually expressed in terms of mean velocity distribution. It will be noted from the γ curves that the fluctuations in the sharp boundary generally extend beyond the mean velocity boundary. A bulge protruding far out apparently carries so little mean velocity increment or defect that its effect cannot be detected by the usual methods.

B.29. Transport Processes in Free Turbulent Flow. In order to solve the equations of motion and heat transfer given in Art. 27 and thus obtain velocity and temperature distributions in y or r , it is necessary to express the quantities on the right-hand side of the equations in terms that can be related to the derivatives of velocity and temperature with respect to y or r . The auxiliary expressions for this purpose have been discussed in Art. 10. Specifically, Eq. 10-12 or 10-13 are used with the coefficients D_u , D_h , ϵ_u , or ϵ_h specified either by general conditions of the problem or expressed in terms of local conditions.

The former usually takes the form of an assumption that the coefficients are constant over a given cross section of the flow but vary from one section to the next. In recent years the following expression proposed by Prandtl [120] has been extensively used:

$$D_u \text{ or } D_h = K(U_{\max} - U_{\min})b \quad (29-1)$$

where b is the width of the region at a given cross section, U_{\max} and U_{\min} are the extremes of mean velocity across the section, and K is an experimentally determined constant of proportionality whose value depends on the quantity D_u or D_h .

Specification of transport in terms of local conditions takes the form of mixing length theory. This theory has already been discussed in Art. 12. Its application to free turbulent flows has been so widely discussed in the literature, for example [6,111], that only a few remarks are called for here. Much of the discussion has had to do with the relative merits of momentum transfer theory on the one hand and Taylor's vorticity transfer theory on the other. Vorticity transfer theory is generally favored on the grounds that it is consistent with a wider distribution of temperature than of velocity, but which of the two theories agrees the better with observed velocity distributions depends on cases.

We shall here concern ourselves with the broader question regarding the foundation of the foregoing procedures rather than with the details of their application. The basis for judgment rests largely on the work of Townsend with the plane wake and that of Corrsin with the round jet. As mentioned in Art. 28, there is evidence that large eddies operate in free turbulent flows to contort the whole flow field and thus transport fluid with smaller scales of turbulence over much of the width occupied by the flow. The next idea to be introduced is that mixing of all properties by large and small scale motions has gone on for a considerable time over the previous course of the flow. In this connection it is advisable to restrict the discussion to jets and wakes, for in these cases all of the properties in question have been put in at the beginning and through mixing have covered much of the cross section during their previous history. Eddies of any scale significant in diffusion will have existed for a considerable time, and their size and intensity found at a particular lo-

cation will depend mainly on their past environment and will reflect the character of the flow as a whole rather than that of any particular locality. The large-eddy part of the structure helps greatly to promote this general averaging. The central idea here is that the lengths and velocities entering into a turbulent transport coefficient are not primarily determined by local conditions. What has been stated here is true to a degree of all turbulent flow, but the greater preponderance of large eddies and the exposure to mixing from the beginning enhance the effects in jets and wakes.

We have the picture, then, that any property that has been in the flow for a considerable length of time should be mixed to a fair degree of uniformity when it has arrived at a particular cross section. Dilution occurs at the sharp boundaries, and also new fluid has recently become turbulent there. Therefore we would not expect complete uniformity everywhere within the sharp boundaries. Experiments show that turbulent energy, temperature in the case of a heated jet or wake, and concentration of a tracer gas in a jet are nearly uniform over the fully turbulent core and decrease gradually in the turbulent bulges as the boundary is approached. The over-all average decrease toward the boundaries is faster than that in the turbulent parts alone due to the absence of any contribution from the nonturbulent parts.

The foregoing behavior does not apply in the same degree to the axial momentum. The mean velocity difference decreases considerably across the core and continues to decrease in the protruding turbulent bulges. This is obviously why the mean velocity distribution is less broad than the mean-temperature distribution, but it is only a superficial explanation since it leaves unexplained why the momentum should have been given preferential treatment in the mixing process.

We must now be concerned with the question of how to express the transfer processes. Mixing length theory and Eq. 29-1 both assume a gradient type of transfer in which the rate can be expressed in terms of the local gradient. This requires that the diffusing movements shall be small compared to the distance over which the gradient changes. This condition may be satisfied as far as the smaller eddies are concerned, but it is obviously not satisfied for eddies comparable in size to the width of the jet or wake. Townsend proposes that the total rate of transport is a combination gradient diffusion by the smaller eddies, which contain most of the turbulent energy, and bulk convection by the larger eddies. Since the gradients in scalar quantities, like heat, matter, and turbulent energy have been reduced due to the long continued mixing, it would appear that these quantities have been transported laterally more by the bulk convection than by gradient diffusion. On the other hand, since momentum has not been so thoroughly mixed, the prospects for gradient diffusion are better.

B · TURBULENT FLOW

With regard to the theories in question, three main facts stand out: (1) only the smaller eddies of this double-structure picture can take part in the gradient diffusion on which the theories are based, (2) the smaller eddies are mixed to a state of near uniformity, and (3) the scale and intensity of all eddies responsible for transfer are determined by general conditions rather than local conditions.

Fact 1 means that we cannot predict to what extent the theories will apply. Fact 2 means that we can make a good case for Eq. 29-1 for that part of the transport which is of the gradient type. Fact 3 means that we must be skeptical of the kind of local dependence on which mixing length theory rests. This refers specifically to Eq. 12-2b and 12-13 of Art. 12 which expresses v and l in terms of local mean flow parameters. Some lessening of local dependence is achieved when l is taken to be constant over a section of the flow and proportional to the width. This is commonly done in free turbulent flows. We see that even with this compromise, mixing length theory is scarcely tenable in free turbulent flows.

Turning to comparisons with measured distributions, we find that mixing length theory cannot be shown to be definitely wrong, although the agreement with observations is rather casual, with vorticity transfer turning out to be better in some cases and momentum transfer being better in others. The vorticity transfer version of the theory when combined with the heat transfer version does at least yield a broader temperature distribution than velocity distribution [121].

Hinze and van der Hegge Zijnen [122] conducted an exhaustive series of experiments in which they measured distributions of velocity, temperature, and concentration of small amounts of added gas in a round air jet. After comparing their results with mixing length theories they concluded that these theories were unsatisfactory, and so set out to explore the possibilities of constant turbulent exchange coefficient. From their measured velocity distributions and the equations of motion and continuity, D_u was determined as a function of radius and axial distance. It was found to remain nearly constant with increasing r from the center outward, and then to decrease in the intermittent zone. They concluded, however, that a constant D_u was a sufficiently good assumption to justify the adoption of the well-known laminar solution. The resulting velocity distribution formula and the expression for D_u are given in Art. 30.

Hinze and van der Hegge Zijnen found that temperature and concentration profiles indicated practically identical exchange coefficients. We shall denote these by the common symbol D_h and refer to the ratio $D_u/D_h = Pr_t$ as the turbulent Prandtl number. (This ratio is known as the Schmidt number when referring to matter in place of temperature.) The value of Pr_t on the axis of the jet was found to be 0.685. However, Pr_t increased steadily with r and became greater than unity for

$U/U_* < 0.2$. This means that D_h decreased where D_u remained constant and decreased more rapidly than D_u in the outer regions.

Corrsin and Uberoi [123] calculated values of Pr_t from their measurements in a heated round jet. Their mean values over the cross section of the jet were very close to the value 0.7. They also obtained an indicated increase from the center outward, but did not regard their accuracy as sufficient to be certain of a definite trend. They noted the striking agreement with the laminar Prandtl number for air at the mean temperature of the jet. Forstall and Shapiro [124] point out, however, that turbulent Prandtl numbers for jets are about 0.7 for various kinds of fluids irrespective of their laminar Prandtl number.

Townsend found in his investigations of the plane wake [119] that both D_u and l remained nearly constant in the central portion of the wake, but fell off rapidly in the outer part. However, D_u divided by the intermittency factor γ was not far from constant over the greater part of the wake.

These pieces of evidence tend to confirm what was conjectured earlier in this article, namely that insofar as theories based on gradient transfer can be applied at all, they should apply better to momentum than to temperature or concentration. The laminar-type solutions of the equations of motion based on some appropriate constant value of D_u over the section have consistently given accurate descriptions of the velocity distribution. Discrepancies occur in the outer part of the flow due to the fact that D_u decreases. Townsend has shown that improvement results for the plane wake if the eddy viscosity ϵ_u is allowed to decrease with the intermittency factor, i.e. as $\gamma \epsilon_u$.

The situation with regard to the diffusion of heat and matter is not so favorable, and transfer based on local gradients is little better than a crude approximation at best. For the round jet, and presumably for the plane jet also, D_h is nowhere constant, but the assumption of constant Pr_t is believed to be acceptable for practical purposes. When Pr_t is constant, the relation between temperature distribution and velocity distribution for the round jet is

$$\left(\frac{\text{temperature}}{\text{ratio}} \right) = \left(\frac{\text{velocity}}{\text{ratio}} \right)^{Pr_t} \quad (29-2)$$

While there is some question about the appropriate value of Pr_t , a reasonable value is $Pr_t \approx 0.7$.

According to Reichardt [125] Eq. 29-2 should be more generally applicable in free turbulent flow. For a review of Reichardt's inductive theory of turbulence, reference is made to [96].

For plane wakes it does not seem possible to calculate temperature distribution on the basis of an exchange coefficient for heat. Paradoxically, mixing length theory gives reasonably good agreement with ob-

B · TURBULENT FLOW

served temperature and velocity distributions when l is assumed constant over the cross section. Momentum transfer theory and vorticity transfer theory give the same results for velocity distribution, but vorticity transfer must be used in connection with the heat transfer equation to get the proper result for temperature distribution. The results are

$$\frac{U_s - U}{U_s - U_0} = \left[1 - \left(\frac{y}{y_s} \right)^{\frac{1}{2}} \right]^2$$

$$\frac{T - T_s}{T_s - T_0} = 1 - \left(\frac{y}{y_s} \right)^{\frac{1}{2}}$$

where U_s and T_s are respectively the velocity and temperature of the free stream, U_0 and T_0 are respectively the velocity and temperature at the center, and y_s is the extreme limit in each case, y_s being the greater for temperature distribution.

We may conclude this discussion by noting that recent findings have given us a clearer physical picture but little by way of a fundamental theory. It has not been possible to clarify the question as to why turbulent motions act differently toward heat and matter than toward momentum. Some discussion of this question is given by Townsend; and since this cannot readily be taken out of context, the reader is referred to [1, pp. 164, 165].

B,30. Velocity Distribution Formulas for Jets and Wakes. The advantage of a constant exchange coefficient is not so much in any marked improvement in accuracy over mixing length theory, but rather that it permits the adoption of laminar-type solutions. When similarity exists, the form of the dependence of the exchange coefficient on x is known, but the absolute magnitude must be found from experiment. The purpose here is to give examples of final results based on this method. For the purpose of comparison a mixing length formula will be shown for one case. It is assumed that mixing length theory and the resulting formulas have been given sufficient attention in other literature, notably in [6,111].

A comparison of formulas for the plane wake, made by Townsend [126], is shown in Fig. B,30. Compared with an observed velocity distribution curve are

1. Mixing length theory, l constant over the width:

$$f_1 = 1.835 \left[1 - \left(\frac{\xi}{0.48} \right)^{\frac{1}{2}} \right]^2 \quad (30-1)$$

2. Constant exchange coefficient:

$$f_1 = 1.835 \exp \left[- \left(\frac{\xi}{0.253} \right)^2 \right] \quad (30-2)$$

3. Modified theory: $\epsilon_\mu = (\epsilon_\mu)_t \gamma$, where $(\epsilon_\mu)_t$ = constant eddy viscosity in the turbulent region, γ = intermittency factor:

$$f_1 = 1.835 \exp \left\{ -14.4 \xi^2 \left[1 + \frac{1}{3} \left(\frac{\xi}{0.35} \right)^4 \right] \right\} \quad (30-3)$$

In 1, 2, and 3, f_1 and ξ are

$$f_1 = \frac{U_* - U}{U_*} \left(\frac{x - x_0}{d} \right)^{\frac{1}{2}}; \quad \xi = \frac{y}{[(x - x_0)d]^{\frac{1}{2}}}$$

x_0 = virtual origin ($x_0/d = +90$)

d = diameter of cylinder producing the wake

In these cases

$$\frac{\epsilon_\mu}{\rho} \equiv D_u = 0.0173 U_* d \quad (30-4)$$

It is seen that mixing length theory makes the distribution too narrow near the axis. The constant exchange coefficient fits in this region but

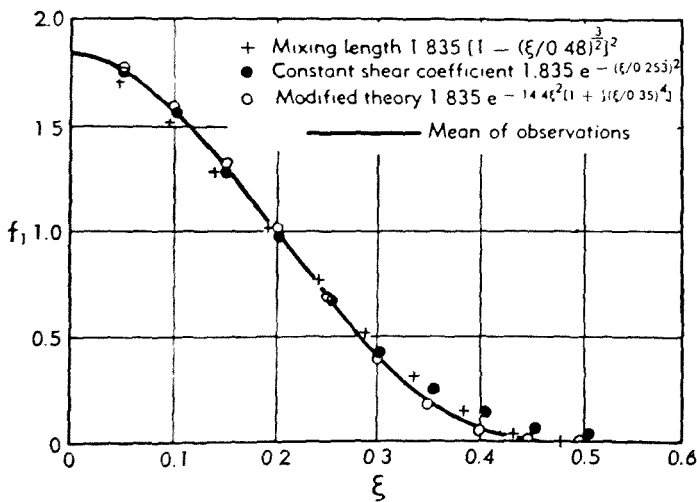


Fig. B,30. Comparison of velocity distribution formulas for plane wake, after Townsend [120].

makes the velocity difference approach zero too slowly in the outer region. In reality ϵ_μ is not constant, and an all-over fit is obtained only by adjusting ϵ_μ , as in Eq. 30-3.

The distribution of axial velocity across the round wake may also be represented by a Gaussian error function. Such representations are characteristically faulty near the outer edges. The round wake has not been investigated so thoroughly as the plane wake.

B · TURBULENT FLOW

The mixing zone between two uniform streams of velocities U_1 and U_2 and the plane jet were treated on the basis of constant exchange coefficient by Görtler [127]. Since this work has been well reviewed by Schlichting [96], only selected results are repeated here. The calculated velocity profile of the mixing zone is in very good agreement with experiment. The calculated distribution of axial velocity in the plane jet is also in good agreement with experiment except in the outer regions where the calculated profile approaches zero too slowly. The formula for the plane jet is

$$U = \frac{\sqrt{3}}{2} \sqrt{\frac{K\alpha}{x}} (1 - \tanh^2 \eta) \quad (30-5)$$

where α = a free constant to be determined by experiment,

$$\eta = \alpha \frac{y}{x}$$

$$K = \text{strength of jet} = \int_{-\infty}^{+\infty} U^2 dy$$

The velocity at the center U_0 is given by

$$U_0 = \frac{\sqrt{3}}{2} \sqrt{\frac{K\alpha}{x}} \quad (30-6)$$

It must be assumed in these formulas that x is the distance from the point where the jet appears to originate. Schlichting quotes Reichardt's experimental value of α as equal to 7.67 and D_u as given by

$$D_u = 0.037 y_t U_0 \quad (30-7)$$

where y_t is the value of y where $U/U_0 = \frac{1}{2}$.

It follows from Eq. 30-5, 30-6, and 30-7 that

$$D_u = \frac{\sqrt{3}}{2} 0.037 \frac{\eta_t}{\sqrt{\alpha}} \sqrt{Kx}$$

$$D_u = 0.0102 \sqrt{Kx} \quad (30-7a)$$

As mentioned in Art. 29, the adaptation of the laminar-type solution for the round jet was investigated by Hinze and van der Hegge Zijnen. Their expression is

$$\frac{U}{U_0} = \frac{1}{\left(1 + \frac{\eta_r^2}{8\alpha_0}\right)^2} \quad (30-8)$$

where $\eta_r = r/(x + x_0)$

x_0 = virtual origin which turned out to be 0.6 times the orifice diameter

$(x + x_0)$ = over-all distance from point where jet appears to originate

α_0 = const = 0.00196

In this case

$$D_u = 0.00196(x + x_0)U_* \quad (30-9)$$

According to Schlichting [96] the velocity at the center may be expressed by

$$U_* = \frac{3}{8\pi} \frac{K_r}{D_u(x + x_0)} \quad (30-10)$$

Here

$$K_r = \text{strength of jet} = 2\pi \int_0^{\infty} U^2 r dr = \frac{\pi}{4} D^2 U_*^2 \quad (30-11)$$

where D is the diameter of the nozzle and U_* is the jet exit velocity. By means of Eq. 30-9 and 30-11, Eq. 30-10 may be written

$$\frac{U_*}{U_*} = \frac{6.92}{\frac{x}{D} + \frac{x_0}{D}} \quad (30-12)$$

According to Hinze and van der Hegge Zijnen the numerical constant in Eq. 30-12 turns out to be 6.39 on the basis of their observed axial distribution of velocity.

When U_* given by Eq. 30-10 is substituted into Eq. 30-9,

$$D_u = 0.0153 \sqrt{K_r} \quad (30-13)$$

In jets, as in wakes, the constant exchange coefficient makes the calculated velocity approach zero too slowly in the outer regions. This discrepancy is tolerated partly because it is in the region where the velocity is low and partly because the reason for it is understood in terms of intermittency.

Since the exchange coefficient D_u is the turbulent kinematic viscosity, it is interesting to compare it to ordinary kinematic viscosity ν . For the plane wake from a cylinder the ratio D_u/ν is found from Eq. 30-4 to be

$$\frac{D_u}{\nu} = 0.0173 \frac{U_* d}{\nu} \quad (30-14)$$

where $U_* d / \nu$ is the Reynolds number of the cylinder. A similar expression may be found for the round jet by replacing K_r in Eq. 30-13 by Eq. 30-11. The result is

$$\frac{D_u}{\nu} = 0.0153 \frac{\sqrt{\pi}}{2} \frac{U_* D}{\nu} = 0.0135 \frac{U_* D}{\nu} \quad (30-15)$$

If, in these two examples, d and D are both one inch and U_* in both cases is 100 ft/sec, the Reynolds number for air at ordinary temperature and pressure is about 4.9×10^4 . The two values of D_u/ν are then found to be 850 and 660 for the wake and jet respectively. These figures serve to

convey an idea of the order of magnitude of the ratio of turbulent viscosity to ordinary viscosity.

When the spreading is linear, as it is for jets, the angle of spreading affords a convenient means of visualizing the size. This angle may be found from Eq. 30-5 and 30-8 in terms of some suitably defined width. If we take this to be the line along which $U/U_0 = \frac{1}{2}$, we find that the plane jet is a wedge with a half angle of approximately $6\frac{1}{2}$ degrees and the round jet is a cone with a half angle of approximately 5 degrees. These angles are independent of the strength of the jet. The spreading of laminar jets, on the other hand, depends on the strength, becoming narrower as the strength increases. The plane laminar jet is not wedge-shaped; the width increases with $x^{\frac{1}{4}}$. These differences between turbulent flow and laminar flow are mentioned as additional illustrations of the effect of an eddy viscosity which is regulated by the flow itself.

B,31. Effect of Density Differences and Compressibility on Jets with Surrounding Air Stationary. In jet propulsion the jet is much hotter than the surrounding air and it issues at a high relative velocity. Density differences and compressibility are therefore expected to be of some importance. When we examine the situation realistically, however, we find that both temperature difference and relative velocity diminish rapidly with distance, and the jet soon behaves much like the constant-density, incompressible jet previously treated. When the jet issues rearward from a moving vehicle, it does not emerge into a surrounding medium at rest but rather into a medium with an axial velocity in the same direction. Under this condition the jet spreads more slowly, and the temperature and relative velocity diminish more slowly with distance from the orifice. The extent over which density and compressibility effects are possibly important therefore depends on the velocity of the outer stream. The effect of an outer velocity will be considered in Art. 32; here the problem is considered for the surrounding medium stationary with respect to the nozzle.

The work of Corrsin and Uberoi on the heated round jet [123] has contributed substantially to what is known about the hot jet issuing into still surrounding air. They studied the jet issuing from a 1-inch orifice with velocities ranging from 65 to 115 ft/sec. The initial temperature rise was made slight when it was desired to study the spread of momentum and heat without introducing significant effects of density difference, and was raised to about 300°C when the effect of density was to be studied. In the latter case the density ratio was $\rho_1/\rho_0 = 2$, where ρ_0 is the density of the jet at the nozzle and ρ_1 is the density of the surrounding air.

The principal effects are illustrated in Fig. B,31a and B,31b taken from the report of Corrsin and Uberoi. Fig. B,31a shows the velocity and temperature profiles 16 nozzle diameters downstream. From these it is

clear that the reduced density corresponding to the higher temperature causes a more rapid spreading of both the velocity and temperature profiles. Again the temperature profile is wider than the velocity profile. Fig. B,31b shows the decrease of velocity and temperature along the axis.

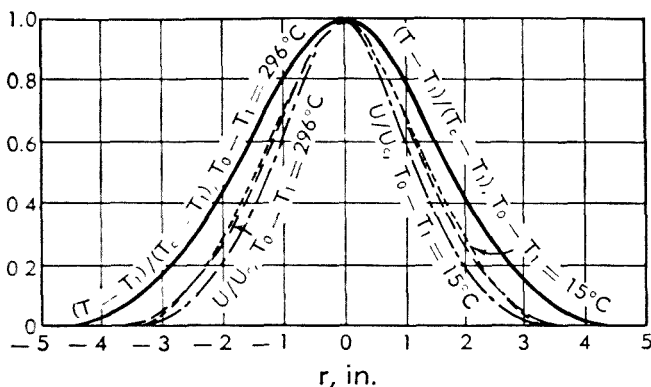


Fig. B,31a. Radial velocity and temperature distribution in round jet showing effect of density, after Corrsin and Uberoi [123]. Section 16 nozzle diameters from orifice. T_0 = initial temperature of jet, T_c = temperature at center, T_1 = temperature of surrounding air.

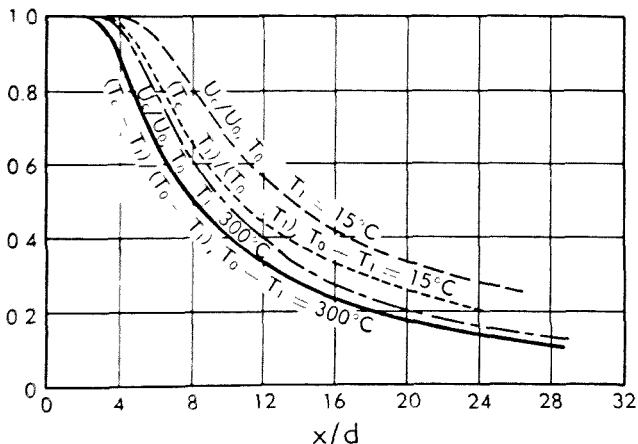


Fig. B,31b. Axial velocity and temperature distribution at center of round jet, after Corrsin and Uberoi [123]. x = distance from orifice, d = diameter of nozzle, T_0 = initial temperature of jet, T_c = temperature at center, T_1 = temperature of surrounding air.

The decreased density causes both velocity and temperature to fall more rapidly than for constant density.

No appreciable change was noted in the shape of the profile in the fully developed jet for $\rho_1/\rho_0 = 2$. Corrsin and Uberoi showed definitely that there was no measurable change in the shape of the total head pro-

B · TURBULENT FLOW

files. However, the density difference was not large after the distance of 7 or 8 nozzle diameters required for the flow to become fully developed. For example, at 15 diameters $\rho_1/\rho_0 = 1.3$ when $\rho_1/\rho_0 = 2$. For a density ratio of this order there is no essential departure from similarity in any of the profiles, so that the spread is found to be proportional to x and the decrease of velocity and temperature along the axis is found to be inversely proportional to x .

Cleaves and Boelter [128] made measurements of velocity and temperature in a round jet with an initial temperature difference of 650°C. The jet issued vertically from a pipe $1\frac{1}{8}$ inches in diameter at velocities ranging from 13 to 56 ft/sec. They did not detect any difference in the radial velocity distribution between the isothermal jet and the hot jet. In short, they found no effect of the decreased density on the rate of spreading of the jet. This disagrees with the results of Corrsin and Uberoi. They did, however, find the velocity on the axis decreased more for the hot jet than for the isothermal jet. The decrease was greater than that found by Corrsin and Uberoi, as would be expected from the higher temperature, but their isothermal results for the velocity on the axis do not agree with those of Corrsin and Uberoi. The Corrsin and Uberoi results should perhaps be given the greater weight in view of the accurate control over experimental conditions.

Since high relative velocities, and the compressibility and heating effects associated with them, are generally found close to a nozzle, the magnitude of these effects is of most interest in connection with the mixing-zone problem. Abramovich [129] investigated the effects by applying the vorticity transfer version of mixing length theory to the plane mixing zone between a stream of uniform velocity and a medium at rest, restricting the treatment to air speeds up to Mach number unity and temperature differences up to 120°C. He found that cooling the stream increased the width of the mixing zone, with the boundary on the stream side showing practically all of the effect. The effect of increasing the velocity was to decrease the width of the mixing zone, again with only the boundary on the stream side being affected. However, the predicted effects were such that practically identical velocity distributions were indicated if on the one hand a low speed stream is cooled to $\Delta T = -60^\circ\text{C}$ and on the other hand a stream of Mach number unity has a stagnation temperature equal to that of the stationary medium (static temperature, $\Delta T = -60^\circ\text{C}$). Thus a jet cooled either by extraction of heat or by adiabatic expansion will have a more rapidly diverging mixing region than a jet having the same static temperature as the surrounding medium. This would not be consistent with the findings of Corrsin and Uberoi.

Gooderum, Wood, and Brevoort [130] measured the density distribution with an interferometer in the mixing zone of a jet issuing from a 3 by 3-inch nozzle at a Mach number of 1.6. The stagnation temperature

of the jet was about the same as that of the surrounding air. The jet was therefore cold, the initial density being 1.5 times that of the surrounding air. The density and velocity were examined across the mixing zone from 2 inches to $7\frac{1}{2}$ inches from the nozzle. The distributions were similar at each cross section, and the velocity distribution could be represented by Tollmien's theoretical curve for incompressible flow [131] in the subsonic portion of the mixing region. Such distributions have the typical s-shape of the Gaussian integral curve, and they reduce to a common curve for different values of x when plotted against $\sigma y/x$, where σ is a scale factor. The width of the mixing region is thus inversely proportional to σ . The value for incompressible flow is generally around 12. Gooderum, Wood, and Brevoort found $\sigma = 15$. The rate of spreading into the jet core and into the surrounding air was therefore less than that for incompressible flow. This would appear to disagree with the trends found by Abramovich, which of course apply to subsonic flow, but is what would be expected from the density effect found by Corrsin and Uberoi in the round jet.

Similar results were reported by Bershader and Pai [132] from measurements on the discharge from a rectangular nozzle 1 by 2 cm at a Mach number of 1.7. Density measurements were made with an interferometer at several closely spaced stations within one nozzle width from the orifice. The density distributions were found to be similar, and σ was found to be 17. The mixing zone was thus narrower than that for incompressible flow. The profile of density ratio is in reasonable agreement with a curve based on Pai's theory [133] which employs the concept of a constant coefficient of eddy kinematic viscosity of the form of Eq. 29-1.

These experimental results on supersonic jets do not distinguish between the effect of a denser jet and the heating effect resulting from internal dissipation. We might assume, however, as pointed out by Pai in relation to laminar flow, that the greater momentum associated with higher density causes the stream to carry farther and thus decrease the divergence of the mixing zone. Evidence to substantiate this assumption is afforded by the work of Keagy and Weller [134] who found wider velocity profiles for helium jetting into air and narrower profiles for carbon dioxide. It may be concluded from this that the observed effects are primarily density effects. Taken as a whole, the observations disagree with the theoretical predictions of Abramovich.

B,32. Effect of Axial Motion of Surrounding Air on Jets. When a jet is projected rearward from a vehicle moving through the air, it effectively emerges into a surrounding medium in motion in the same direction as the jet. Some attention is now given to the effect of this motion on the characteristics of the jet. We do not consider other cases, likewise of importance, where the jet is projected forward or at an angle to a moving stream.

It appears that no basic investigations have been carried out which would give us information on the turbulent structure and the boundary configuration when the surrounding medium is moving. Corrsin and Kistler [117] call attention to the limiting case where a turbulent and a nonturbulent stream are in contact with no mean relative velocity, and infer that the diffusing mechanism will be much the same as when a relative velocity exists. If this is so, it follows that mixing again depends on the velocity and scale of the mixing motions as determined by a relation of the type of Eq. 29-1. We know that travel of the surrounding stream along with the jet lessens the divergence and decay of jet velocity. In a very real sense the jet fluid rides along with the outer stream and reaches a distance x from the nozzle in a shorter time. Fluid has had less time to diffuse and as a consequence has traveled a shorter distance laterally. Correspondingly, it has had less time to mix, and it would be expected that a greater distance is now required for the similarity regime to prevail. In the absence of any firm knowledge of the turbulent structure, the usual concepts are applied by investigators in this field, namely that either mixing length or turbulent exchange coefficient are constant over a cross section.

Using mixing length theory for momentum transfer, Kuethe [109] investigated the plane mixing region between streams moving in the same direction with different relative velocities and also treated the mixing zone of the round jet from the nozzle to the end of the potential core for the case where the outside medium is at rest. Görtler [127] later developed the relations for the plane mixing region between two streams on the basis of a turbulent exchange coefficient given in the form of Eq. 29-1. Szablewski [135] then extended this method to the core-containing region of the round jet for the case where the surrounding stream has different velocities. Squire and Trouncer [136], using mixing length theory, applied to momentum transfer developed relations for the characteristics of the round jet for various velocities of the surrounding stream, including both the initial core-containing region and the fully developed region. In addition they calculated the inflow velocity in the region surrounding the jet. All of the methods apply to incompressible, isothermal flow.

All of the methods agree, at least qualitatively, in showing a marked effect of velocity of the outer stream on the rate of jet spreading and decay of velocity differences. The effect depends on the ratio U_1/U_0 , where U_1 is the outer stream velocity and U_0 is the jet exit velocity. As the ratio increases, the divergence decreases, the core region extends farther from the nozzle, and the velocity increments decrease more slowly with x . When $U_1/U_0 = 0$, the core region extends only to about 5 orifice diameters from the nozzle. When $U_1/U_0 = 0.5$, the distance is increased to 11 diameters according to Szablewski and to 8.1 diameters according to Squire and Trouncer. Each of these two methods requires that a single

constant be evaluated by experiment, and for this purpose existing data for still surrounding air were used. Szablewski's method indicates somewhat greater effects, but it is difficult to judge the reliability of these methods due to the basic assumptions and approximations made in the solutions. No attempt will be made here to reproduce the developments and final formulas, all of which tend to be cumbersome. Squire and Trouncer achieved some simplification by arbitrarily adopting a cosine velocity profile which for the fully developed jet takes the form

$$\frac{U - U_1}{U_\infty - U_1} = \frac{1}{2} \left(1 + \cos \pi \frac{r}{r_1} \right) \quad (32-1)$$

where U_1 is the velocity of the surrounding stream, U_∞ the velocity on the jet axis, r the radial distance from the axis, and r_1 the radius of the jet boundary.

We turn next to experiment, and here we find a comprehensive investigation conducted by Forstall and Shapiro [124] aimed at testing the analytical formulation of Squire and Trouncer and additionally comparing mass transfer and momentum transfer. For obtaining the mass transfer 10 per cent by volume of helium was added to the jet as a tracer. Values of U_∞ up to 225 ft/sec and values of U_1 up to 90 ft/sec were used. Velocity ratios U_1/U_∞ ranged from 0.2 to 0.75.

Velocity and concentration profiles downstream from the end of the potential region could be closely represented by a formula of the type of Eq. 32-1. The assumption of this formula by Squire and Trouncer was therefore well justified. The profiles remained substantially similar at all values of x and were independent of the velocity ratio U_1/U_∞ .

In order to avoid the uncertainty in specifying the extremes of the jet, the size parameters r_{mean} and r_{eff} were adopted, where r_{mean} is the radius where the velocity is the mean of its value on the axis and in the outside stream, and r_{eff} is the radius where the concentration is $\frac{1}{2}$ the concentration on the axis. Expressing these in terms of the diameter of the nozzle D the rate of spreading with x/D was found to be greater for concentration than for velocity. A turbulent Schmidt number of about 0.7 was indicated (compare Art. 29). The experiments checked the law of jet divergence derived by Squire and Trouncer.

Both concentration and velocity were found to decay inversely with x/D . In general, concentration showed more of a drop than did the velocity, but the difference in behavior was small. The inverse law amounts to a faster decrease with x/D than that predicted by the Squire and Trouncer theory, although the theory gives the general order of magnitude of the center line properties.

Forstall and Shapiro give the following empirical formulas for the round jet in a surrounding stream of equal density to serve as rough rules for the velocity field:

(109)

B · TURBULENT FLOW

Formulas

- (i) $\frac{x_e}{D} = 4 + 12\lambda$
- (ii) $\frac{U_e - U_1}{U_0 - U_1} = \frac{x_e}{x}$
- (iii) $\frac{2r_{mv}}{D} = \left(\frac{x}{x_e}\right)^{1-\lambda}$
- (iv) $\frac{U - U_1}{U_e - U_1} = \frac{1}{2} \left(1 + \cos \frac{\pi r}{2r_{mv}}\right)$

Symbols

- U_1 = velocity of surrounding stream
 U_0 = exit velocity of jet at nozzle
 λ = U_1/U_0
 x = axial distance from end of nozzle
 x_e = distance to end of potential core
 U_e = center line velocity of jet for $x > x_e$
 D = diameter of nozzle
 r = radial distance from axis
 U = velocity at r
 r_{mv} = radius where $U = \frac{U_e + U_1}{2}$

It is noted that formula (i) for the case where $\lambda = 0$ does not agree with the one given by Hinze and van der Hegge Zijnen, which is

$$\frac{U_e}{U_0} = \frac{6.39}{\frac{x}{D} + 0.6}$$

Reference should be made to Pai's book [111, p. 120] for another form of (ii) and further discussion of the effect of a surrounding stream.

Turning next to the heated jet in a surrounding stream, we have the problem of the combined effects of a stream velocity and density differences on the velocity and temperature fields. Some experimental information on the temperature field of the round jet in a supersonic stream was obtained by Rousso and Baughman [137] in connection with an NACA program on jets aimed primarily at answering certain engineering problems. The only known account of work attempting to solve the transfer problem is the paper by Szablewski [138], in which a theoretical development is given, and the experimental work of Pabst [139] is displayed as a test of the theory. The analysis applies specifically to the round jet and includes large density differences. It does not include the case where the surrounding air is stationary.

It is left to the reader to consult [138] for the lengthy analytical development and the complete results. In brief, Szablewski bases his development on turbulent exchange coefficients given by the Prandtl expression (Eq. 29-1). These are introduced into the usual equations expressed in the form of continuity equations for mass, momentum, and heat. The ratio of the exchange coefficient for momentum to that for heat and mass (the turbulent Prandtl number, Pr_t) was taken to be 0.5 on

the basis of Pabst's results. The computed examples cover the range

$$\frac{U_1}{U_0} = 0.5, 0.25, 0.05$$

$$\frac{T_0}{T_1} = 1, 1.75, 2.5$$

where U_1, T_1 = outer stream velocity and absolute temperature respectively

U_0, T_0 = jet exit velocity and absolute temperature respectively. Pabst's measurements of velocity and temperature distributions in a round jet were made with $U_0 \cong 400$ m/sec, $U_1 = 18, 101$, and 188 m/sec, and $T_0 = 300^\circ\text{C}$ ($T_0/T_1 \cong 2$). Since Szablewski's account of this work appeared to cover the significant points, the original work of Pabst was not consulted.

The following are the major conclusions:

1. The theoretical predictions for small density differences agree with other work regarding the direction of the effect of an outside stream, namely to decrease the rate of spreading of both velocity and temperature. The predicted asymptotic boundary (jet so far from nozzle that nozzle size has no effect) varies as x^4 for any value of U_1 except zero.
2. An outside stream reduces the rate of velocity and temperature fall along the axis. This is qualitatively confirmed by experiment, but there is some question about the accuracy of Pabst's temperature measurements. The asymptotic variation predicted by theory is x^{-4} for any value of U_1 except zero.
3. When $U_1 \neq 0$ the asymptotic velocity profile is given by

$$\frac{U - U_1}{U_c - U_1} = \exp \left[- \left(c \frac{r}{r_1} \right)^2 \right]$$

where U_c is the velocity at the center, r_1 is the radius of the jet boundary, and c is a shape factor. The temperature profile is

$$\frac{T - T_1}{T_c - T_1} = \left(\frac{U - U_1}{U_c - U_1} \right)^{Pr_1}$$

where Pr_1 is taken as 0.5. These distribution functions when fitted to Pabst's measurements at 16, 20, and 24 nozzle diameters downstream show reasonably good agreement.

4. Reduced jet density, due to elevated temperature, increases the rate of velocity and temperature fall along the axis. Apparently Pabst's work does not provide any test of this effect. However, this is consistent with the findings of Corrsin and Uberoi for $U_1 = 0$.
5. Reduced jet density, due to elevated temperature, decreases the rate

B · TURBULENT FLOW

of spreading of both velocity and temperature. The effect of the temperature on the width is given as proportional to $[1 + (T_0 - T_1)/T_1]^{-\frac{1}{2}}$. Pabst's work, as quoted by Szablewski, does not provide any test of this effect. The effect is opposite to that found by Corrsin and Uberoi for $U_1 = 0$.

Conclusion 5 appears to be inconsistent with conclusion 4. Conclusion 5 can, however, be made to appear reasonable by following a suggestion by Squire and Trounec to the effect that compressibility or heating might be dealt with in terms of an "equivalent jet." Since the momentum

$$\frac{\pi}{4} D^2 \rho U_0 (U_0 - U_1)$$

is maintained at all sections, an equivalent incompressible jet should behave like a compressible jet when the momentum is the same. Heating a jet decreases $\rho U_0 (U_0 - U_1)$ by decreasing ρ . We should obtain the same effect without heating by keeping ρ the same and decreasing $U_0 (U_0 - U_1)$. This can be done either by decreasing U_0 or by increasing U_1 . By either means U_1/U_0 is increased, and this clearly has the effect of decreasing the divergence of the velocity field. Presumably the divergence of the temperature field would follow that of the velocity field.

The tentative conclusion drawn from the present information is that the effect of density on spreading characteristics reverses in going from the case where $U_1 = 0$ to the case where $U_1 > 0$. More experimental results covering a greater range of conditions are needed to clarify the situation.

Not all of the information on jets has been covered in this brief survey. Pai, for example, gives a mathematical procedure for dealing with turbulent jets by employing methods analogous to those for laminar flow. For this, the reader is referred to his book [111]. An extensive bibliography given by Forstall and Shapiro [124] will be helpful to readers wishing to pursue the subject of jets further.

CHAPTER 6. TURBULENT STRUCTURE OF SHEAR FLOWS

B.33. The Nature of the Subject. Dating from about 1925 many investigators have applied the hot wire anemometer in aerodynamic experiments in an effort to learn something about turbulence through measurement. Over the years these efforts have borne fruit; consequently there are many separate pieces of information contributing to our present knowledge of turbulence and the turbulent structure of various flow fields.

B · TURBULENT FLOW

of spreading of both velocity and temperature. The effect of the temperature on the width is given as proportional to $[1 + (T_0 - T_1)/T_1]^{-\frac{1}{2}}$. Pabst's work, as quoted by Szablewski, does not provide any test of this effect. The effect is opposite to that found by Corrsin and Uberoi for $U_1 = 0$.

Conclusion 5 appears to be inconsistent with conclusion 4. Conclusion 5 can, however, be made to appear reasonable by following a suggestion by Squire and Trounec to the effect that compressibility or heating might be dealt with in terms of an "equivalent jet." Since the momentum

$$\frac{\pi}{4} D^2 \rho U_0 (U_0 - U_1)$$

is maintained at all sections, an equivalent incompressible jet should behave like a compressible jet when the momentum is the same. Heating a jet decreases $\rho U_0 (U_0 - U_1)$ by decreasing ρ . We should obtain the same effect without heating by keeping ρ the same and decreasing $U_0 (U_0 - U_1)$. This can be done either by decreasing U_0 or by increasing U_1 . By either means U_1/U_0 is increased, and this clearly has the effect of decreasing the divergence of the velocity field. Presumably the divergence of the temperature field would follow that of the velocity field.

The tentative conclusion drawn from the present information is that the effect of density on spreading characteristics reverses in going from the case where $U_1 = 0$ to the case where $U_1 > 0$. More experimental results covering a greater range of conditions are needed to clarify the situation.

Not all of the information on jets has been covered in this brief survey. Pai, for example, gives a mathematical procedure for dealing with turbulent jets by employing methods analogous to those for laminar flow. For this, the reader is referred to his book [111]. An extensive bibliography given by Forstall and Shapiro [124] will be helpful to readers wishing to pursue the subject of jets further.

CHAPTER 6. TURBULENT STRUCTURE OF SHEAR FLOWS

B.33. The Nature of the Subject. Dating from about 1925 many investigators have applied the hot wire anemometer in aerodynamic experiments in an effort to learn something about turbulence through measurement. Over the years these efforts have borne fruit; consequently there are many separate pieces of information contributing to our present knowledge of turbulence and the turbulent structure of various flow fields.

For the most part the measured quantities are the velocity fluctuations, their mean square values, their time derivatives, space and time correlations, probability distributions, and energy spectra. In a few cases measurements have been made of temperature fluctuations, including correlations, spectra, and velocity-temperature correlations. Due to limitations inherent in the hot wire technique, very few measurements have yet been made in the compressible flow range. Low speed boundary layers, jets, and wakes have been the principal objects of investigation.

Theoretical studies on the turbulent structure of shear flows are not abundant because of the difficult nature of the statistical theories of turbulence and the additional complications arising from anisotropy and inhomogeneity associated with shear flows. Nevertheless, it becomes a lengthy task to present and discuss both the experimental and theoretical sides of the subject. We therefore restrict the present coverage to a listing of references. Qualitative aspects of structure have been discussed in previous articles, and the references there cited will be repeated here only by number. The list covers mainly relatively recent works which are available to us, and it can by no means pretend to be complete. Classification is by subject, each being headed by a brief discussion. Since many works cover topics belonging in different classes, the grouping must not be considered as rigid.

B.34. References on Structure of Shear Turbulence.

General considerations on vorticity and structure of turbulence. The stretching of vorticity and the formation of vortex sheets play an important role in shear turbulence. Studies of these phenomena are generally theoretical, and often have to be based on a simple and isotropic model.

- Agostini, L., and Bass, J. Les théories de la turbulence. *Publs. sci. et tech. Ministère air France* 237, 1950.
- Betchov, R. An inequality concerning the production of vorticity in isotropic turbulence. *J. Fluid Mech.* 1, 497–504 (1956).
- Burgers, J. M. The formation of vortex sheets in a simplified type of turbulent motion. *Proc. Acad. Sci. Amsterdam* 53, 122–133 (1950).
- Corrsin, S. Hypothesis for skewness of the probability of the lateral velocity fluctuations in turbulent flow. *J. Aeronaut. Sci.* 17, 396–398 (1950).
- Djang, F. G. A kinetic theory of turbulence. *Chinese J. Phys.* 7, 176 (1948).
- Liepmann, H. W. Aspects of the turbulence problem. *J. Math. and Phys.* 3, 321–342, 407–426 (1952).
- Lin, C. C. On Taylor's hypothesis in wind tunnel turbulence. *Mem. Nav. Ord. Lab.* 10775, 1950.
- Lin, C. C. On Taylor's hypothesis and the acceleration terms in the Navier-Stokes equations. *Nav. Ord. Rept.* 2306, 1952.
- Munk, M. M. *A Simplified Theory of Turbulent Fluid Motion.* Catholic Univ. of America, 1955.
- Pai, S. I. *Viscous Flow Theory. II: Turbulent Flow.* Van Nostrand, 1957.
- Theodorsen, Th. Mechanism of turbulence. *Proc. Second Midwestern Conf. Fluid Mech., The Ohio State Univ.*, 1952.

Statistical theories of shear and inhomogeneous turbulence. In statistical theories of turbulence, it is important to study the structure of correlations and spectral functions on the basis of hydrodynamical equations of motion. The spectral tensor in anisotropic turbulence has a much more complicated form than in isotropic turbulence. Exact mathematical theories are not yet possible. Dimensional arguments and simplifying reasoning are necessary. If a reasonably simple equation of motion of one-dimension is used, such as in Burgers' model, the solution can be obtained exactly, and many characteristics of turbulence can be studied without introducing simplifying assumptions at an early stage.

- Burgers, J. M. Some considerations on turbulent flow with shear. *Proc. Acad. Sci. Amsterdam B56*, 125–136, 137–147 (1953).
- Burgers, J. M., and Mitchell, M. On homogeneous non-isotropic turbulence connected with a mean motion having a constant velocity gradient. *Proc. Acad. Sci. Amsterdam B56*, 228–235, 343–354 (1953).
- Kampé de Fériet, J. Le tenseur spectral de la turbulence homogène non isotrope dans un fluide incompressible. *Proc. Seventh Intern. Congress Appl. Mech., London*, 6–26 (1948).
- von Kármán, Th. The fundamentals of the statistical theory of turbulence. *J. Aeronaut. Sci.* 4, 131 (1937).
- Monin, A. S. Characteristics of anisotropic turbulence. *Doklady Akad. Nauk. S.S.R.* 75, 621–624 (1950).
- Parker, E. N. The concept of physical subsets and application to hydrodynamic theory. *Naval Ord. Test Station Tech. Mem.* 988, China Lake, Calif., 1953.
- Rotta, J. Statische Theorie nichthomogener Turbulenz I, II. *Z. Physik* 129, 547 (1951); 131, 51 (1951).
- Tchen, C. M. On the spectrum of energy in turbulent shear flow. *J. Research Natl. Bur. Standards* 50, 51 (1953).
- Tchen, C. M. Transport processes as foundations of the Heisenberg and Obukhoff theories of turbulence. *Phys. Rev.* 93, 4 (1954).

Structure of turbulence in wall-bounded flow (boundary layer, channel and pipe). Turbulent measurements are made on energy, shear stresses, correlation, spectral functions of energy, and shear stress. In the case of the boundary layer, the flow is complicated by the fact that there exist a laminar sublayer near the wall and an irregular outer limit producing a region of intermittent turbulence near the free edge of the boundary layer. The intermittencies and the probability of their occurrence are important for the understanding of the boundary layer, and for the formulation of a realistic theory of the boundary layer structure. Phenomenological theories are based on transport concepts (such as mixing length) to express nonlinear turbulent terms. Other theories assume some definite relation between the fourth and second orders of correlations, and a third group of theories make some assumption involving physical and dimensional reasoning on the role of the turbulent pressure.

- Chou, P. Y. On velocity correlation and the solutions of the equations of turbulent fluctuation. *Quart. Appl. Math.* 3, 38–54 (1945).
- Chou, P. Y. Pressure flow of a turbulent fluid between two infinite parallel plates. *Quart. Appl. Math.* 3, 198–209 (1945).

- Chou, P. Y. On velocity correlations and the equations of turbulent vorticity fluctuation. *Natl. Tsing-Hua Univ. Sci. Rept.* 5, 1-18 (1948).
- Chou, P. Y. The turbulent flow along a semi-infinite flat plate. *Quart. Appl. Math.* 5, 346-353 (1947).
- Dryden, H. L. Recent advances in the mechanics of boundary layer flow. *Advances in Applied Mechanics*, pp. 1-40. Academic Press, 1948.
- Eskinazi, S., and Yeh, H. An investigation on fully developed turbulent flows in a curved channel. *J. Aeronaut. Sci.* 23, 23-35 (1956).
- Fage, A., and Townsend, H. C. H. An examination of turbulent flow with an ultra-microscope. *Proc. Roy. Soc. London A135*, 656-677 (1932).
- Favre, A., Gaviglio, J., and Dumas, R. Nouvelles mesure dans la couche limite d'une plaque plane, des intensités de turbulence, et des corrélations dans le temps; spectres. *Recherche aéronaut. Paris* 38, 7-12 (1954).
- Favre, A., Gaviglio, J., and Dumas, R. Couche limite turbulente: Corrélations spatio-temporelles doubles; spectres. *Recherche aéronaut. Paris* 48, 3-14 (1955).
- Johnson, D. S. Turbulent heat transfer in a boundary layer with discontinuous wall temperature. *The Johns Hopkins Univ. Dept. of Aeronaut. Rept.*, 1955.
- Klebanoff, P. S. Characteristics of turbulence in a boundary layer with zero pressure gradient. *NACA Tech. Rept. 1247*, 1955.
- Laufer, J. Some recent measurements in a two-dimensional turbulent channel. *J. Aeronaut. Sci.* 17, 277-287 (1950).
- Laufer, J. The structure of turbulence in fully developed pipe flow. *NACA Rept. 1174*, 1955.
- Ludwig, H., and Tillman, W. Untersuchungen über die Wandschubspannung in turbulenten Reibungsschichten. *Ing.-Arch.* 17, 288-299 (1949).
- Malkus, W. V. R. Outline of a theory of turbulent shear flow. *J. Fluid Mech.* 1, 521 (1956).
- Mattioli, E. Una formula universale per lo spettro nella turbolenza di parete. *Atti accad. sci. Torino* 90, 1956.
- Mattioli, E. Richerche teoriche e sperimentali sulla turbolenza di parete. *Aerotecnica* 36, (2), 1956.
- Michel, R. Contribution à l'étude des couches limites turbulentes avec gradient de pression. *Publs. sci. et tech. Ministère air France* 252, 1951.
- Newman, B. G. Skin friction in a retarded turbulent boundary layer near separation. *Dept. of Supply, Australia, Aeronaut. Research Lab. Rept. A73*, 1950.
- Rotta, J. Beitrag zur Berechnung der turbulenten Grenzschichten. *Ing.-Arch.* 19, 31 (1953).
- Rotta, J. Schubspannungsverteilungen und Energiedissipation bei turbulenten Grenzschichten. *Ing.-Arch.* 20, 195-207 (1952).
- Sandborn, V. A., and Braun, W. H. Turbulent shear spectra and local isotropy in the low-speed boundary layer. *NACA Tech. Note 3761*, 1956.
- Schubauer, G. B. Turbulent processes as observed in boundary layer and pipe. *J. Appl. Phys.* 25, 188-196 (1954).
- Steketee, J. A. Some problems in boundary layer transition. *Univ. Toronto Inst. Aerophys. Rept.* 38, 1956.
- Szablewski, W. Berechnung des turbulenten Strömung in Rohr auf der Grundlage der Mischungsweg-hypothese. *Z. angew. Math. u. Mech.* 31, 13-142 (1951).
- Szablewski, W. Berechnung des turbulenten Strömung Langs einer ebenen Platte. *Z. angew. Math. u. Mech.* 31, 309 (1951).
- Taylor, G. I. Correlation measurements in a turbulent flow through a pipe. *Proc. Roy. Soc. London A157*, 537-546 (1936).
- Townsend, A. A. The structure of the turbulent boundary layer. *Proc. Cambridge Phil. Soc.* 47, 375-395 (1951).
- Walz, A. Näherungstheorie für kompressible turbulente Grenzschichten. *Z. angew. Math. u. Mech.*, 50-56 (1956).
- Walz, A. Nouvelle méthode approchée de calcul des couches limites laminaire et turbulente en écoulement compressible. *Publ. sci. et tech. Ministère air France* 309, 1956.

B · TURBULENT FLOW

Yeh, H., Rose, W. G., and Lien, H. Further investigation on fully developed turbulent flows in a curved channel. *The Johns Hopkins Univ. Dept. Mech. Eng. Rept.*, 1956.

Cited references [73,76,77,87,89,93].

Structure of turbulence in a free flow (jet, wake). In a free flow, the intermittencies produced near the boundary of the flow play an important role in the characteristics of the flow and the structure of turbulence. The shear flow in the present case has a weak mean velocity gradient, so that the spectrum of energy is not far from the spectrum of an isotropic turbulence. However, here a spectrum of shear exists, in contrast to its absence in isotropic flow.

Chou, P. Y. On an extension of Reynolds' method of finding apparent stress and the nature of turbulence. *Chinese J. Phys.* 4, 1-33 (1940).

Corrsin, S., and Uberoi, M. S. Spectra and diffusion in a round turbulent jet. *NACA Rept. 1040*, 1951.

Hinze, J., and van der Hegge Zijnen, B. G. Heat and mass transfer in the turbulent mixing zone of an axially symmetrical jet. *Proc. Seventh Intern. Congress Appl. Mech., London*, 1948.

Kalinske, A. A., and Pien, C. C. Eddy diffusion. *Ind. Eng. Chem.* 36, 220-223 (1944).

Kovácsnay, L. S. G. Hot-wire investigation of the wake behind cylinders at low Reynolds numbers. *Proc. Roy. Soc. London A198*, 174-190 (1949).

Laurence J. C. Intensity, scale, and spectra of turbulence in mixing region of free subsonic jet. *NACA Rept. 1292*, 1956.

Laurence, J. C., and Stickney, T. M. Further measurements of intensity, scale, and spectra of turbulence in a subsonic jet. *NACA Tech. Note 3576*, 1956.

Squire, H. B. Reconsideration of the theory of free turbulence. *Phil. Mag.* 39, 1-20 (1948).

Swain, L. M. On the turbulent wake behind a body of revolution. *Proc. Roy. Soc. London A125*, 647-659 (1929).

Tamaki, H., and Oshima, K. Experimental studies on the wake behind a row of heated parallel rods. *Proc. First Japan. Natl. Congress. Appl. Mech.*, 459-464 (1951).

Cited references [94,112,113,114,115,116,121,123,124,126].

Structure of turbulence connected with turbulent diffusion and heat transfer. In both the statistical and phenomenological theories of the structure of shear turbulence, of bounded or free flows, turbulent diffusion plays an important role. A thorough coverage of turbulent diffusion is not intended, and only those works dealing with the mechanism of diffusion which help in better understanding the structure of turbulence are listed below, leaving aside works mainly connected with applications of diffusion.

Batchelor, G. K., Binnie, A. M., and Phillips, O. M. The mean velocity of discrete particles in turbulent flow in a pipe. *Proc. Phys. Soc. London B68*, 1095-1104 (1955).

Batchelor, G. K., and Townsend, A. A. Turbulent diffusion. *Surveys in Mechanics*, pp. 353-399. Cambridge Univ. Press, 1956.

Beckers, H. L. Heat transfer in turbulent tube flow. *Appl. Sci. Research A6*, 147 (1956).

Brier, G. W. The statistical theory of turbulence and the problem of diffusion in the atmosphere. *J. Meteorol.* 7, 283-290 (1950).

- Davies, D. R. The problem of diffusion into a turbulent boundary layer from a plane area source, bounded by two straight perpendicular edges. *Quart. J. Mech. and Appl. Math.* 7, 467-471 (1954).
- Dryden, H. L. Turbulence and diffusion. *Ind. Eng. Chem.* 31, 416 (1939).
- Ellison, T. H. Atmospheric turbulence. *Surveys in Mechanics*, pp. 400-430. Cambridge Univ. Press, 1956.
- Frenkiel, N. F. On the statistical theory of turbulent diffusion. *Proc. Natl. Acad. Sci.* 38, 509-515 (1952).
- Frenkiel, F. N. Application of the statistical theory of turbulent diffusion to micro-meteorology. *J. Meteorol.* 9, 252-259 (1952).
- Frenkiel, N. F. Sur la mesure de la diffusion de la chaleur. *Groupement fran^c. d^evelop. recherches a^tronaut.*, 1946.
- Hunze, J. O. Turbulent diffusion from a source in turbulent shear flow. *J. Aeronaut. Sci.* 18, 565 (1951).
- Inoue, E. On the temperature fluctuations in a heated turbulent field. *Geophys. Notes, Geophys. Inst., Tokyo Univ.*, 3, 1950. *Geophys. Mag.* 23, (1), 1951.
- Inoue, E. Some remarks on the dynamical and thermal structure of a heated fluid. *J. Phys. Soc. Japan* 6, 392 (1951).
- Kitojima, K. On the mixing length of turbulence. *Kyushu Univ. Research Inst. Fluid Eng. Rept.* 4, 43-54 (1948).
- Lee, T. D. Note on the coefficient of eddy viscosity in isotropic turbulence. *Phys. Rev.* 77, 842 (1950).
- Levich, V. G. Diffusion. *Doklady Akad. Nauk. S.S.R.* 78, 1105-1108 (1951).
- Liu, V. C. Turbulent dispersion of dynamic particles. *J. Meteorol.* 13, 399-405 (1956).
- Monin, A. S. Equations of turbulent diffusion. *Doklady Akad. Nauk. S.S.R.* 105, 256-259 (1955).
- Ribaud, G. Some remarks on the subject of heat and momentum transfer in the boundary layer. *C. R. Acad. Sci. Paris* 240, 1, 25-28 (1955).
- Taylor, G. I. The dispersion of matter in turbulent flow through a pipe. *Proc. Roy. Soc. London A223*, 446 (1954).
- Tchen, C. M. Enige Wiskundige Betrekkingen Welke een Rol Spelen in Diffusie-problemen. *Verhandl. Acad. voor Wet.* 53, 400-410 (1944).
- Tchen, C. M. Stochastic processes and the dispersion of the configurations of linked events. *J. Research Natl. Bur. Standards* 46, 480-488 (1951).
- Wieghardt, K. On diffusion phenomena in turbulent boundary layer. *Z. angew. Math. u. Mech.* 28, 346-355 (1948).
- Cited references [25, 26, 27, 116, 119, 122].

Instrumentation for the measurement of turbulence. What has been learned about the structure of turbulence from experiment has depended largely on the instruments available for making observations and measurements. Here the hot wire anemometer has played a predominantly important role. The number and accuracy of quantities measured have gone hand in hand with the development of hot wire probes and the adaptation of electronic circuits to amplify the signal, compensate for thermal lag of the hot wire, and perform a variety of operations such as adding, multiplying, and differentiating signals. The following references therefore pertain mainly to the hot wire and its auxiliary equipment.

- Dryden, H. L., and Kuethe, A. M. The measurement of fluctuations of air speed by the hot-wire anemometer. *NACA Rept.* 320, 1929.
- Fage, A. Studies of boundary-layer flow with a fluid-motion microscope. *50 Jahre Grenzschichtforschung*, pp. 132-146. (Ed: H. Görtler and W. Tollmien.) Vieweg, Braunschweig, 1955.

B · TURBULENT FLOW

- Kovásznay, L. S. G. Turbulence in supersonic flow. *J. Aeronaut. Sci.* 20, 657-675 (1953).
- Kovásznay, L. S. G. Development of turbulence-measuring equipment. *NACA Rept. 1209*, 1954.
- Laufer, J., and McClellan, R. Measurements of heat transfer from fine wires in supersonic flow. *J. Fluid Phys.* 1, 276-289 (1956).
- Laurence, J. C., and Landes, L. G. Auxiliary equipment and techniques for adapting the constant-temperature hot-wire anemometer to specific problems in air-flow measurements. *NACA Tech. Note 2843*, 1952.
- Mock, W. C., Jr. Alternating-current equipment for the measurement of fluctuations of air speed in turbulent flow. *NACA Rept. 598*, 1937.
- Newman, B. G., and Leary, B. G. The measurement of the Reynolds stresses in a circular pipe as means of testing a hot wire anemometer. *Dept. of Supply, Australia, Aeronaut. Research Lab. Rept. A72*, 1950.
- Ossofsky, E. Constant temperature operation of the hot-wire anemometer at high frequency. *Rev. Sci. Instr.* 19, 881-889 (1948).
- Sansborn, V. A. Heat loss from yawed hot wires at subsonic Mach numbers. *NACA Tech. Note 3563*, 1955.
- Schubauer, G. B. A turbulence indicator utilizing the diffusion of heat. *NACA Rept. 524*, 1935.
- Spangenberg, W. G. Heat-loss characteristics of hot-wire anemometers at various densities in transonic and supersonic flow. *NACA Tech. Note 3381*, 1955.
- Tchen, C. M. Heat delivery in a compressible flow at subsonic and supersonic speeds. *NACA Tech. Note 2436*, 1951.
- Überoi, M. S., and Kovásznay, L. S. G. Analysis of turbulent density fluctuations by the shadow method. *J. Appl. Phys.* 26, 1955.
- Weske, J. R. A hot-wire circuit with very small time lag. *NACA Tech. Note 881*, 1943.
- Willis, J. B. Review of hot-wire anemometry. *Council for Sci. and Ind. Research, Div. of Aeronautics, Australia, Rept. A34*, 1945.
- Wise, B., and Schultz, D. L. Turbulent measurements in supersonic flow with the hot-wire anemometer. *Brit. Aeronaut. Research Council Rept. FM 2390*, 1955.

B,35. Cited References.

1. Townsend, A. A. *The Structure of Turbulent Shear Flow*. Cambridge Univ. Press, 1956.
2. Batchelor, G. K. *The Theory of Homogeneous Turbulence*. Cambridge Univ. Press, 1953.
3. Reynolds, O. *Phil. Trans. A186*, 123 (1894), or *Papers 2*, 535.
4. Lorentz, H. A. *Abhandl. theoreti. Physik 1*, 43 (1907).
5. Lamb, H. *Hydrodynamics*, 6th ed. Dover, 1945.
6. Goldstein, S. *Modern Developments in Fluid Dynamics*, 1st ed., Vol. 2. Clarendon Press, Oxford, 1938.
7. Howarth, L. *Modern Developments in Fluid Dynamics, High Speed Flow*, 1st ed., Vol. 2. Clarendon Press, Oxford, 1953.
8. Rubesin, M. W. A modified Reynolds analogy for the compressible turbulent boundary layer on a flat plate. *NACA Tech. Note 2917*, 1953.
9. Crocco, L. Sulla Transmissione del Calore da una Lamina Piana a un Fluido Scorrente ad alta Velocita. *Aerotecnica 12*, 181-197 (1932).
10. Squire, H. B. Heat transfer calculation for aerofoils. *Brit. Aeronaut. Research Council Repts. and Mem.* 1986, 1942.
11. Ackerman, G. *Fortsch. Gebiete Ingenieurw.* 13, 226-234 (1942).
12. Mack, L. M. An experimental investigation of the temperature recovery factor. *Calif. Inst. Technol. Jet Propul. Lab. Rept. 20-80*, 1954.
13. Stalder, J. R., Rubesin, M. W., and Tendeland, T. A determination of the laminar-transitional, and turbulent-boundary-layer temperature-recovery factors on a flat plate in supersonic flow. *NACA Tech. Note 2077*, 1950.

B,35 · CITED REFERENCES

14. Seban, R. A. *Analysis for the Heat Transfer to Turbulent Boundary Layers in High Velocity Flow.* Ph.D. Thesis, Univ. Calif., Berkeley, 1948.
15. Shirokow, M. *Tech. Phys. USSR* 8, 1020–1027 (1936).
16. Stine, H. A., and Scherrer, R. Experimental investigation of the turbulent-boundary layer temperature-recovery factor on bodies of revolution at Mach numbers from 2.0 to 3.8. *NACA Tech. Note 2664*, 1952.
17. Tucker, M., and Maslen, S. H. Turbulent boundary layer temperature recovery factors in two-dimensional supersonic flow. *NACA Tech. Note 2296*, 1951.
18. Lobb, K. R., Winkler, E. M., and Persh, J. *J. Aeronaut. Sci.* 22, 1–9 (1955).
19. van Driest, F. R. *J. Aeronaut. Sci.* 18, 145–160 (1951).
20. Spivack, H. M. Experiments in the turbulent boundary layer of a supersonic flow. *North Amer. Aviation Rept. AL-1052, APL/JHU CM-615*, 1950.
21. Chapman, S., and Cowling, T. G. *The Mathematical Theory of Non-Uniform Gases.* Cambridge Univ. Press, 1953.
22. Lorentz, H. A. *The Theory of Electrons.* Dover, 1952.
23. Van Vleck, J. H., and Weisskopf, V. G. *Rev. Mod. Phys.* 17, 227 (1945).
24. Bhatnagar, P. L., Gross, E. P., and Krook, M. *Phys. Rev.* 94, 511 (1954).
25. Tchen, C. M. *Mean Value and Correlation Problems Connected with the Motion of Small Particles Suspended in a Turbulent Fluid.* Thesis, Delft, 1947. Mededeeling No. 51 uit het Laboratorium voor Aero-en Hydrodynamica der Technische Hogeschool te Delft.
26. Burgers, J. M. On turbulent fluid motion. *Calif. Inst. Technol. Hydrodynam. Lab. Rept. E-34.1, Chap. 5*, 1951.
27. Tchen, C. M. *J. Chem. Phys.* 20, 214–217 (1952).
28. Reynolds, O. *Proc. Manchester Lit. Phil. Soc.* 14, 7–12 (1874); *Collected Papers 1*, 81–85.
29. Chapman, D. R., and Kester, R. H. *J. Aeronaut. Sci.* 20, 441–448 (1953).
30. Reichardt, E. Heat transfer through turbulent friction layers. *NACA Tech. Mem. 1047*, 1943.
31. Colburn, A. P. *Trans. Am. Inst. Chem. Engr.* 29, 174–210 (1933).
32. Rubesin, M. W., Maydey, R. C., and Varga, S. A. An analytical and experimental investigation of the skin friction of the turbulent boundary layer on a flat plate at supersonic speeds. *NACA Tech. Note 2305*, 1951.
33. Pappas, C. C. Measurement of heat transfer in the turbulent boundary layer on a flat plate in supersonic flow and comparison with skin-friction results. *NACA Tech. Note 3222*, 1954.
34. Coles, D. *J. Aeronaut. Sci. Readers' Forum* 19, 717 (1952).
35. Coles, D., and Goddard, F. E. Direct measurement of skin friction on a smooth flat plate at supersonic speeds. Paper presented at 8th Intern. Congr. Theoret. and Appl. Mech., Istanbul, 1952.
36. Liepmann, H. W., and Dhawan, S. *Proc. First U.S. Natl. Congr. Appl. Mech.*, Chicago, 869–874 (1951).
37. Dhawan, S. Direct measurements of skin friction. *NACA Tech. Note 2567*, 1952.
38. Wilson, R. E. *J. Aeronaut. Sci.* 17, 585–594 (1950).
39. Brinich, P. F., and Diacomis, N. S. Boundary-layer development and skin friction at Mach number 3.05. *NACA Tech. Note 2742*, 1952.
40. Fallis, W. B. Heat transfer in the transitional and turbulent boundary layers of a flat plate at supersonic speeds. *Univ. Toronto Inst. Aerophys., UTIA Rept. 19*, 1952.
41. Slack, E. G. Experimental investigation of heat transfer through laminar and turbulent boundary layers on a cooled flat plate at a Mach number of 2.4. *NACA Tech. Note 2888*, 1952.
42. Monaghan, R. J., and Cooke, J. R. The measurement of heat transfer and skin friction at supersonic speeds. Part III: Measurements of overall heat transfer and of the associated boundary layers on a flat plate at $M_1 = 2.43$. *Roy. Air Establishment Tech. Note Aero. 2129*, 1951.
43. Monaghan, R. J., and Cooke, J. R. The measurement of heat transfer and skin

B · TURBULENT FLOW

- friction at supersonic speeds. Part IV: Tests on a flat plate at $M_1 = 2.82$. *Roy. Air Establishment Tech. Note Aero. 2171*, 1952.
44. Frankl, F. Heat transfer in the turbulent boundary layer of a compressible gas at high speeds. Also Frankl, F., and Voishel, V. Friction in the turbulent boundary layer of a compressible gas at high speeds. *NACA Tech. Mem. 1032*, 1942.
 45. Frankl, F., and Voishel, V. Turbulent friction in the boundary layer of a flat plate in a two-dimensional compressible flow at high speeds. *NACA Tech. Mem. 1053*, 1943.
 46. von Kármán, Th. Mechanical similitude and turbulence. *NACA Tech. Mem. 611*, 1931.
 47. Schoenherr, K. E. *Trans. Soc. Nav. Arch. and Marine Eng. 40*, 279–313 (1932).
 48. Prandtl, L. *Göttingen Ergebnisse 4*, 27 (1932).
 49. Clemmow, D. M. The turbulent boundary layer flow of a compressible fluid along a flat plate. *Brit. Directorate of Guided Weapons Research and Develop. Rept. 50/6*, 1950.
 50. van Driest, E. R. Proceedings of the Bureau of Ordnance symposium on aeroballistics. Comments on paper by R. E. Wilson, *NAVORD Rept. 1961*, 264–267 (1950).
 51. Li, T.-Y., and Nagamatsu, H. T. Effects of density fluctuations on the turbulent skin friction of an insulated flat plate at high supersonic speeds. *Calif. Inst. Technol. Guggenheim Aeronaut. Lab. Mem. 5*, 1951.
 52. Ferrari, C. *Quart. Appl. Math. 8*, 33–57 (1950).
 53. Smith, F., and Harrop, R. The turbulent boundary layer with heat transfer and compressible flow. *Roy. Aircraft Establishment Tech. Note Aero. 1759*, 1946.
 54. Eckert, H. U. *J. Aeronaut. Sci. 16*, 573–584 (1950).
 55. Monaghan, R. J. Comparison between experimental measurements and a suggested formula for the variation of turbulent skin friction in compressible flow. *Brit. Aeronaut. Research Council C.P. 45*, 19260, 1951.
 56. Cope, W. F. The turbulent boundary layer in compressible flow. *NPL Eng. Dept., Brit. Aeronaut. Research Council 7634*, 1943.
 57. Tucker, M. Approximate turbulent boundary-layer development in plane compressible flow along thermally insulated surfaces with application to supersonic-tunnel contour correction. *NACA Tech. Note 2045*, 1950.
 58. Tucker, M. Approximate calculation of turbulent boundary-layer development in compressible flow. *NACA Tech. Note 2337*, 1951.
 59. Young, G. B. W., and Janssen, E. *J. Aeronaut. Sci. 19*, 229–236 (1952).
 60. von Kármán, Th. The problems of resistance in compressible fluids. *Mem. Reale Acad. D'Italia*, Rome, 1936.
 61. Falkner, V. N. *Aircraft Eng. 15*, 65 (1943).
 62. Hill, F. K. *J. Aeronaut. Sci. 23*, 35 (1956).
 63. Korkegi, R. H. *J. Aeronaut. Sci. 23*, 97 (1956).
 64. Hakkinen, R. J. *Measurements of Skin Friction in Turbulent Boundary Layer at Transonic Speeds. Ph. D. Thesis*, Calif. Inst. Technol., 1953.
 65. O'Donnell, R. M. Experimental investigation at a Mach number of 2.41 of average skin-friction coefficients and velocity profiles for laminar and turbulent boundary-layers and an assessment of probe effects. *NACA Tech. Note 3122*, 1954.
 66. Coles, D. *J. Aeronaut. Sci. 21*, 433–448 (1954).
 67. Dönh, F. *Fortsch.-Aro. Gebiete Ingenieurw.-Wes. 282*, 1926.
 68. Blasius, H. *Mitt. Forschung. Ver. deut. Ing. 131*, 1–34 (1913).
 69. Prandtl, L. *Aerodynamic Theory*, Vol. 3, Durand, W. F. ed. Durand Reprinting Committee, Calif. Inst. Technol., 1943.
 70. Prandtl, L. Recent results of turbulence research. *NACA Tech. Mem. 720*, 1933. (Transl. *Z. Ver. deut. Ing. 7*, (5), 1933.)
 71. von Kármán, Th. *Nachr. Ges. Wiss. Göttingen*, 58–76 (1930).
 72. Clauser, F. H. The turbulent boundary layer. *Advances in Appl. Mech. 4*, 1–51. Academic Press, 1956.

B.35 · CITED REFERENCES

73. Millikan, C. B. A critical discussion of the turbulent flows in channels and circular tubes. *Proc. Fifth Intern. Congress Appl. Mech., Cambridge, Mass.*, 386-392 (1938).
74. Schultz-Grunow, F. New frictional resistance law for smooth plates. *NACA Tech. Mem. 986*, 1941. (Transl. *Luftfahrtforschung* 17, 239-246, 1940.)
75. Freeman, H. B. Force measurements on a $\frac{1}{10}$ -scale model of the U.S. airship "Aron." *NACA Rept. 432*, 1932.
76. Klebanoff, P. S., and Diehl, Z. W. Some features of artificially thickened fully developed turbulent boundary layers with zero pressure gradient. *NACA Rept. 1110*, 1952.
77. Laufer, J. Investigation of turbulent flow in a two-dimensional channel. *NACA Rept. 1033*, 1951.
78. von Kármán, Th. *J. Aeronaut. Sci.* 1, 1-20 (1934).
79. von Kármán, Th. Mechanische Ähnlichkeit und Turbulenz. *Proc. Third Intern. Congress Appl. Mech., Stockholm*, 1, 85-93 (1930).
80. Schlichting, S. *Ing.-Arch.* 7, 1-34 (1936).
81. Squire, H. B., and Young, A. D. The calculation of the profile drag of airfoils. *Brit. Aeronaut. Research Council Repts. and Mem.* 1838, 1938.
82. Kempf, G. *Werft, Reederei, Hafen*, 10, (11), 234-239 (1929); (12), 247-253 (1929).
83. Clauser, F. H. *J. Aeronaut. Sci.* 21, 91-108 (1954).
84. von Doenhoff, A. E., and Teterin, N. Determination of general relations for the behavior of turbulent boundary layers. *NACA Rept. 772*, 1943.
85. Coles, D. *J. Fluid Mech.* 1, Part 2, 191-226 (1956).
86. Landweber, L. *Trans. S.N.A.M.E.* 61, 5 (1953).
87. Schubauer, G. B., and Klebanoff, P. S. Investigation of separation of the turbulent boundary layer. *NACA Rept. 1030*, 1951.
88. Newman, B. G. Some contributions to the study of the turbulent boundary layer near separation. *Dept. Supply, Australia, Rept. ACA-53*, 1951.
89. Ludwieg, H., and Tillmann, W. Investigation of the wall-shearing stress in turbulent boundary layers. *NACA Tech. Mem. 1285*, 1950. Transl. from *Z. angew. Math. u. Mech.* 29, 15-16, 1949.
90. Ruetenik, J. R., and Corrsin, S. Equilibrium turbulent flow in a slightly divergent channel. *50 Jahre Grenzschichtforschung*. (Ed: H. Görtler and W. Tollmien), 446-459. Vieweg, Braunschweig, 1955.
91. Lees, L., and Crocco, L. *J. Aeronaut. Sci.* 19, 649-676 (1952).
92. Ross, D., and Robertson, J. *J. Appl. Mech.* 18, 95-100 (1951).
93. Rotta, J. On the theory of the turbulent boundary layer. *NACA Tech. Mem. 1344*, 1953. Transl. Über die Theorie der turbulenten Grenzschichten. *Mitt. Max-Planck-Inst., Göttingen*, 1, 1950.
94. Liepmann, H. W., and Laufer, J. Investigation of free turbulent mixing. *NACA Tech. Note 1257*, 1947.
95. Nikuradse, J. Laws of flow in rough pipes. *NACA Tech. Mem. 1292*, 1950. Transl. *Strömungsgesetze in rauhen Rohren*. Ver. deut. Ing. *Forschungsheft 361*, 1933.
96. Schlichting, H. *Boundary Layer Theory*. McGraw-Hill, 1955.
97. Hama, F. R. *Trans. Soc. Nav. Arch. and Marine Engrs.* 62, 333-358 (1954).
98. Buri, A. A method of calculation for the turbulent boundary layer with accelerated and retarded basic flow. *Brit. Ministry Aircraft Production R. T. P. Transl. 2073*. From *Thesis 652*, Federal Tech College, Zurich, 1931. (Also available from *CADD, Wright-Patterson Air Force Base*, as *AT143493*.)
99. Gruschwitz, E. *Ing.-Arch.* 2, 321-346 (1931).
100. Garner, H. C. The development of turbulent boundary layers. *Brit. Aeronaut. Research Council Repts. and Mem.* 2133, 1944.
101. Teterin, N., and Lin, C. C. A general integral form of the boundary-layer equation for incompressible flow with an application to the calculation of the separation point of turbulent boundary layers. *NACA Tech. Note 2168*, 1950.

B · TURBULENT FLOW

102. Fediaevsky, K. Turbulent boundary layer of an airfoil. *NACA Tech. Mem. 882*, 1937. Transl. *Central Aero-Hydrodynam. Inst., Moscow, Rept. 282*, 1936.
103. Ross, D., and Robertson, J. M. *J. Appl. Phys. 21*, 557–561 (1950).
104. Granville, P. S. A method for the calculation of the turbulent boundary layer in a pressure gradient. *The David W. Taylor Model Basin Rept. 752*, 1951.
105. Kuethe, A. M., McKee, P. B., and Curry, W. H. Measurements in the boundary layer of a yawed wing. *NACA Tech. Note 1946*, 1949.
106. Ashkenas, H., and Riddell, F. R. Investigation of the turbulent boundary layer on a yawed flat plate. *NACA Tech. Note 3383*, 1955.
107. Young, A. D., and Booth, T. B. The profile drag of yawed wings of infinite span. *College of Aeronautics, Cranfield, Rept. 38*, May 1950.
108. Townsend, A. A. *Proc. Roy. Soc. London A190*, 551–561 (1947).
109. Kuethe, A. M. *J. Appl. Mech. 2*, (3), 1935. In *Trans. Am. Soc. Mech. Eng. 57*, A-87, A-95 (1935).
110. Birkhoff, G., and Zarantonello, E. H. Jets, wakes, and cavities. *Applied Math. and Mech.*, Vol. 2. Academic Press, 1957.
111. Pai, S.-I. *Fluid Dynamics of Jets*. Van Nostrand, 1954.
112. Corrsin, S. Investigation of flow in an axially symmetrical heated jet of air. *NACA Wartime Rept. ACR 3L28*, 1943.
113. Townsend, A. A. *Proc. Roy. Soc. London A190*, 551–561 (1947).
114. Townsend, A. A. *Australian J. Sci. Research, Series A 1*, 161–174 (1948).
115. Townsend, A. A. *Proc. Roy. Soc. London A197*, 124–140 (1949).
116. Townsend, A. A. *Phil. Mag. 41*, 890–906 (1950).
117. Corrsin, S., and Kistler, A. L. The free-stream boundaries of turbulent flows. *NACA Rept. 1244*, 1955.
118. Klebanoff, P. S. Characteristics of turbulence in a boundary layer with zero pressure gradient. *NACA Tech. Note 3178*, 1954.
119. Taylor, G. I. *Proc. London Math. Soc. 20*, 196–212 (1921).
120. Prandtl, L. *Z. angew. Math. u. Mech. 22*, 241–243 (1942).
121. Taylor, G. I. *Proc. Roy. Soc. London A135*, 685–702 (1932).
122. Hinze, J. O., and van der Hegge Zijnen, B. G. *Appl. Sci. Research A1*, 435–461 (1949).
123. Corrsin, S., and Uberoi, M. S. Further experiments on the flow and heat transfer in a heated turbulent air jet. *NACA Rept. 998*, 1950.
124. Forstall, W., and Shapiro, A. H. *J. Appl. Mech. 17*, 399–408 (1950). In *Trans. Am. Soc. Mech. Eng. 72*, 1950.
125. Reichardt, H. *Z. angew. Math. u. Mech. 24*, 268–272 (1944).
126. Townsend, A. A. *Australian J. Sci. Research, Series A, 2*, 451–468 (1949).
127. Görtler, H. Berechnung von Aufgaben der freien Turbulenz auf Grund eines neuen Näherungsansatzes. *Z. angew. Math. u. Mech. 22*, 244–254 (1942).
128. Cleeves, V., and Boelter, L. M. K. *Chem. Eng. Progr. 43*, 123–134 (1947).
129. Abramovich, G. N. The theory of a free jet of a compressible gas. *NACA Tech. Mem. 1058*, 1944. Transl. *Central Aero-Hydrodynam. Inst., Moscow, Rept. 377*, 1939.
130. Goorderum, P. B., Wood, G. C., and Brevoort, M., J. Investigation with an interferometer of the turbulent mixing of a free supersonic jet. *NACA Rept. 963*, 1949.
131. Tollmien, W. Calculation of turbulent expansion processes. *NACA Tech. Mem. 1085*, 1945. Transl. from *Z. angew. Math. u. Mech. 6*, 1926.
132. Bershad, D., and Pai, S. I. *J. Appl. Phys. 21*, 616 (1950).
133. Pai, S. I. *J. Aeronaut. Sci. 16*, 463–469 (1949).
134. Keagy, W. R., and Weller, A. E. A study of freely expanding inhomogeneous jets. *Heat Transfer and Fluid Mech. Inst., Univ. Calif.*, 89–98 (1949). Am. Soc. Mech. Eng., New York.
135. Szablewski, W. Contributions to the study of the spreading of a free jet issuing from a nozzle. *NACA Tech. Mem. 1811*, 1951. Transl. Zur Theorie der Ausbreitung eines aus einer Düse austretenden freien Strahls. *Untersuch. u. Mitt. Nr. 8003*, Sept. 1944.

(122)

B,35 · CITED REFERENCES

136. Squire, H. B., and Trouncer, J. Round jets in a general stream. *Brit. Aeronaut. Research Council Repts. and Mem.* 1974, 1944.
137. Rousso, M. D., and Baughman, E. L. Spreading characteristics of a jet expanding from choked nozzles at Mach 1.91. *NACA Tech. Note 3836*, 1956.
138. Szablewski, W. The diffusion of a hot air jet in air in motion. *NACA Tech. Mem. 1288*, 1950. Transl. Die Ausbreitung eines Heissluftstrahles in Bewegter Luft. *GDC/2460*, Sept. 1946.
139. Pabst, O. Die ausbreitung heisser Gasstrahlen in bewegter Luft. *Untersuch. u. Mitt., Part II, UM 8007*, 1944.
140. Rubert, K. F., and Persh, J. A procedure for calculating the development of turbulent boundary layers under the influence of adverse pressure gradients. *NACA Tech. Note 2478*, 1951.
141. Ross, D. *Trans. Am. Soc. Civil Eng. Paper 2838, 121*, 1219–1254 (1956).
142. Spence, D. A. *J. Aeronaut. Sci. 23*, 3–15 (1956).